NTNU – Trondheim
Norwegian University of
Science and Technology

Drilling in Salt Formations and Rate of Penetration Modelling

Mats Håpnes

NORWEGIAN UNIVERSITY OF SCIENCE AND TECHNOLOGY

Abstract

Faculty of Engineering Science and Technology

Department of Petroleum Engineering and Applied Geophysics

Master of Science

Drilling in Salt Formations and Rate of Penetration Modelling

by Mats Håpnes

As the industrialization of the world is growing, both energy consumption and demand are steadily increasing. Hydrocarbons have been an important energy provider for several decades, but the production from mature oil and gas producers is now declining. In order to meet this rise in energy demand, new hydrocarbon deposits must be found and produced. Because large oil and gas reservoirs are associated with salt formations, this may be an important energy source for the future. Salt's low permeability and ability to deform under stress and temperature, makes it an ideal hydrocarbon-trap.

The initial objective of this thesis was to establish which challenges are related to drilling for pre-salt hydrocarbons, and propose solutions for how to overcome these challenges. When drilling towards these oil and gas reservoirs, the first problems may occur already in the formations above the salt structures. The density of salt does not increase with burial depth. When its density becomes lower than of the surrounding formations, salt will start to migrate and push through the overlying rocks. Due to the combined effect of compaction disequilibrium and salt tectonics, complex stress patterns can be created in the formations surrounding the salt structures. This may lead to many hazardous scenarios, created by rubble zones and recumbent beds. When drilling inside salt formations, it is salt's ability to creep and flow that may cause problems. Salt flow may cause borehole deformation

that impedes with the drilling and casing operations. When a wellbore has been drilled, salt can creep into the removed rock volume. This may cause situations such as stuck-pipe, hole instability, and high levels of shock and vibration when drilling. Salt flow is a positive function of time, so minimizing the time factor will decrease the possibility of salt flow related problems. One of the measures to minimize exposure time is to perform drilling operations quickly. Hence, a high rate of penetration (ROP) is beneficial when drilling in salt.

As part of proposing solutions to the drilling challenges in salt, two new drillbit technologies have been evaluated. These bits may be beneficial in order to overcome many of the problems related to salt drilling. Based on the results obtained in previous studies, these bits are capable of reducing the shock and vibration levels while drilling. This is because these bits are able to drill smoother than conventional PDC bits. Further, the reduced shock and vibration levels will allow an increase in WOB and rotary speed. Based on previous studies, these are the two of the most important parameters to ROP. Thus, these two new drillbit technologies might be able to increase ROP when drilling in salt.

Another goal for this thesis was to establish which parameters have the most effect on ROP when drilling in salt formations. Knowing this could help minimize the challenges faced due to salt creep and flow. Therefore, a modelling attempt was performed using Bourgoyne and Young's ROP model. This model uses multiple linear regressions to calculate a straight line that best fits the data used in the model. In this attempt, data acquired from a well drilled in salt formation was used. Due to lack of variation in the drilling data, several parameters had to be discarded from the model in order to obtain physically meaningful results. This led to only three variables being used in the model. This was weight on bit (WOB), rotary speed of the drillstring, and jet impact force. It was found that the parameter that had most effect on ROP in salt was WOB, followed by rotary speed, and last, jet impact force.

NORGES TEKNISK-NATURVITENSKAPELIGE UNIVERSITET

Abstrakt - Norsk

Fakultet for Ingeniørvitenskap og Teknologi

Institutt for Petroleumsteknologi og Anvendt Geofysikk

Master i Teknologi/Sivilingeniør

Boring i saltformasjoner og modellering av penetrasjonsrate

av Mats Håpnes

Ettersom industrialiseringen av verden vokser, er både energiforbruket og -etterspørselen stadig økende. Hydrokarboner har vært en viktig energikilde i flere tiår, men produksjonen fra modne olje- og gassprodusenter er nå avtagende. For å møte denne voksende energietterspørselen må nye hydrokarbonforekomster bli funnet og produsert. Ettersom store olje- og gassreservoarer er tilknyttet saltformasjoner, kan utvinning av hydrokarboner i disse områdene være en viktig energileverandør for fremtiden. Saltets lave permeabilitet og evne til å deformere under trykk og temperatur, gjør det til en ideell hydrokarbonfelle.

Et av målene med denne avhandlingen var å kartlegge hvilke utfordringer som kan oppstå ved boring etter pre-salt hydrokarboner, samt foreslå løsninger for hvordan disse kan overkommes. Ved boring etter disse olje- og gassreservoarene kan det oppstå problemer allerede i formasjonene over saltstrukturene. Tettheten av salt øker ikke med overdekningdybde. Når dens tetthet blir lavere enn de omkringliggende formasjoner, kan salt migrere og presse seg gjennom de overliggende bergartene. På grunn av den kombinerte effekten av ubalanse i kompasjon og salttektonikk, kan komplekse spenningsmønstre oppstå i formasjoner som omgir saltstrukturer. Dette kan føre til mange farlige situasjoner, forårsaket av soner med knust stein og foldede lagdelinger. Ved boring i saltformasjoner er det saltets evne til å flyte som kan forårsake problemer. Flytende salt kan føre til deformasjon

av borehullet, noe som kan vanskeliggjøre bore- og foringsrøroperasjoner. Når en brønn er boret kan salt flyte inn og erstatte det fjernede bergartsvolumet. Dette kan føre til situasjoner som fastklemt borestreng, hullustabilitet, og høye nivåer av støt og vibrasjoner under boring. Saltstrømming er positiv korrelert med tid, slik at minimering av tidsfaktoren vil redusere muligheten for saltstrømmingsrelaterte problemer. Ett av tiltakene for å minimalisere eksponeringstiden er å utføre boreoperasjoner raskt. Derfor er en høy penetrasjonsrate gunstig ved boring i salt.

Som et ledd i å foreslå løsninger på utfordringene ved boring i salt har to nye borekroneteknologier blitt evaluert. Disse kan være fordelaktige for å overkomme mange av utfordringene knyttet til boring i salt. Basert på resultatene oppnådd i tidligere studier, er disse borekronene i stand til å redusere støt- og vibrasjonsnivået under boring. Dette skyldes at disse borekronene er i stand til å bore jevnere enn konvensjonelle PDC-borekroner. Det reduserte støt- og vibrasjonsnivået tillater en økning i vekt på borekronen og rotasjonshastighet. Basert på tidligere studier er dette to av de viktigste parametrene til penetrasjonsraten. Derfor kan disse to nye borekroneteknologiene øke penetrasjonsraten ved boring i salt.

Et annet mål for denne avhandlingen var å avdekke hvilke parametere som har mest effekt på penetrasjonsraten ved boring i saltformasjoner. Kunnskap om dette kan bidra til å redusere utfordringene knyttet til saltflyt. Dette ble gjort ved å gjennomføre et modelleringsforsøk ved å benytte Bourgoyne og Youngs penetrasjonsratemodell. Denne modellen bruker flere lineære regresjoner for å beregne en rett linje som passer best til de dataene som brukes i modellen. I dette forsøket ble det benyttet data fra en brønn boret i saltformasjon. På grunn av manglende variasjon i boredataene måtte flere parametere forkastes fra modellen for å oppnå fysisk meningsfulle resultater. Dette førte til at kun tre variabler ble brukt i modellen. Disse var vekt på borekronen, rotasjonshastighet på borestrengen og stråleslagkraft. Parameteren som viste seg å ha størst påvirkning på penetrasjonsraten var vekt på borekronen, etterfulgt av rotasjonshastigheten og deretter stråleslagkraft.

Acknowledgements

I want to thank my supervisor John-Morten Godhavn for providing me with feedback, remarks and useful comment throughout my learning process of this master thesis.

I would also like to thank Espen Hauge for his assistance in this project.

Contents

List of Figures

List of Tables

Abbreviations

BHA	Bottomhole Assembly
BHP	Bottomhole Pressure
CDE	Conical Diamond Element
CPM	Cost per Meter
DEI	Diamond Enhanced Inserts
FIT	Formation Integrity Test
GoM	Gulf of Mexico
LOT	Leak off Test
LWD	Logging While Drilling
MWD	Measurement While Drilling
NPT	Non Productive Time
OECD	Organisation for Economic Co-operation and Development
PDC	Polycrystalline Diamond Compact
ppg	pounds per gallon
psi	pounds per square inch
ROP	Rate of Penetration
rpm	revolutions per minute
RSS	Rotary Steerable Systems
TD	Total Depth
TCI	Tungsten Carbide Insert
TVD	True Vertical Depth
UCS	Unconfined Compressive Strength
WBM	Water Based Mud
WOB	Weight on Bit

Symbols

$a_1 - a_8$	Coefficients in the penetration rate equation	-
D	Depth	ft
d_b	Bit diameter	inch
F_j	Hydraulic impact force beneath the bit	lbf
$f_1 - f_8$	Functions defining the effect of various drilling variables	-
g_p	Pore pressure gradient	lbm/gal
gpm	Gallons per minute	-
lbf	Pound force	-
lbm	Pound mass	-
ln	Natural logarithm	base e
log	Common logarithm	base 10
lpm	Liters per minute	-
q	Flow rate	gpm
$x_1 - x_8$	Effect of parameters on penetration rate	-
γ	bulk density	kg/m^3
$\bar{\gamma}$	mean bulk density	kg/m^3
σ	stress	Pascal
$\sigma_v, \sigma_{hmin}, \sigma_{HMAX}$	principal earth stresses	Pascal
ϕ	porosity	%

Dedicated to my girlfriend Ida Olivia for providing me with words of encouragement and support throughout the process. It is much appreciated.

Chapter 1

Introduction

The industrialization and electrification of non-OECD countries, especially China, has increased the worlds energy consumption with 2,2 % per annum from 2005 to 2014 [1]. Even though this phase of high energy consumption growth draws to a close, the prediction is that the primary energy demand will increase by 41 % between 2012 and 2035, with an average growth of 1,5 % per annum, as seen in Figure 1.1. All energy sources have to be increased to meet the energy demand. Figure 1.2 shows the predicted energy source growth in the decades to come. It can be calculated from this figure that the growth for oil and gas is 0,8 and 1,9 % per annum, respectively. Since production in mature oil and gas provinces are declining, new and challenging reserves such as pre-salt oil and gas, have to be discovered and produced in order to meet this increasing energy demand.

The oil industry discovered in the 1990's that vast hydrocarbon reserves could be found beyond the continental shelves, and under thousands of meter of water. When exploring these pay zones, engineers were faced with a foreign operating environment. The discovery that these pay zones were covered by immense, thick sheets of salt made this effort intimidating, as this required new and innovative solutions in order to reach the hydrocarbon reserve's [2]. Drilling these formations were considered to be full of risks. Therefore, it was agreed that the best way of dealing with salt interval was to avoid them all along. However, new technologies have been developed, allowing safer drilling in salt. Over the next decade, a significant amount of exploration and field developments will take place in the salt provinces around the world [3]. Salt is essentially impermeable and are excellent traps for hydrocarbons. Large oil and gas reservoirs are, therefore, associated with

salt structures. These are found, among others, in the Gulf of Mexico, the North Sea, Iran, offshore Brazil and West Africa, and in Kazakhstan [4].

Several challenges arise when drilling in salt formations. Unlike the adjacent formations, when buried, salt maintains its density. Due to gravity, salt will start to migrate upwards when its density becomes lower than the surrounding rocks, creating rubble zones around the salt. Well control is challenging as predicting pore pressure, fracture gradients and the existence of fractures is difficult. Shock and vibration levels have also proven to cause problems in these formations.

The most pronounced characteristic of salt is its ability to creep under isovolumetric conditions, when subjected to any differential stress [3]. This can lead to undergauge hole conditions when drilling, since salt will flow into the wellbore and thereby replacing the volume removed by the drillbit [2]. This may occur quickly, especially at high temperatures, therefore, the ROP is important when drilling in salt formations. If the well can be drilled in a short amount of time, this minimizes risk of borehole closure due to salt creep. Being able to establish which parameters affect ROP most when drilling in salt, would be huge a benefit.

The motivation for this thesis is to describe the challenges that are associated with drilling for pre-salt hydrocarbons, and give a better understanding for how to overcome these challenges. In addition, an attempt is made in order to find out which parameters have the most effect on ROP when drilling in these formations. This is done by modelling the ROP, using data from a deepwater salt well, in combination with Bourgoyne and Young's ROP model. This may help contribute to safer and more efficient drilling in salt formations.
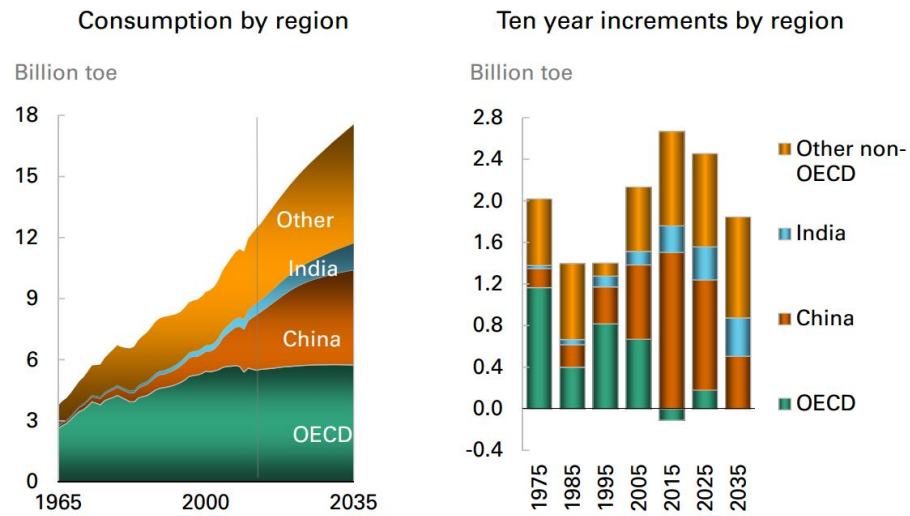
FIGURE 1.1: Predicted energy outlook towards year 2035 [1].
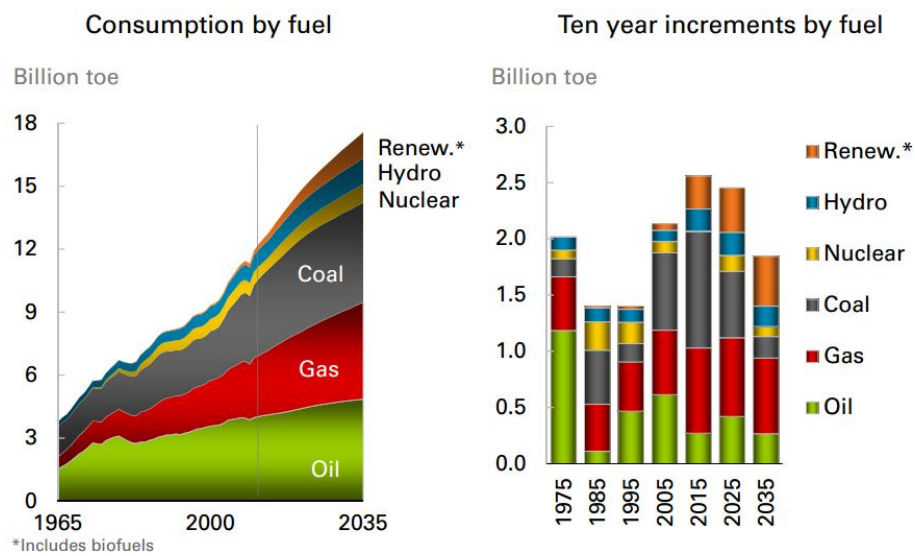
FIGURE 1.2: Fuel growth over the forecast period[1].

Chapter 2

Background Theory

This chapter will present general information regarding salt, how salt formations and salt domes arise, and about drilling in salt. This is to provide the reader a basic knowledge regarding these topics before more detailed information is presented in later chapters.

2.1 Origin and Characteristics of Salt

Drilling in, and through salt was for a long period avoided due to the challenges that was present when drilling these formations. However, large oil and gas reservoirs are associated with salt structures. This, combined with the predictions that all the "easy oil" has been found [5], are drivers for salt drilling. In the recent years and over the next decade, a substantial amount of new field developments and exploration will take place in salt structures all over the world.

Salt structures can be found in several locations around the world, see Figure 2.1. Exploration oil and gas drilling are especially targeting the domal structures in the Gulf of Mexico, Williston basin, the North Sea, Iran, and Brazilian and West African offshore basins. Sub-salt resources are found in the GoM salt tongue regions, in large areas in Kazakhstan (Kashagan and Tengiz), and in other areas [4].

Salt deposits are created by gradual evaporation and desiccation of salt water that has been confined, similar to the salt flats at Great Salt Lake of Utah, USA today. There exists several types of salt, depending on their chemical composition. The

most ordinary salt is halite, *NaCl*. Other salts and minerals often associated with salt deposits are:

- Sodiums: principally halite ($NaCl$).

- Sulphates: gypsum ($CaSO_4 \cdot 2(H_2O)$) and anhydrite ($CaSO_4$).

- Potassium salts: sylvite (KCl), carnalite ($KMgCl_3 \cdot 6H_2O$), and polyhalite ($K_2Ca_2Mg(SO_4)_4$)

- Other less known salts include:

    - Chlorides: bischofite ($MgCl_2 \cdot 6(H_2O)$) and tachyhydrite ($CaMg_2Cl_6 \cdot 12(H_2O)$)

    - Sulphates: langbeinite ($K_2Mg_2(SO_4)_3$), kieserite ($MgSO_4 \cdot (H_2O)$) and epsomite ($MgSO_4 \cdot 7(H_2O)$)

    - Potassium halide: kainite ($K_4Mg_4Cl_4(SO_4)_4 \cdot 11(H_2O)$)
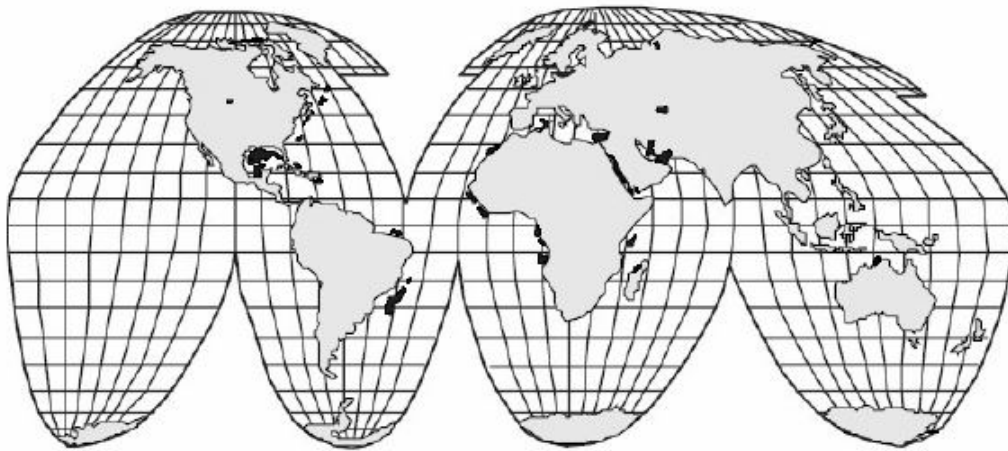
FIGURE 2.1: Major global salt deposits, indicated by black shaded areas [3].

Salt can creep and/or deform. This ability is one of the unique and problematic characteristics of salt. It is believed that this ability is because salt does not increase in density with burial depth [6]. When layers of sediments are deposited on top of salt and begins to compact, eventually a critical depth is reached where the density of the overburden becomes equal to the density of the salt. At this point, salt flow begins [7]. Given long enough time, this salt flow can result in characteristic salt structures, including nappies, domes, sheet and canopies. Salt that

has migrated from its originally deposited location is referred to as *allochthonous salt.* The creep rate is dependent on several factors, including (1) temperature, (2) differential stress, (3) confining pressure, (4) grain size, and (5) presence of inclusions of free water or free gas bubbles [8]. Temperature and stress differentials are the main drivers for salt creep.

As seen in Figure 2.2, if the temperature is increased, this will cause the creep rate to increase. The creep rate increases abruptly for temperatures from 200 to 400°F ($\approx$ 93,3 to 204,4°C). If the temperature exceeds 400°F, salt becomes almost completely plastic and will flow readily if differential pressure is applied [8]. Drilling long salt sections differ from drilling other geological formations due to these unique properties. These differences include (1) wellbore stability, (2) drilling fluids, (3) cementing, (4) casing design, and (5) directional control.

As mentioned earlier, salts ability to creep under isovolumetric conditions when subjected to any differential stress is its most pronounced feature [7]. This behavior may cause undergauge hole conditions when drilling. In addition, it leads to salt diapirs. Salts time-dependent response to an enforced stress difference can be divided into steady-state (long term) and transient (early time) responses [7].

Even though the deformation and strength properties of salt are believed to be affected by impurities and salt chemistry [7], creep testing on several different high-purity halite salts shows a reasonable consistency in creep rates, see Figure 2.3.
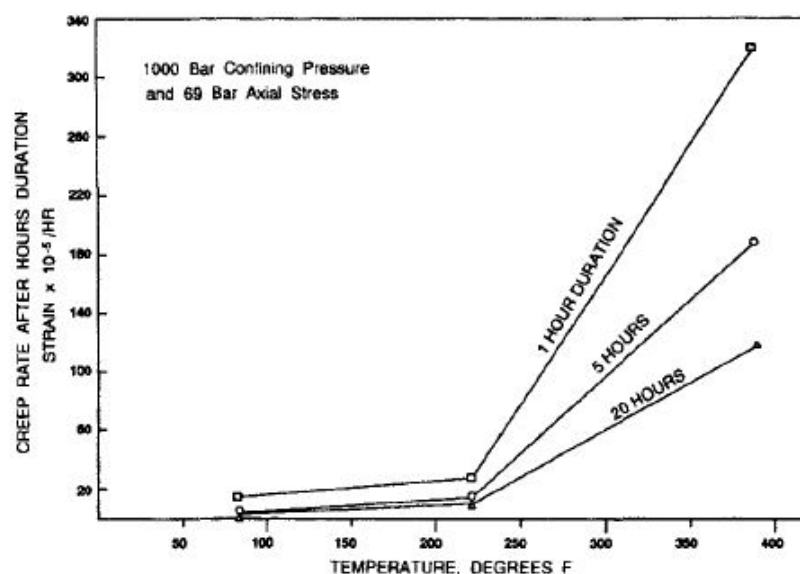
FIGURE 2.2: The effect of temperature on salt-creep rate [8].
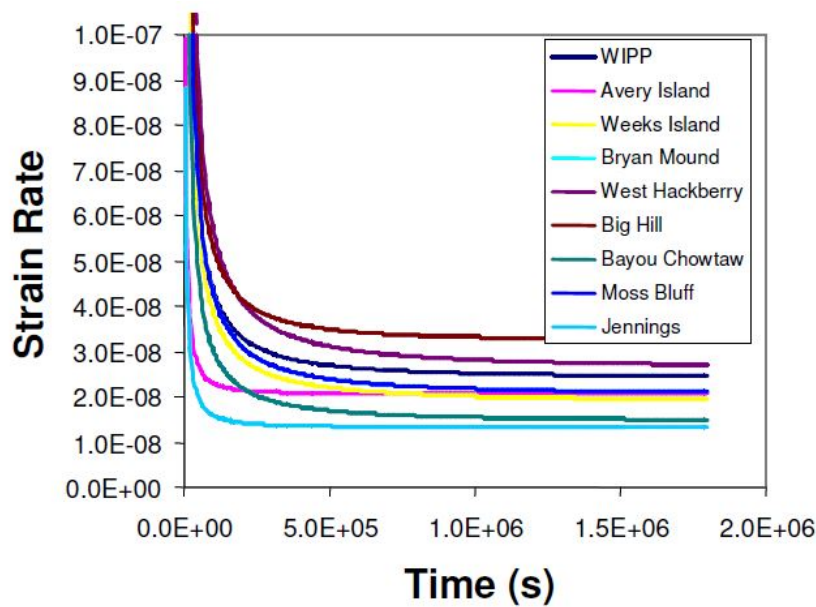
FIGURE 2.3: Comparison of creep rates for New Mexico and Louisiana high purity halite salts [3].

Salt is known for having a relatively low unconfined compressive strength (UCS). Willson and Fredrich [3] reported the UCS for salt in the range between 3000 to 3500 psi. Even though the UCS is relatively low for salt, a substantially higher torque and WOB are required when drilling these formations, compared to other formations with similar UCS. The reason for this need of extra energy is due to the plastic nature of the salt and its ability to creep into the newly drilled wellbore. The two mentioned reasons represent some of the biggest challenges to drillers.

Depending on the purity, the *in-situ* salt density usually averages around $\approx$ 2,10 g/cm^3. In very pure salt, e.g. the salt found along the US gulf coast, which consists of 97 % halite, the density is 2,17 g/cm^3 [8].

2.1.1 *In-Situ* Conditions

Stresses and Temperatures: The typical geothermal gradient for sedimentary basins is in the order of 20 - 25°C/km, but this will vary with geographic location. E.g. in the deep waters of GoM, these temperature gradients are in the order of 15°C/km, while there are cases in the North Sea where gradients within salt have approached 38°C/km [9].

It is assumed and confirmed through leak of tests[1] (LOT) and formation integrity tests[2] (FIT), that $\sigma_v = \sigma_{HMAX} = \sigma_{hmin} = \bar{\gamma} \cdot z$, where $\bar{\gamma}$ is the mean overburden bulk density. Isotropic stresses are only found in very soft muds and in viscous rocks, hence the *in-situ* stresses in frictional materials (such as shale, sandstone and limestone) are always differing. Since salt can be seen as a viscous fluid, underbalance occurs when the mud pressure in the borehole is lower than the vertical stress, $p_b < \sigma_v$.

Permeability and Pore Pressures: When salt is under stress, it continues to compact, displacing brine, until the porosity is totally occluded ($\phi < 2 - 4$ %). If the temperature and the stresses are high, the compaction will continue until only a brine filled porosity of 0,3 to 1,5 % remains. The remaining porosity consists of thin, dendritic voids at the grain boundary's [9]. Flow through salt only occurs in non-salt lithologies or through introduced flaws, when viewed in an engineering time scale (< 100 years). Filter cakes do not form in salt, hence 100 % of the mud pressure acts on the salt wall. This is also assumed for rocks where the pores are filled up with precipitated salt since there is no inter-communicating flow path. The concept of pressure as a state descriptor is therefore, in these cases not useful.

2.2 Salt Domes

A *salt dome* is a large geological structure that is located subsurface [10]. It is a vertical cylinder of salt, with a diameter larger than 1000 meters, which is embedded in horizontal or inclined strata. The salt consists of mainly halite, but other evaporates as well. The term *salt dome* includes both the core of salt and the surrounding strata, which is domed by the salt core. *Salt pillows* and *salt walls* are other geological structures where salt is the main component. These are genetically related to salt domes and *salt anticlines*, which basically are rocks that have been folded by upward migrating salt. Gypsum and shale form the cores of similar geologic structures. All these structures, including salt domes, are known as *diapiric structures*, or *diapirs*, from the Greek word diapeirein, which means "to pierce." The common denominator in all instances is that the embedded material

---

[1]A test to determine the fracture pressure of the formation and shoe, by increasing the bottomhole pressure (BHP) until the formation breaks down.

[2]A method for determining the formation and shoe strength by increasing the BHP to designed pressure

has pierced the surrounding rocks. The factors that cause the upward flow are believed to be [10]:

1. **Gravitational Forces**
   When light rocks are overlain by heavier rocks, the lighter rocks will rise towards the surface.

2. **Tectonic forces (earth-deformation)**
   A mobile material is squeezed by lateral stress through a less mobile material.

3. **A combination of both gravitational and tectonic forces**

The interrelationship of salt structures, including salt domes are presented diagrammatically in Figure 2.4. Gravitational stress alone is enough to develop the "classic" salt dome from bedded salt. Salt domes may, in addition, be developed from salt walls and salt anticlines as a base. The formation of salt domes from salt anticlines is a result from the superposition of gravitational stress on salt masses that initially developed due to tectonic stress.
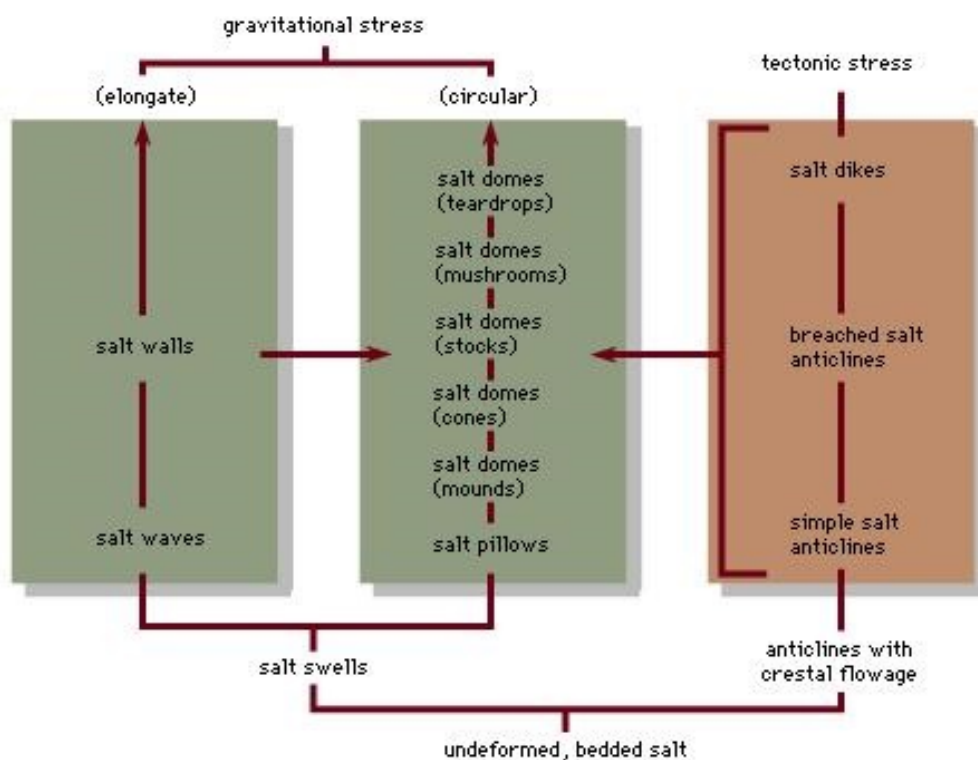
FIGURE 2.4: The interrelationship of salt structures, including salt domes [10].
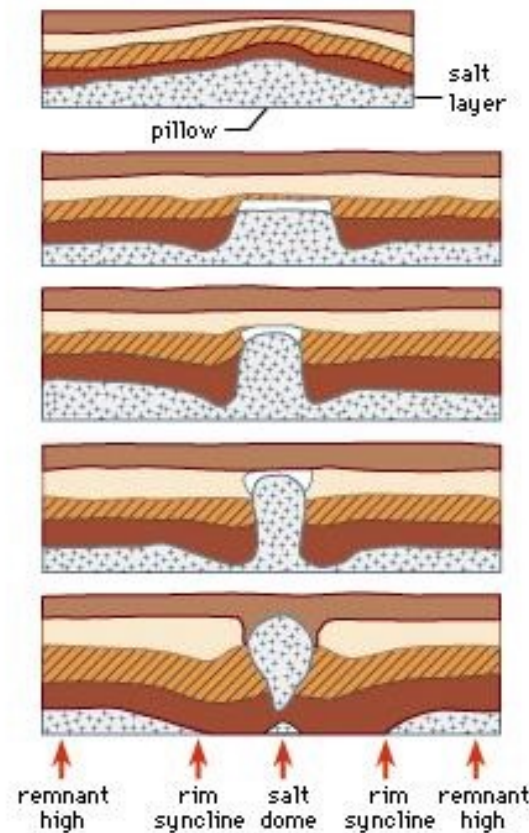
FIGURE 2.5: The development of salt domes [10].

2.2.1 Physical Characteristics of Salt Domes

A salt dome is basically a core of salt and an envelope of surrounding strata. Sometimes the salt core contains a *cap rock* in addition to salt. A cap rock is a layer of hard impervious rock, which may sheath the salt core, and in many cases provide a seal for oil, gas, or coal. The size of a salt dome varies substantially [10]. Most often the diameter is larger than a kilometer, and it may be above 10 km. The typical salt dome is at least 2 km high in the subsurface, and some are known to be higher than 10 km.

The content of salt domes varies. In the North American Gulf Coast, the cores of the salt domes consist virtually of pure halite (sodium chloride) with small amounts of anhydrite (calcium sulfate) and traces of other minerals. Here layers of black halite and anhydrite are interbedded with layers of pure white halite. In Germany, the salt dome cores consist of halite, sylvite, and other potash minerals. In the Iranian salt domes, halite, anhydrite and marl (argillaceous limestone) are mixed together with large blocks of limestone and igneous rock.

In interbedded salt-anhydrite and salt-potash the layers are complexly folded. The folds are vertical and more complex in the outer edge of the salt. From studies performed in German domes, it has been determined that the older material is generally in the center of the salt core, and the younger material is located at the edges. Another study of halite grains in some of the Gulf Coast salt domes indicates a complex pattern of orientation that varies both horizontally and vertically in the domes. E.g. in a Caspian salt dome, the mineral grains at the edges are horizontal, while the grains in the center are vertical.

A cap rock is a cap of limestone-anhydrite ranging from 0 to 300 m thick. The cap is often divided into three zones, more or less horizontally. These zones are an upper calcite zone, a middle transitional zone characterized by the presence of gypsum and sulfur, and a lower anhydrite zone. These zones are irregular and are generally gradational with each other. The contact between gypsum and anhydrite can, occasionally, be quite abrupt. It is believed that the cap rock is created from solution of salt from the top of the salt core, which leaves a residue of insoluble anhydrite [10]. This is again altered to gypsum, calcite, and sulfur. It is assumed that solution happens in the circulating and shallow-water zone. All known deeply buried salt domes with a cap rock have once been shallow and then subsequently buried.

In the Gulf Coast salt domes, a common feature is the shale sheath. The shape of these shale sheaths may completely encase the salt, like a sheath. It may also be limited to the lower portions of the salt. Shale sheaths are most common in the deeper portions of salt domes whose tops are near the surface or on deeply buried salt domes. The fluid pressure within the shale is significantly higher compared to the surrounding rocks. In addition, the stratification (bedding planes) of the shale is distorted. It is indicated from the fossils found in the shale, which is older than the surrounding sediments, which the shale comes from an older, and therefore, deeper layer.

There are three ways that the strata around salt cores can be affected. It can (1) be lifted up, (2) lowered, or (3) it can be unaffected while the surrounding strata subsides relatively. When the strata has been uplifted, it has the structural features of domes or anticlines. Characteristically the strata (including cap and sheath if present) is domed around or over (or both) the core and dip down into the surrounding synclines. When the strata is domed around circular domes, it is generally broken by faults that radiate out from the salt. These faults may be more

linear on elongated domes or anticlines with one fault or set of faults predominant. Lowered strata develop into synclines and a rim syncline may fully or partially encircle the domal uplift. Unaffected strata develops into highs surrounded by low areas. These heights are called turtleback highs or remnant highs. The vertical relief is smaller in these highs compared to the salt domes among which they are interspersed. In some instances, the present-day structure of strata around salt domes does not coincide with the position of the salt. The explanation for this offset relationship is that the center of the salt dome has been shifted somewhere between the late and the early uplift.

2.2.2 Origin of Salt Domes

Folded salt structures have in general been associated with the same forces that caused the folding. Salt structures, including diapiric or piercement structures, develop as a result of gravitational forces, tectonic forces, or a combination of these forces [10]. These forces can happen at the same time or where one force follows the other. Regardless of the force, for a diapiric structure to develop, it is required that there is a rock that can flow.

Even though rock flow rate is small, the results of it can clearly be seen in (1) stonework that sags, (2) mine and tunnel openings that flow shut, (3) and glaciers of rock salt that move down mountainsides like an ice glacier. Because of relatively high pressure and temperature due to burial depth, considerable movement of plastic material can occur, given very long periods of time. E.g. if a salt moves with one millimeter a year, over a period of one million years, that equals a net movement of 1000 meters. Halite, sylvite, gypsum, and high-pressure shale are some of the most common rocks that are able to flow. In addition, these rocks have lower densities than consolidated rock, such as sandstone. Therefore, if buried by sandstone, these rocks would be gravitationally unstable. These are all deposited by normal processes of sedimentation and are widespread in sedimentary strata.

Through studies of models and natural salt structures, the sequence of events in the development of salt domes has been reconstructed, see Figure 2.5. To start with, salt is deposited and buried by denser sedimentary strata. After some time, the salt and overlying strata turns unstable and the salt begins to flow from an undeformed bed to a rounded salt pillow. The overlying strata becomes domed when the flow continues into the center of the pillow. A rim syncline is formed

at the same time since the area from which the salt flowed subsides. The strata overlying the salts are subjected to tension, and fractures develop. Eventually, when the overlying strata has been spread apart, the salt breaks through the center of the vaulted area. This creates a plug-shaped salt mass in the center of the domed, upturned, and pierced strata. The upward growth of the salt continues apace with additional deposition of strata. Therefore, the position of the salt mass is maintained near or at the surface. If the deposition of salt stops during the dome growth, the development will cease and the dome will maintain whatever stage it has reached, and the dome is buried [10].

2.2.3 Distribution of Salt Structures

Salt structures can be developed in any aqueous basin where salt deposits later have been overlaid with thick sedimentary strata, or tectonically deformed, or both. Salt structures are widespread, except for the shield areas. Salt domes generated by gravitational instability alone are limited to areas where there has not been any architectonic stress. However, some salt domes occur in areas that have been subjected to tectonic stress. The largest areas of salt structures in the world are (1) the Gulf of Mexico region of North America, (2) the North German-North Sea area of Europe, and (3) the Iraq-Iran-Arabian Peninsula of the Middle East.

2.2.4 Economic Significance of Salt Domes

The geometrical shape of salt domes makes them excellent traps for hydrocarbons, because the surrounding sedimentary strata has been domed upwards and blocked off. In the domes of Mexico, the United States, Germany, the North Sea, and Romania, large accumulations of oil and natural gas occur. In the salt dome areas off the coast of Louisiana, huge supplies of oil have been found. In this region, some individual salt domes are believed to contain more than 500.000.000 barrels of oil. The salt domes in the Gulf Coastal Plain of Texas and Louisiana will be an important source of hydrocarbons in the United States for many years to come. The salt domes in the northern part of Germany have produced oil for several years, and in the North Sea exploration for salt dome oil has extended production offshore.

In addition to being good traps for hydrocarbons, salt domes are a major source of salt and potash in the Gulf Coast and in Germany. Large quantities of sulfur can be found in the cap rock of shallow salt domes in the Gulf Coast. Other sources that can be extracted from domes by underground mining and by brine recovery are halite and sylvite.

Another usage of salt domes is storage of liquefied propane gas. This is done by drilling into the salt and forming a cavity by subsequent solution [10]. Cavities like these have been considered as sites for disposal of radioactive wastes.

2.3 Drilling in Salt

2.3.1 Wellbore Stability

It is normal for the vertical *in-situ* stress in a typical sand/shale formation to be the same as the overburden stress and that the horizontal stress is slightly less than the vertical stress. In salt the *in-situ* stress is assumed to be identical in all directions and equal to the weight of the overburden stress. When drilling, if the hydrostatic pressure from the mud is lower than the salt stress, then salt will begin to creep into the wellbore. When temperature and differential pressure between the salt stress and the mud weight hydrostatic pressure is increased, the salt creep rate is increased. This is rarely a problem at shallow depths, but at greater depths this will result in increased creep rate. If salt starts to creep into the wellbore, this can reduce the wellbore radius, causing an undergauge hole, which can lead to stuck pipe and casing collapse loading [8].

Leyendecker and Murray developed in 1975 a widely used guideline for determining the mud weight needed to prevent and control salt creep. This guideline is presented in Figure 2.6. The curves in this figure were developed based on static plastic theory with finite-element techniques [11]. Since these curves are for specific downhole conditions of stress, temperature, and creep rate, Barker, Feland, and Tsao developed a simple analytical equation for determining mud weights to control salt creep [8]. This equation allows calculations at different stress, temperature, and closure-rate combinations. The equation is based on steady-state creep of salt formations. The wellbore radius after salt creep is given by

$$r = \frac{r_0}{\exp^{(\Delta\ t)(\frac{3\gamma}{4n-2})(A)(\exp^{-\frac{B}{T}})(\sigma_\infty - p)^n}}$$ (2.1)

where $\gamma = (n+1)/2$.
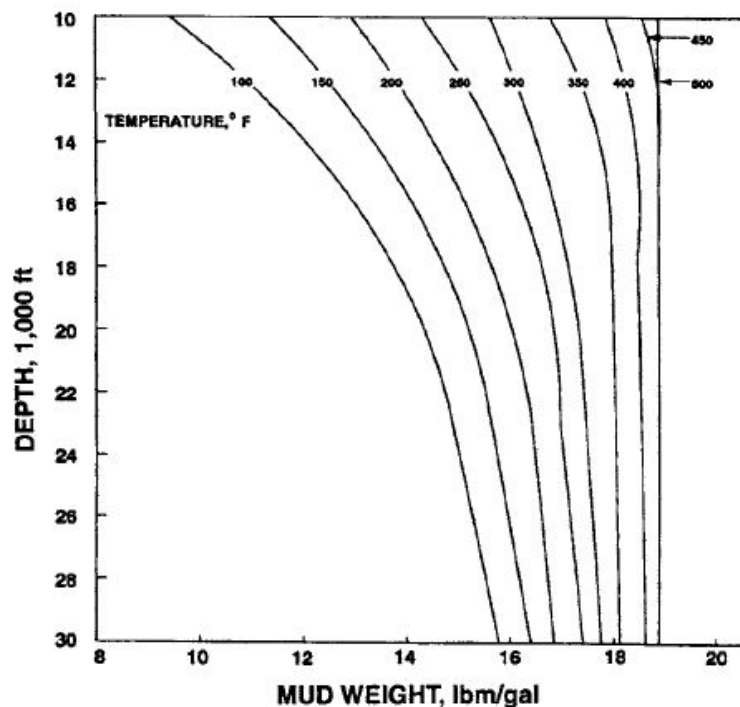
FIGURE 2.6: The mud weight required for 0,1%/hr area closure at various temperatures [11].

2.3.2   Drilling Fluids

When drilling in salt sections, there are two types of water based muds that can be used, in addition to oil based muds. For long salt sections usually a water-based mud is used, which will integrate either a low or a high concentration of salt. It is very difficult to match the formation salt dissolution and erosion, with wellbore creep, using a low-salt mud. This is due to the large difference in salt creep and dissolution rate between the top and bottom of a long salt section. This results in an erratic wellbore diameter with depth. By using highly salt saturated water based mud or an oil-based mud the dissolution of salt during drilling can be controlled.

Hole enlargement can be a problem even though a highly salt saturated mud is used. This is because of the effect temperature has on salt solubility. Cold salt saturated mud is pumped downhole when drilling. The bottomhole temperature will heat up this mud and the mud then becomes undersaturated. As this mud returns up the annulus[3], it dissolves formation salt and thereby increasing the wellbore diameter. When this mud reaches the surface, the lower temperature will cause excess salt to precipitate out. This process will repeat itself when the mud is circulated. In order to overcome this problem, several inhibitors have been created to supersaturate salt muds even at low temperatures. Another solution to this problem is to heat up the mud at the surface to maintain a saturated mud at all times during circulation [12].

The problem of hole enlargement from dissolution can be eliminated by using oil based mud. However, using oil based muds will increase reaming time, and there is an increased chance for minor stuck pipe incidents in the resulting gauge hole. Pumping freshwater pills have proven successful in order to free a drill string stuck in salt, but this requires careful planning and implementation.

2.3.3 Cementing

One of the most important aspects of drilling long salt sections successfully is effective cementing of casing. Cementing is a very important factor in preventing unequal loads on casing that can lead to casing collapse, and to achieve good zonal isolation. If there is poor cement displacement in zones of hole enlargement that could lead to non-uniform salt loading and casing deformation and collapse.

Cementing casing strings across large salt formations can be a challenge. It is important to use cement slurries that are salt saturated in order to prevent salt dissolution. However, high salt concentration makes mixing these slurries difficult and can over-retard the cement. Additives for fluid loss control and dispersants are also required. To avoid over-retarded cement, salt free cements and semi-saturated cements has been used to cement casing's opposite massive salt sections. There exists a concern that the low salt cement used will lose strength over time [13]. Cement failure may occur eventually due to the ion exchange between calcium and magnesium found in brines.

---

[3]An annulus is the ring-shaped void space bound by two concentric circles

Grant, Dodd and Gardner [14] suggested using a small concentration of *KCl* in the cement in order to provide a degree of salinity balance between a salt formation and low salt cement. This cement mixture has been proved successful for cementing casing across salt formations in several field applications, when combined with controlled fluid loss and free water. Special additives have been developed, in the late 1980s, to eliminate the disadvantages when using highly salted cements [12]. The problem of over-retardation and compressive strength development has been solved by using specific fluid loss additives and dispersants for salt cement slurries.

2.3.4 Casing Design

In extended salt sections, one of the most frequent causes of wellbore losses is casing deformation and collapse. Normally, when designing casing through long salt sections, it is assumed that the casing is empty inside (there is no pressure acting inside the casing). Further, it is assumed that the external hydrostatic pressure gradient is equal to the overburden stress [15]. Although this method has been successful in the gulf basin, often hole washouts and poor cement displacement in the salt formation cause unusual, non-uniform loading that is difficult to predict and to quantify. To overcome this problem, several modifications have been proposed to the traditional salt casing design [16] [17]. These are:

- Increase the pipe thickness instead of the pipe grade, in order to increase collapse resistance.

- The resistance to non-uniform loading and the radial deformation of the pipe is decreased when applying a uniform load on a single pipe subjected to non-uniform loading. This will again decrease the chance of getting equipment stuck inside the casing.

- If uniform and non-uniform loading is combined, the systems resistance to non-uniform loading is increased. This will also decrease the radial deformation of the inner pipe.

2.3.5 Directional Control

Salt is a relatively soft material. Due to this, drilling by scraping action is considered being the best. This occurs, among others, when using polycrystalline bits.

Conventional rock bits can also be used. Several thousands of feet of salt have been drilled with traditional rock bits. In addition, side-cutting reamers or mills above the bit and eccentric or bi-centered bits have been used to drill salt. By using these bits and assemblies a reduction in wellbore radius can be permitted from its drilled radius, and therefore, will not result in an undergauge hole.

It can be difficult to obtain directional control while drilling long salt sections because usually the wellbore radius is either enlarged or undergauge. When undersaturated mud is used, this will often result in hole enlargement on the low side of the wellbore. This will again make building and maintaining the wellbore angle difficult. This becomes especially observable when entering a salt dome with a slight wellbore angle using undersaturated salt mud. Dissolution can create a hole enlargement in the top of the salt which will allow the wellbore to drop quickly to vertical. This will create ledges and a substantial dogleg that can result in huge problems.

When drilling salt with conventional directional drilling bottomhole assemblies (BHA), creep of salt or ledges formed can often lead to stabilizer hang-up. In order to drill directional wells successfully in salt, the use of oriented, hydraulic, positive displacement motors with either undergauge or no stabilizers may be required. This will be discussed in further detail later in this paper.

Chapter 3

Geomechanical Considerations for Salt Drilling

In this chapter potential geomechanical and pore pressure-related risks are presented. It will give the reader detailed knowledge regarding the challenges that are presented when drilling in and around salt. This knowledge may help ensure successful well constructions in these formations.

3.1 Through-, Sub- and Near-Salt Drilling Hazards

Drilling within or close to salt present several drilling hazards that can occur, as shown in Figure 3.1. The occurrences of these hazards are dependent upon the movement of the salt body relative to the lithification state of the adjacent sediments [3].

Area of tectonic instability: Toe-thrusts outboard of a salt upwelling can give rise to a local stress regime different from the stresses acting generally on the basin. This can happen where active lateral salt deformation is occurring. Here, where the minimum horizontal stress will be near the overburden stress and the maximum horizontal stress will surpass the overburden stress, thrust faulting stress regimes can occur. In these areas, wellbore instability can be a problem. Figure 3.2 shows a generalized view of the stress regimes around a salt dome that has pushed

outwards against the surrounding rock in all directions. The magnitude of plastic deformations imposed on the country rock determines the extent of these stress regimes and the magnitudes of the stress contrast. This is due to the elastoplastic nature of the faulting processes [9].

Rubble zone: Depending on the geometry of the salt body, rubble zones may be created *in-situ* if the neighboring rock is not able to withstand the imposed stressed developed from salt emplacement or fluid migration. There are two scenarios where this can happen. The first is that the total stresses can be undisturbed, but elevated, and pore pressure increase can cause rock failure by reducing the minimum effective stress. This is typical for structural "highs" or inverted bowls in the base salt topography, and in drillout conditions where the pore pressure is high and there is a small pore-fracture window. The second cause of rubble zones is when the salt body interferes with the near salt stresses. This leads to a difference in the horizontal stresses or can boost the shear stress enough to cause rock failure *in-situ* [18].

"Invisible" salt wing with trapped pressure: Areas of high trapped pore pressure can arise around the edges of the salt, where there can be restricted dewatering pathways, or in the areas of creation of structural highs. Large pore pressure differentials can also occur in *salt welds* due to its excellent sealing ability. In addition, these wings may be hard to recognize from seismic before drilling because of the poor seismic resolution around salts.

Tar bands: The main problem that is associated with *tar* is the difficulty in keeping an open borehole. Often, when running of casing, the hole can be fully plugged with tar, causing the casing to be stuck in this "sticky" material even though under-reaming is employed while drilling. It is believed that tar migrates up fractures associated with salt movement. Tar thickness above 35 meters has been encountered. It is speculated that tar bodies of this size once flowed over the sea bed and were later buried by sediments and the rising salt body [19].

Major sub-salt pressure regression: When exiting salt, in order to control salt creep in through-salt sections, mud weight may have to be increased to the next (sub-salt) casing setting depth level. Reducing the pore pressure, in a major sub-salt regression case, could give rise to a differential sticking problem if there are permeable formations below the salt. Loss situations may occur when the fracture gradients are reduced, if the reversing pore pressure is not diagnosed in real-time

monitoring operations. When these situations are encountered, the recommended solution is to set casing prior to exiting salt.

Recumbent or overturned beds: Salt bodies undergoing large lateral movement can create complex near salt sediment deformation. These movements can make nearby formations overturned and highly fractured and faulted. This may again lead to losses, rubble zones, and high stresses causing wellbore instability.

Base salt depth error: One of the biggest challenges to sub-salt well design is the velocity uncertainty in the sub-salt regime, that leads to uncertainty in the sub-salt pore pressure. E.g. if it is a 12 % error in the velocity, this could lead to a 1,5 ppg uncertainty in the estimated pore pressure [3]. These uncertainties may, in addition, affect the salt base depth prediction, leading to uncertainty in casing setting depth.

Salt gouge at low effective stress: Zones of elevated lateral shear can create a gouge zone of plasticized sediment where there exists large amounts of relative displacement between the base salt and the close by formation. In these sediments, the pore pressure can be high, and almost equal to the overburden. Due to the high deformation rate into the borehole when drilled with an underbalanced mud weight, these sediments can cause tight hole or stuck pipe situations. Casing deformation can, in extreme cases, be a problem caused by these formations.

Dirty salts causing tight hole conditions: High gamma-ray reading is an indication of dirty salts, due to their content of sylvite, polyhalite and carnallite, which are radioactive potassium salts. When these salts are encountered the chances for tight hole conditions is increased.

High pressure associated with seams or inclusions: Pressure traps may exist inside the salt in terms of rafts of fractured dolomite, or included shales that can cause a *kick*[1] while drilling. There have been recorded water kicks as high as 18 ppg in the Plattendolomit interbedded salt/dolomite formation in the Southern North Sea. Even though these flow volumes usually are relatively small, they can cause well control problems. When planning a well through salt sections, suture zones should be a cause for concern. If sutures can be identified from seismic, it is recommended to set casing so that high mud weights can be used to counteract any influxes or creeping sediments.

---

[1]A kick is when formation fluids flow into the wellbore during drilling operations. This can occur when the pressure in the formation fluids exceeds the wellbore pressure.

Mud loss in highly fractured carapace facies: A rising salt body may carry older, more lithified sediments upwards with it. When these sediments that previously have been under high pressure and *in-situ* stresses get "depressurized," they may become fractured and can lead to losses. Losses can additionally be promoted by extension zones in sediments overlying the salt which has been laterally displaced, due to relatively low horizontal stresses. Difficulties with lost circulation can be an issue where salt is encountered at great depths. This is due to the faulted sediments at the top of the salt.

Overpressured sediments in carapace/rafted sediments: Older rafted sediment that have been brought upwards by salt diapirism is associated with overpressure in carapace formations. The rate at which salt rise may outpace the ability of these rafted sediments to dewater (disregarding fracturing). This may result in a residual component of higher pore pressure in these sediments. If the salt deformation rate has increased in recent times, then there might be a possibility that the newer sediments over the salt could exhibit more modest relative overpressure. In these areas tight-hole and *gumbo*[2] shale behavior may prevail.

High temperature salt loads casing: The deformation rate of salt (creep rate) is governed by the temperature of the salt, and the stress differences between the overburden stress and the borehole hydrostatic pressure. High salt temperatures increases deformation rate. E.g. in a deepwater GoM well where the top of salt was at approximately 2770 mTVD.SS with a temperature of 48°C, and the base salt was at 5800 mTVD.SS with a temperature of 93°C. If this salt section were drilled using a mud weight equivalent to a fixed pressure differential below the overburden, then the creep rate at the bottom of the hole would be expected to be one-hundred times faster due to temperature effects alone. In situations like this, tight hole conditions when drilling, and casing loading over the well lifetime are important aspects of the well design and construction process.

Trapped sediment on salt seams: The pore pressure in sediments trapped on salt seams may be high, and the sediment itself can be highly plasticized. To be able to withstand the squeezing tendency of the formation when drilling these suture zones, mud weights greater than 90% of the overburden is required.

---

[2]Gumbo is a generic term for soft, sticky, and swelling clay formations.

Salt shear zones: Salt shear zones may exist due to the coalescence of salt bodies, or as a consequence of faulting of sub-salt formations [3]. A typical risk associated with these shear zones is deformable zones with high pressure.
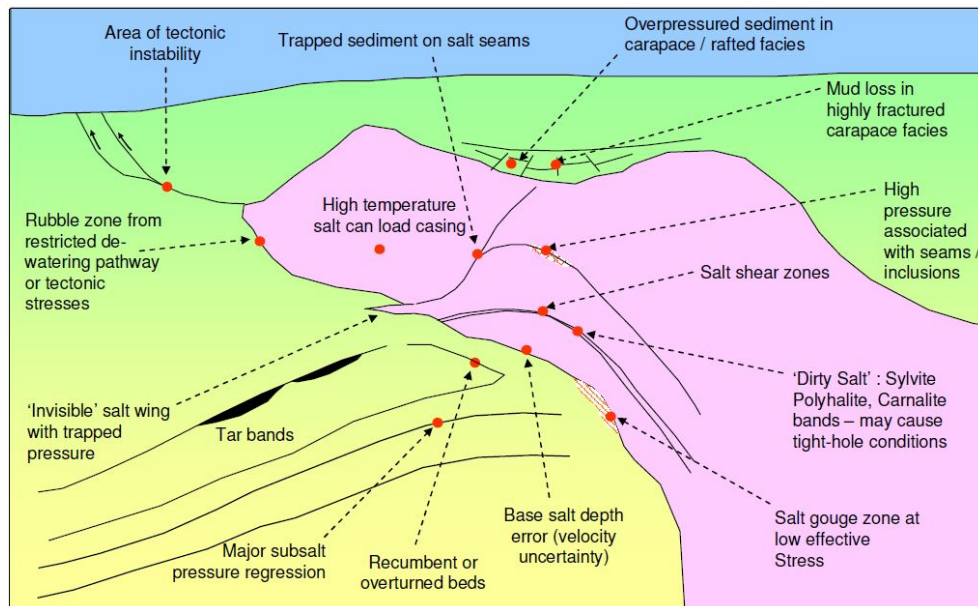
FIGURE 3.1: Schematic of potential through, and near-salt geomechanical hazards [3].
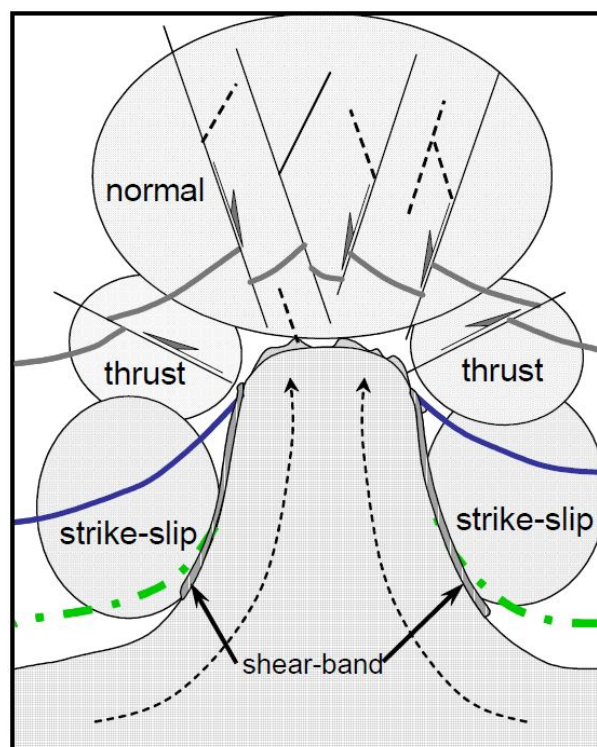
FIGURE 3.2: Generalized stress regimes around a salt dome [9].

3.2 Deformation Styles Adjacent to Salt

Understanding the mechanics of deformation of sediments near salt, in addition with clarifying the rate of sediment lithification relative to diapirism, is important to identifying geomechanical risks adjacent to salt.

3.2.1 Diapirism and the Down-Building of Sediments

It is the style of diapirism that controls sediment deformation adjacent to salt. There are two processes involved, (1) where salt pierces overlying sediments, and (2) where sediment down-building and diapirism happens at the same time. The second process has been well documented [20] and Figure 3.3 shows an example of a diapiric structure with significant down-building of adjacent sediments.

In Figure 3.3, well developed frictional drag zones can be seen in the sediments close to the salt. This happens due to a "smearing" action that occurs when the sediments are dragged along with the salt as the rising salt body moves relative to the subsiding formations. An upturned salt "pedestal" may exist if the salt is rooted to a deeper salt sheet. This also leads to an upturn in sediments [21]. The mechanical forces acting on these upturned sediments can be quite different. Therefore, these upturned sediments should be distinguished from those caused by frictional drag in the assessment of geomechanical risk.
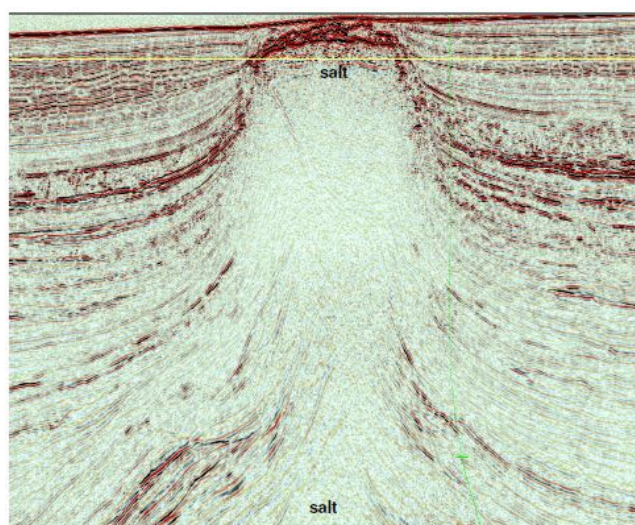
FIGURE 3.3: Seismic section of a columnar diapir showing well developed sediment down-building [20].

3.2.2 Classification of Drag Zones Adjacent to Diapirs

Drag zones are the high strain zones generated in sediments adjacent to the flanks of a growing diapir [3]. These drag zones are created where the surrounding overburden is revolved into a sharp dipping "on-lapping" geometry relative to the diapir walls. These zones could be confused with broader zones of an upturn which are produced by bed's molding to the form of an underlying salt pedestal, see Figure 3.5. Because of the steeply-inclined attitude of the rotated bedding in the drag zones, it is difficult to get good seismic resolution around diapirs.

Alsop et al. [22] defined four deformation patterns in drag zones adjacent to salt, see Figure 3.4. Deformation of homogeneous formations next to salt occurs in a predominantly plastic manner with little faulting. Deformed sediments may be "smeared" along the salt walls, creating a gouge zone, where near surface diapirism and sedimentation occurs. Their lateral extent can be limited to only a few feet in width. For heterogeneous overburdens, especially those that were partially lithified at the time of diapirism, considerable faulting extending several hundred meters from the salt wall may occur. Salt exits into homogeneous formations should therefore, from a geomechanical and drilling perspective, pose little difficulties. The exception is possibly in the narrow gouge zone that can be present in the case of quickly down built sediments close to the diapir. In these cases, the risk of high angle well exits causing a "parallel to bedding" mode of borehole failure is low.

From a wellbore stability point of view, the largest risks would be in inclined salt exits or vertical well trajectories in heterogeneous competent formations next to salt diapirs [3]. The sediments must be relatively old (to have been lithified) at the startup of diapirism in order for this to have occurred. Wells drilled to deeper structural targets may meet these more lithified sediments, and could therefore undergo a larger set of drilling difficulty.
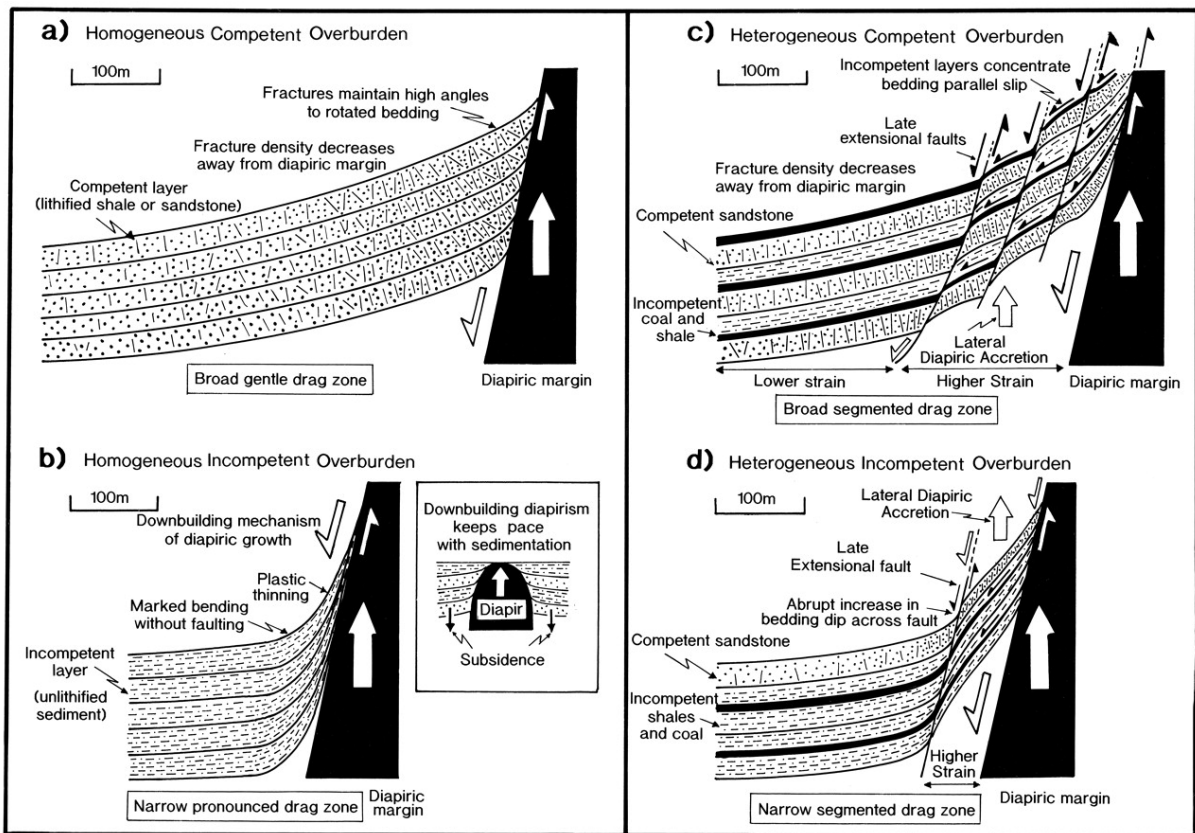
FIGURE 3.4: Classification of drag zone styles adjacent to diapirs [22].
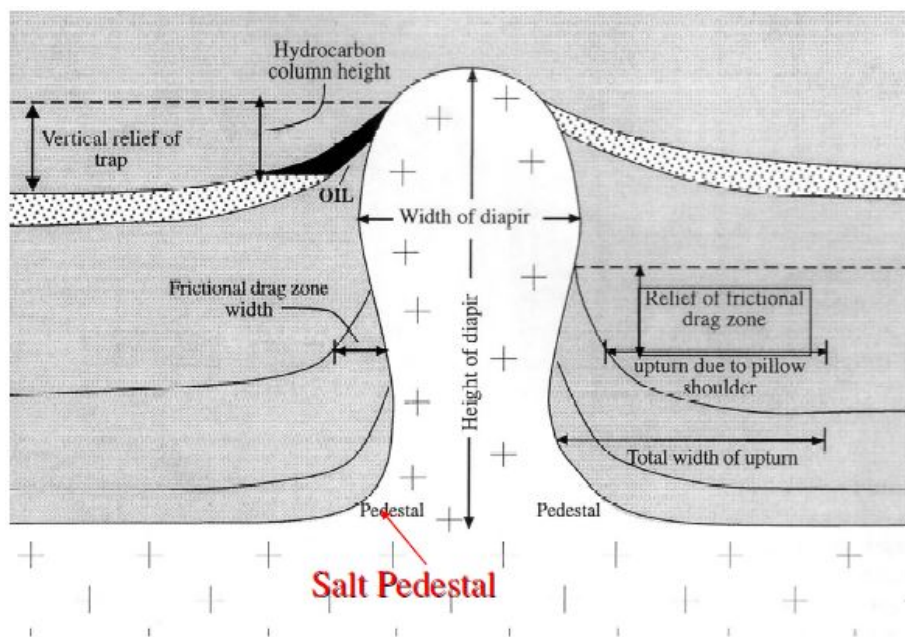
FIGURE 3.5: Upturned zones above salt pedestals and frictional drag zones [21].

3.2.3 Drag Zones and Overturned Sediments Below Salt Sheets and Overhangs

If subsequently buried, salt diapirs can bulge out of the sea floor and flow laterally as a "salt glacier," forming salt overhangs. The style of motion is latitudinally, in a tank-tread style [23]. In unconsolidated and weakly lithified sediments underneath salt extrusions. Significant deformations will occur due to this.

3.2.4 Toe Thrusts Adjacent to Salt Nappies

In the proximity of near surface occurrences of salt, normal faulting can occur close to the escarpment edge, matching local relief in the underlying salt [24]. Outboard of salt, toe thrusts may occur and will be subjected to a thrust-faulting stress regime. The minimum horizontal stress will be roughly the same as the overburden, and the maximum horizontal stress will be larger than the overburden, see example in Figure 3.6. Due to this, regions above the salt can be characterized by relatively low fracture gradients, from a geomechanical well design point of view. In addition, sediments in frictional balance under a normal faulting stress regime may be weak, and regions close to the salt sheet can be highly stressed. When designing mud weights for sections drilled through these regions, these conditions must be taken into consideration.

Present day examples of toe thrust may still exist in their residual form adjacent to salt tongues, which have been, on a later stage, covered by thicker layers of newer sediments. When designing a well, the existence of perturbed stresses and fractured/faulted rock cannot be disregarded, even though most likely the stresses have equilibrated to a condition approaching that of a lithostatic or normal faulting regime. The risk of wellbore instability is larger when drilling immediately outside of a salt diapir tongue compared to drilling at a greater distance outside of the salt [18].
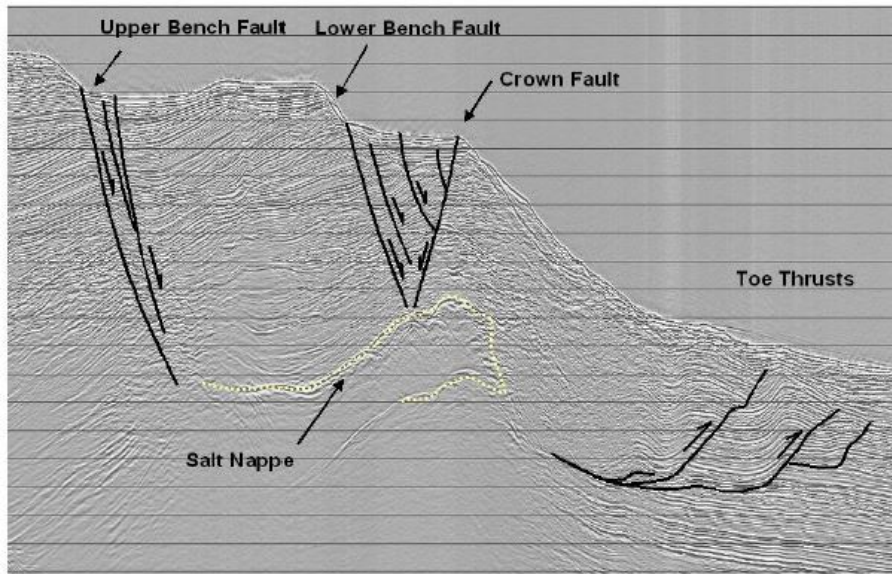
FIGURE 3.6: Normal faulting above, and toe thrust faults adjacent to the Mad Dog salt nappe [24].

3.2.5 Radial and Circumferential Faulting around Salt Diapirs

Several faulting styles exist around piercing diapirs. Sometimes these can form reservoir closures and traps in their own right. A good example of these can be found in the East Texas Basin, see Figure 3.8. The radial faults are formed when salt is removed at depth instead of the active piercing of sediments by a rising salt diapir. They also develop at some distance from the salt stock.

It is common to see radial faulting around piercing diapirs. This can clearly be seen adjacent to salt diapirs in deep water and in the North Sea, see Figure 3.7. It is shown in the deep water example that the radial fault pattern transforms into a polygonal fault pattern away from the diapir. Wellbore instability and lost circulation while drilling can be caused by both these styles of faulting [3].
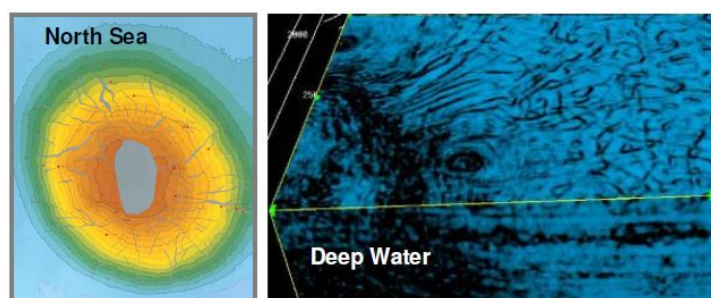
FIGURE 3.7: Radial faulting styles around piercing diapirs [3].
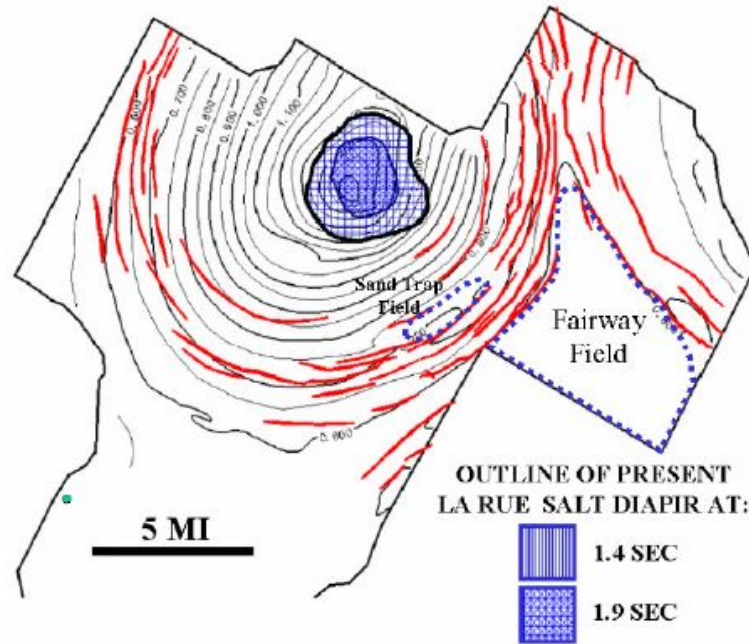
FIGURE 3.8: Mapped ring faults surrounding the La Rue salt diapir in East
Texas [3].

3.3 Pore Pressure beneath Salt

Due to the lack of trust in discriminating seismic interval velocities in the zones
beneath salt, a major technical challenge is the prediction of the pore pressure.
However, at the Pompano field located in the US Gulf of Mexico, a large number of
sub-salt wells have been able to give good characterization of the basal shear zone
pore pressure variations stretching away from the salt. Harrison [25] reported that
dipmeter, pressure, and paleontologic data suggests a highly structurally distorted
zone approximately 400 ft thick underneath the base of the salt with a sharp basal
contact between the underlying country rock and the older rock in the shear zone.
The characteristics of this contact are of a reverse fault that insulates the deformed
drag zone close to the salt face. Harrison indicates that across of the 400 ft thick
zone a $\approx$ 1 ppg pore pressure variation occurs. This variation in the sub-salt
pore pressure is larger than what is typically predictable from seismic velocity
interpretation before drilling. Due to this, the insecurity of the pore pressure
underneath salt remains a substantial challenge to well design and construction.

3.4 Prediction of Perturbed Stresses Adjacent to Salt

In recent years, the awareness of intrusive salt bodies in the overburden and their interference with the *in-situ* stresses, in and around the salt, has increased [18]. These amended stress states can have significant consequences. If the stress state in the near salt region is altered, then the pore pressure will be altered too. Often the causes of formation instability that can be encountered when drilling around salt diapirs are a combination of these stress and pressure variation.

3.4.1 Formation Instability Near-Salt Diapirs

There have been several cases of formation related drilling problems close to salt diapirs [26][27][28]. The existence of "rubble" or "brecciated" zones that occur in the drag zones of adjacent sediments that have been distorted upwards by the diapiric process [22], may be the reason for these drilling problems. Fredrich [18] found indications in his work that stress anisotropy can be created in these regions. Stress rotations can be generated in the near salt formations, as well as promoting differences in horizontal stresses, due to the necessity for lithostatic stresses in salt, and continuity of deformations at the salt/formation interface. If the mentioned differences are adequately large, *in-situ* shear failure of the near salt formations may occur. Fredrich speculated that this could be an additional cause of rubble zones adjacent to salt [18].

An example of the impact of stress perturbations and rotations on borehole stability in a vertical well is illustrated in Figure 3.9 (a), (b), and (c). The figures shows the required minimum mud weights (in ppg) for acceptable stability. The mud weights are plotted as function of inclination and wellbore azimuth. In Figure 3.9 (b) and 3.9 (c) the impact that non-uniform and rotated stresses can have on the required mud weight are illustrated. If a near-salt vertical well is drilled using a mud weight equal to what is required for far-field conditions, losses are possible. It can be seen from these two figures that including rotations have a great impact on the stability predictions. In addition, when rotations are included, a pronounced directionality results in the preferred drilling direction and the required mud weights. As wells are often deviated to exit the salt at a high angle to

access laterally remote reserves, or deviated towards the salt to access formations beneath a salt tongue, this directionality is of great relevance to oil-well drilling.

In deviated wells, especially those deviating in towards the salt body, the effects of stress disturbance and rotation on mud weight are most pronounced. However, care must be exercised, even when drilling a vertical well. "Rubble zones" may exist around a diapir and when drilling with a highly overbalanced mud, these zones can suffer pronounced time dependent instability. Under these conditions, irrevocable instability can be caused if drilling fluid penetrates into the fractured surrounding rock, driven by the substantial pressure differential, and thereby reduces the effective overbalance. Hence, even when drilling a vertical well, it is important that dependable predictions of the minimum required mud weight be made, to make sure that the applied overbalance is not too large. Another unfavorable stress condition on the rock is if the shear stresses are higher than the far-field stresses. This can create rubble zones by failing the rock *in-situ*, and can lead to severe instability problems.
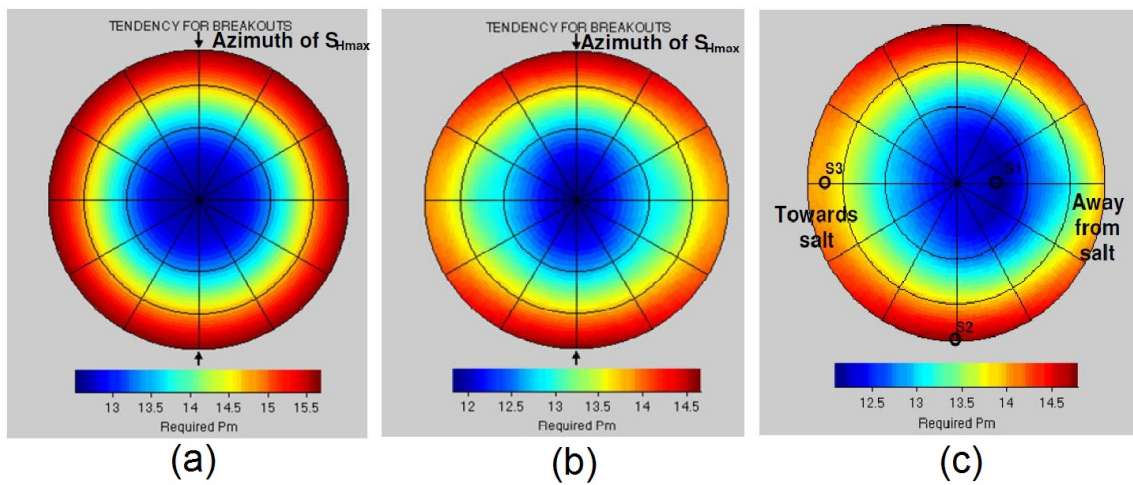
FIGURE 3.9: (a) Required mud weight for far field conditions,(b) Required mud weight for near salt condition, ignoring stress rotation,(c) Required mud weight for near salt conditions, including stress rotations [18].

Chapter 4

Directional Drilling in Salt

This chapter presents the challenges introduced when drilling directionally in salt formations. Technologies and equipment to overcome these challenges are also presented. The purpose is to give the reader better understanding of how to plan and drill directionally through salt in a safe and successful manner.

4.1 Directional Well Planning

In order to be able to drill directional wells through salt successfully, a key factor is directional well planning. The drilling can be split into the following categories:

1. Above salt kickoff and build, followed by drilling a tangential section through the salt

2. Kickoff in the salt and build angle

3. Steering in salt to manage collision risk

It is important when planning to drill directional wells through salt, that geomechanical risks and limits are factored into the planning phase. The complex origins and interactions involved in the creation of salt bodies, and the risk and limits that arise due to this were previously discussed in Chapter 4.

A goal when designing well trajectories should be to avoid salt seams and inclusions (if visible on the seismic), in addition to try to exit the salt at the flattest or

lowest dip area available. By doing this, the added instability and related issues that can occur from rotation of stresses at higher dipping salt bases can be avoided [6]. The natural build-walk tendency of salt is another directional consideration that is related to the geomechanical properties of salt. It has previously been experienced when drilling in the same salt body, that the natural formation tendency can push the drilling assembly in completely different directions, depending on where in the salt body, the drilling is taking place. The reason for this is believed to be due to the varying stress directions and magnitudes that can exist in distinct areas of the salt body. This underpins the theory that salt bodies are an amalgamation of several salt sheets. Understanding the magnitude and direction of this tendency is important to ensure that too abrupt doglegs are not planned. In crowded development scenarios where wellbore nudging may be necessary to maintain the anti-collision separation needs, this becomes even more essential. In these scenarios, wells drilled from the same template will tend to take the identicle directional trend. This trend shows that good directive control is needed, and that this natural tendency needs to be integrated in the drilling plan when possible, to avoid unwanted approaches to offset wells.

The trajectory design while drilling salt is impacted by drilling mechanics. The contact between the BHA, drillstring and salt wellbore increases as the inclination of the wellbore is increased. This leads to an increase in torque and drag, in addition to an increase in the potential for stick-slip[1] and other dynamics that are related to vibration.

It is crucial to have a uniformly round hole to be able to drill directionally as the casing and cement design relates to hole geometry and, therefore, can be tied back into the directional deliverables. For this purpose, rotary steerable systems (RSS) have proven their ability to deliver high-quality wellbores with lower doglegs, fewer ledges and smoother build rates. Because of the higher hole quality, RSS has been used to drill straight holes through salt in the GoM. Here they have been able to exploit the extra fracture gradient over thick salt sections in the deepwater to run fewer casing strings, compared to drilling outside of the salt [6]. To prepare for the unknown pressure environment below the salt, often full strings of heavy wall casing are run before exiting the salt. For this to be feasible, a high-quality hole is

---

[1]If the friction between the drillbit and the formation gets too high; the bit may "stick" and the rotation will either be reduced or come to a complete stop. When this occurs, the energy stored in the drillstring will accumulate and be stored as several turns of twist in the string. When the energy level gets to a certain level, it will overcome the friction force and be released. The string will then spin out of control and create, possible, destructive vibrations.

needed. This is because these casing runs often are one-way trips, and therefore, requires problem-free running of casing to the bottom.

Willson et al. [29] found in their studies that there can be more to gain from assuring a good hole quality, compared to using cement in the casing-salt annulus. If the hole is uniform, this will allow a uniform loading of the casing in salt (due to salt creep), and thereby preventing casing deformation, as seen in Figure 4.1. If an irregular hole is drilled in salt, this will require cementing of the casing-salt annulus to prevent non-uniform loading, and eventually casing deformation. Additionally, the casing centralization requirements will be changed if the hole section needs an effective cement job over the length of the pipe. If the centralization is increased, this will lead to an increase in the rigidity of the casing string and may therefore limit the allowable hole profile.

The benefits of uniform loading on casing extend over the life of the well, by reducing the chance of losing the well due to casing deformation and collapse. From this perspective alone, the additional cost of using RSS to achieve better hole quality of the wellbore can be readily justified [6].

Uniform loading   Nonuniform loading   Loading over a limited contact arc
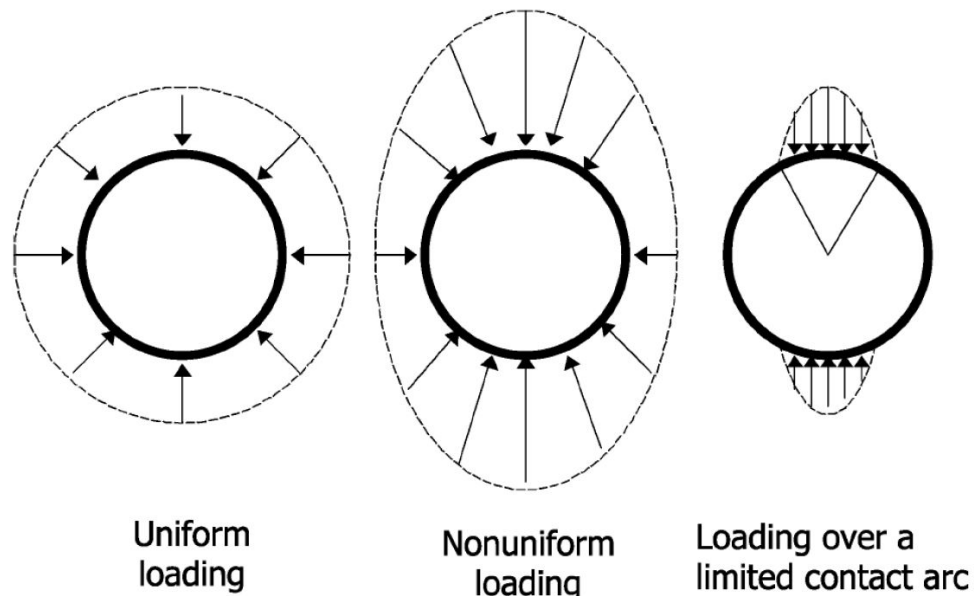
FIGURE 4.1: Schematic of non-uniform load configurations conventionally assumed for through salt casing design [29].

4.2 Riserless Drilling of Salt

In deepwater applications where the top of salt is shallow below the mudline ($<$ $\approx$ 750 m), riserless drilling of the top of salt may be conducted. These holes are usually large (26" to 22") and typically drilled vertically using salt saturated mud with returns to the sea floor. In these scenarios, the intervals drilled can range from $\approx$ 100 - 750 m, depending on well construction and design requirements.

The BHA design in these sections is with respect to the salt interval. The formation above the salt is often controlled drilled. The major concern is hole cleaning. Deviation is not a problem in the high permeability, unconsolidated overlying formation, since it will drill with low WOB. The BHA is therefore designed for drilling the salt [6]:

1. Directional control is needed to avoid high doglegs caused by the natural directing walk tendency of salt. The larger the salt interval that must be drilled is, the bigger the build and walk potential. High doglegs at shallow depths can cause severe issues further down in the well, considering casing wear, weight transfer, and torque.

2. Since there is a finite amount of mud on hand when drilling riserless, it is necessary to drill these sections as quick as possible. The faster it can be drilled; the less is the chance of running out of available mud before reaching the section total depth (TD). To be able to drill at an optimum ROP, bit selection and BHA design becomes crucial. Other advantages of drilling with higher ROP are rig time savings and reducing the volume of mud needed.

Based on the two points above, the key feature of BHA design when drilling salt section's riserless is (1) good directional control, (2) the ability to deliver consistently high ROPs throughout the section, and (3) the BHA must be strong enough to be able to drill the whole section in one run, as an unplanned trip in this section will require the mobilization and building of additional mud.

For this scenario there are three basic BHA options available:

1. **Conventional rotary pendulum assembly:** The reaction when exposed to the salt tendencies is unknown. To control these tendencies, often the

WOB has to be lowered thus reducing the ROP. In addition, this assembly offers no directional control.

2. **Steerable positive displacement motor:** This alternative offers good directional control in order to counteract salt tendencies, but the ROP is often reduced to unacceptable levels (up to 60 % in many cases) due to slide drilling[2]. Drilling in rotating mode only, thus letting the assembly follow the natural build and walk tendencies of the formation, can be attempted if the natural tendency is in line with the desired kickoff direction later in the well.

3. **Rotary steerable assemblies:** The benefits of using RSS is good directional control, in addition with the removal of slide drilling, thus enabling optimum ROPs to be upheld throughout the salt interval. Some RSS can drill almost perfect vertically, without input or encroachment from the directive driller. This can save valuable time when drilling these intervals, as time spent on orienting a steerable motor or trying to hold a toolface in salt is eliminated.

4. **Powered RSS:** Significant improvement in ROP when drilling salt intervals have been achieved when using RSS coupled with high torque, low speed motors (Powered RSS) [30].

It is not recommended to use drilling jars in these large hole sizes for any of the above BHAs as they are often the weak point in the string [6]. However, jars are seldom necessary in this interval since stuck pipe instances are rare. In such sizeable holes, wall contact is minimum in addition to low differential pressures. If stuck in salt, fresh water can open up the hole, and unstable holes can be circulated out with ease.

It is beneficial to use polycrystalline diamond compact (PDC) bits to improve the ROP while drilling salt. This is because mill tooth or insert bits often induce tracking in the salt, thus reducing the ROP. The shearing nature of PDC bits are much more suited to drill in salt. To be able to produce the same ROP using a mill tooth bit as with a PDC bit, typically a higher WOB would be required, see Figure 4.2.

---

[2]Slide drilling is when the drillstring is stationary and only the drillbit is rotated while drilling. This increases the friction between the drillstring and the borehole wall significantly, compared to drilling with drillstring rotation.

The best alternative for drilling these intervals would often be powered RSS when aligned with stable PDC bits. Powered RSS delivers the torque right at the bit. This will help to overcome the potential stick-slip that can be generated by large PDC bits, by permitting an increase in revolutions per minute (rpm). Higher ROPs can be achieved when drilling through salt, by increasing the torque and rpm at the bit. One of the negative sides of doing this is that the measurement while drilling (MWD) and logging while drilling (LWD) sensors must be places further behind the bit. Another disadvantage is that another tool is added to the BHA with the potential for failure.

In recent years, the ability to perform jet-in operations using RSS with a high torque, low speed mud motor in the riserless sections has been possible. This allows operators to pick up the RSS/motor BHA, with 36" structural pipe latched on, jet the conductor, un-jay and drill ahead with all the benefits of RSS and PDC bits [6]. This will reduce valuable operating time on deepwater rigs that is not equipped with dual derricks.
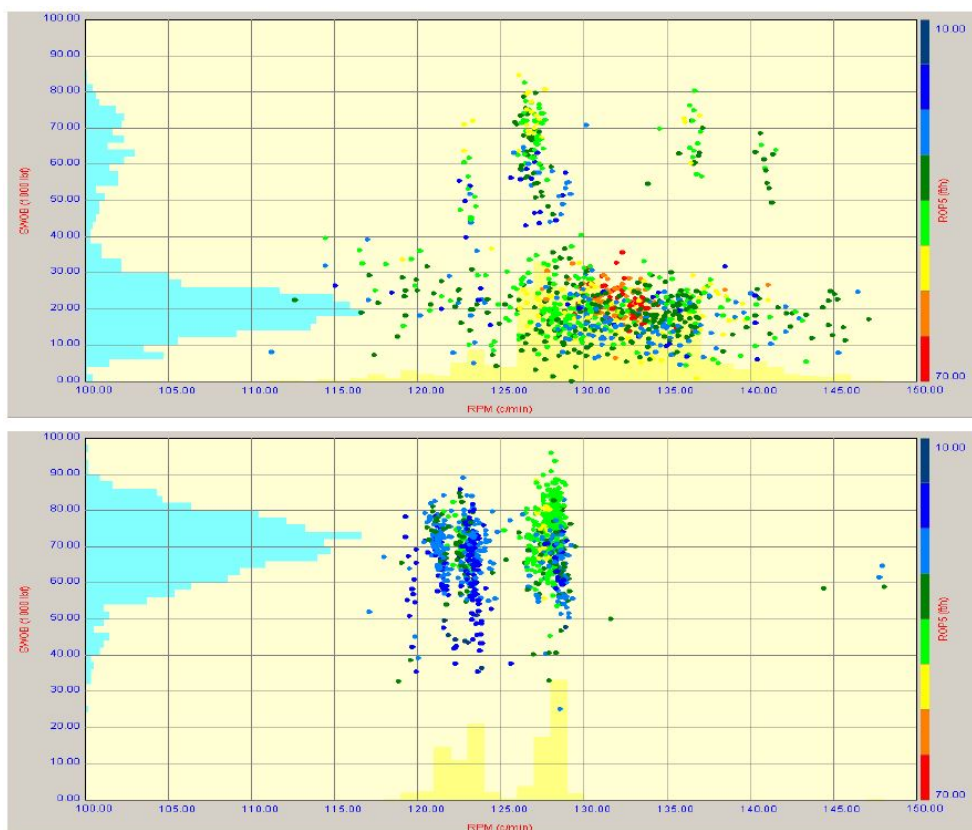
FIGURE 4.2: ROP Cross-plots for 26" PDC bit in salt (upper plot) and 26" mill tooth bit in salt both run in the same well. The plot indicates a best ROP of 60 ft/h with the PDC bit versus 45 ft/h with the mill tooth bit [6].

4.2.1 Riserless Drilling Challenges

Salt entry. The risk when entering salt are mainly due to stress regime changes in the interval just over the salt arising from its migration. These situations represent a risk of wellbore stability. When the salt top is deep, fractured or faulted formations have often been encountered. It is believed that these formations have been formed as the older, higher pressured sediment was forced upwards by the underlying salt and later fractured as the pressure "bled-off". Where this is the case, there is a risk for loss circulation while drilling into the top of the salt. If these zones have not been "bled-off", there is a risk of drilling into an over-pressurized zone on top of the salt.

It is recommended, when approaching the top of the salt, to reduce the ROP and/or WOB to give the drillers more time to interpret and react to the above-mentioned risks before entering the salt. An indication that the top of the salt has been reached is an increase in torque and a reduction in ROP. It is recommended to have a gamma-ray measurement within 10 ft from the bit to provide useful lithological confirmation that the change in drilling parameters can be correlated to the top of the salt.

Shock and vibration. One of the most challenging parts of drilling in salt is the shock and vibrations. Too large vibrations can cause downhole tools to fail or twist-off, which leads to the need for an additional trip and adding to the rig's nonproductive time (NPT). There are several mechanisms that can cause shock and vibrations, including (1) unstable or overly aggressive bits, (2) poorly matched bit-reamer combinations, (3) ratty or laminated salt intervals, (4) and creeping salts [6].

The best ways to identify the ideal drilling parameters for smooth drilling is through real-time analysis of run data, and adjust the rpm and WOB parameters to the vibration levels observed. In addition, guidelines for optimizing bit-reamer compatibility and BHA design can be obtained by predrill vibration modelling.

Inclusions. There are two reasons for why inclusions in the salt may present a hazard to the drilling operation:

1. **The impact of drilling in non-homogeneous formation while simultaneously under-reaming.** The ROP differs from formation to formation,

and different parameters to drill efficiently are required. When an inclusion is encountered while simultaneously, drilling and under-reaming, the bit and the under-reamer may be drilling in various formations. This can result in that the bit out-drills the reamer, and thereby cause an ineffective weight transfer to the reamer. This can, in turn, result in large shock and vibration's levels that can damage the BHA components.

2. **The uncertainty of pore pressure within the inclusion.** Depending on the mechanism that formed the inclusion and its lithology, the inclusion can be both abnormally or sub-normally pressured. Both these scenarios represent a drilling hazard. Kicks, loss circulation and stuck pipe can occur in these situations.

Tar. Drilling through tar zones represents a considerable drilling hazard. Some of the largest risks related to tar include (1) pack-offs, (2) swabbing, (3) damage to BHA components, and (4) difficulty in running casing. Tar is most often found in the base of salt. Romo et al. [31] presented in their work two recommendations to reduce the problems related to tar. These are (1) to avoid it completely, and (2) to drill these intervals as quickly as possible. To be able to avoid tar at the base of salt, identifying a specific base of salt exit target box must be done. This may require kicking off in salt to intersect the target [6]. In order to drill the interval as quickly as possible indicates that drilling with positive displacement mud motors are unsuitable when drilling salt/tar applications. This is because sliding ROP in salt has been reported to be as low as 50 % of the rotating ROP. In addition, rotation of the drillstring and the BHA is an important factor to prevent stuck pipe in tar.

Salt Exit. The same situation is present with salt exit as with salt entry regarding disturbance of the normal surrounding stress regimes, due to migration of the salt body. This introduces significant risks when at the salt exit phase of drilling. The hazards associated with drilling through the salt base are [3] (1) rubble zones, (2) sub-salt pressure uncertainty, (3) depth errors on base of salt, and (4) overturned beds. These hazards look similar to those when entering the top of salt, but experience has shown that the risks when exiting the base of salt are much bigger.

4.3 Equipment and Technologies

New technology developments have made great improvements in directional drilling through salt. Some of the technology enablers include [6]:

Rigs. The ability to drill through salt was greatly improved with the 5th generation drilling rigs. The improvements made on these rigs are:

- Increased torque at increased rotary speeds. This is favorable for salt drilling.

- Improved hydraulics with larger drill strings and higher pressure pumps.

- Increased hook rating. This is beneficial for running long, heavy casing strings through thick salt sections.

- Increased storage capacities. When drilling riserless into salt with salt saturated mud in a pump and dump method, great storage capacity is important. In addition, a high volume of cement, which must be stored on the drilling rig, is required for large holes.

Rotary Steerable Systems. The slide/rotate mechanism of drilling with positive displacement mud motors has proven to be inefficient and unsuccessful in salt, especially in directional drilling. There are several advantages of drilling with RSS such as increased ROP, more consistent doglegs and a smoother wellbore. RSS is a cost-effective option for salt drilling in deepwater operations.

Bits. It is recommended to avoid aggressive bits with six blades or less and 19 mm cutters when drilling in salt. This is because these bits can generate drilling related shocks that can cause tool-failure or parting of the BHA components. A good rule is to use 13 mm (or 16 mm for larger than 18" bits) cutters and more than seven blades on the bit. It is important that the cutter is compatible with any concentric reaming device being used, and that the bit should not out-drill the reamer. PDC bits have shown great stability for directional drilling in salt. However, it is important with a good gauge length for maintaining the stability for large (18-1/8" to 26") PDC bits.

Under-reamers. The usage of under-reamers is essential for salt drilling applications when drilling salts that have a strong creep tendency. The advantage of

running a concentric reamer on the BHA is huge. It gives the driller added insurance and time by simultaneously drilling and opening the hole, which gives the drill crew better chances of successfully running the casing. To make sure that the bit does not out drill the reamer (which can induce shock, vibration and stick slip to the BHA) it is important to ensure that the cutting structure of the reamer match the bit.

Sub-salt imaging. Because of the large difference in seismic velocity between salt (14.500 - 15.200 ft/second) and the surrounding sediments (often less than half of the velocity in salt), often the seismic imaging through thick salt bodies are distorted when using traditional time-migration methods [32]. This made it difficult for drillers to locate the intended drilling target. This problem has been solved, to some degree, by 3-D prestack depth imaging, which refines the seismic image and reduces the time migration data errors by an order of magnitude. Still large uncertainties exist, but new methods are under development that will reduce the drilling risks significantly. When these improvements are ready, it will help to increase the predrill positional accuracy of base of salt and dips, salt inclusions, reduce the pore pressure uncertainty underneath the salt and better image rubble zones.

Real-time monitoring. Salt drilling is complex. One measurement to deal with this complexity is to use real-time monitoring or operation support centers. These are useful for improving communication between the offshore and office teams. The data from the operation needs to be quickly turned into information that can be shown with minimum latency, in the right context and in a format which is beneficial for the people who are making the decisions. These centers are able to monitor pore pressure predictions, torque and drag, shocks, and vibrations and hole cleaning. In addition, these centers allow early detection of problems, to facilitate optimum drilling parameters, and reduce NPT.

Measurements While Drilling. The measurements required for drilling in salt are similar to those used when drilling in other harsh environments. These include (1) vibrational data (lateral, axial and torsional), (2) torque measurements, (3) stick-slip, (4) downhole WOB, and (5) annular pressure for ECD measurements.

One of the latest developments being adapted for salt drilling is the option to transmit different data arrangements into the telemetry tool [6]. This means that, e.g. while drilling salt, the telemetry bandwidth is optimized with vibration and

stick-slip data points, but once out of the salt the tool can be switched over to another preprogrammed data frame, like ECD data points.

Logging While Drilling. Even though few petrophysical measurements are required in salt, some measurements can help to improve drilling performance.

- Gamma-ray: It can measure changes in lithology associated with entering the top of salt, drilling an inclusion or exiting salt and correlate these with drilling parameters (ROP, WOB, torque). It is usually placed within 10 ft of the bit.

- Sonic: To improve the accuracy of models through inclusions and in the interval under salt, compressional data is used in real-time pore pressure measurements while drilling. It is important for post drilling geomechanical modeling of the salt to gather sonic shear data. The stress regimes in the salt can be determined by these models and show if the stress is changing with depth into the salt. This data is used when constructing the next well. To minimize the impact on sonic data from drilling noise, a rigorous BHA design is required.

- Seismic while drilling: This can be used to update the base of salt depth in real-time from the seismic checkshots obtained. Adjusting the salt base may cause a shift in the prognosis target depth below the salt. Trajectory changes can then be made to alter the inclination in salt in order to hit the target and avoiding the need for side-tracking.

Chapter 5

New Drillbit Technology Suitable for Drilling in Salt

In this chapter two new drillbit technologies will be presented. The properties of these bits and how they can be beneficial when drilling in salt will be discussed. The aim is to create an interest for these bits, which may lead to initiative for testing their properties in salt formations.

5.1 The Kymera Hybrid Drillbit

The first hybrid drillbit concepts dates all the way back to the 1930s when Scott and Bettis [33] in 1932 developed the first prototype of a hybrid bit. The concept behind the hybrid drillbit was to develop a bit that would improve the roller-cone bits limitations in drilling in shale and other plastically behaving rocks, while maintaining its ability to drill hard and abrasive formations. The prototype bit designed by Scott and Bettis was a combination of a fishtail and a roller-cone bit, see Figure 5.1. The fixed-blade of the fishtail bit was not as affected by the combination of chip hold-down and/or bit balling as the roller-cone bit. This is because they act as mechanical scrapers that continuously scour the borehole bottom [34]. Scott and Bettis' prototype never succeeded commercially because the fixed part of the bit, the fishtail, would wear to early, which resulted in large wear flats that reduced the ROP to less than what could be achieved using just a roller-cone bit.

In the 1980s the concept of a hybrid bit was reintroduced when the wear-resistant fixed-cutter PDC bits were developed, but again with mixed results [34]. The poor results were mainly due to structural deficiencies in the designs and the lack of durability of the first PDC cutters. Significant improvements have been made in the PDC cutter technology since then, and fixed-blade PDC bits have replaced roller-cone bits in nearly all applications, except for those where the roller-cone bit are uniquely suited. These situations are (1) hard, abrasive and interbedded formations, (2) complex directional-drilling applications, (3) and general applications in which the torque requirements of a conventional PDC bit exceeds the capabilities of a given drilling system [34]. These are the applications in which the hybrid bit can improve the performance of a roller-cone bit substantially, with a lower level of harmful dynamics compared with a common PDC bit.
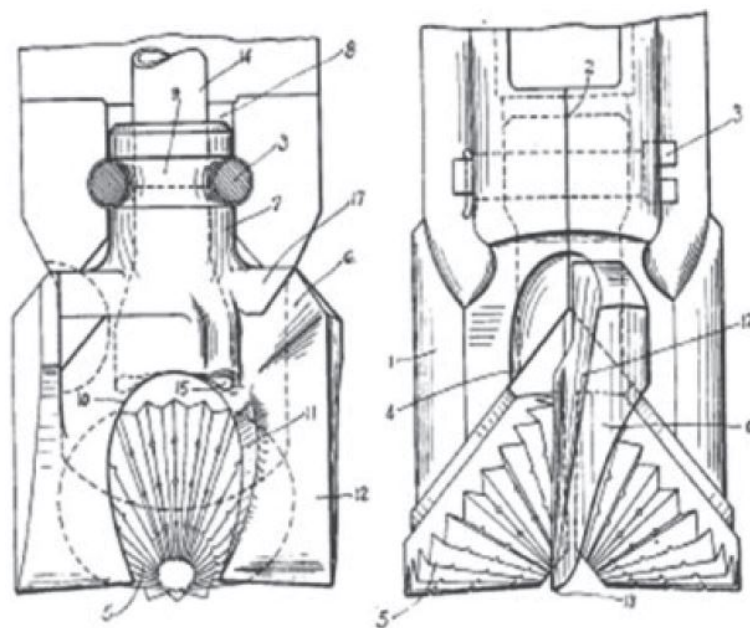
FIGURE 5.1: The first hybrid drillbit prototype [33].

5.1.1 Kymera Hybrid Bit Design

In 2009 Baker Hughes introduced their "Kymera" hybrid drillbit with two basic designs. These was (1) a two-cone, two-bladed version for smaller diameter boreholes and (2) a three-cone, three-bladed version for larger diameter boreholes, see Figure 5.2 and 5.3. These bits are based on the proven four- and six-bladed PDC-bit designs, but the secondary blades have been replaced by truncated rolling cutters.

The result of this is that the central portion of the borehole is only cut by the PDC cutters on the primary blades, while the more difficult outer portion is cut by a combination of the cutting elements of the rolling cutters and the fixed blades. In order to open up a space in front of the blades for the cuttings to return and for the placement of the nozzles, the rolling cutters are oriented toward the backside of the blades.
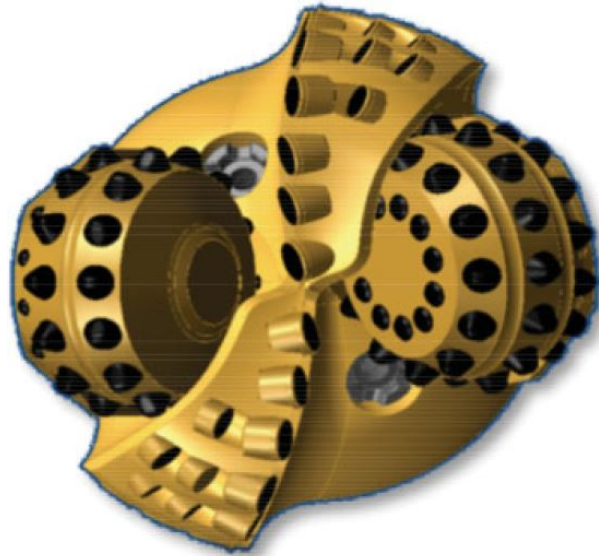
FIGURE 5.2: Two-cone/two-blade hybrid bit [34].

FIGURE 5.3: Three-cone/three-blade hybrid bit [34].

5.1.2 Drilling Mechanics

The drilling mechanism of the Kymera hybrid bit is a continuous shearing and scraping by the fixed-blade bit, combined with the subsequent crushing by the roller-cone bit. However, the performance of the bit is highly dependent on formation or rock type, strength and structure.

Pessier and Damschen [34] conducted several tests for examine the drilling mechanics of the hybrid bit compared to PDC- and roller-cone bits. These tests was performed in three various rocks with different rock strengths.

Medium-Strength Carbonate. The first test was performed in Carthage marble with UCS of approximately 15.000 psi, with 3.000 psi BHP, 9,5 lbm/gal water-based mud (WBM) and run at a constant 120 rpm with increasing WOB. In this test, two different types of the two-cone, two-bladed hybrid bit were used. These two versions were (1) cone leading and (2) blade leading. The terms specify which cutting structure that is dominating. In the cone leading version the rolling cutter forego the PDC blade, which are aligned in the same radial paths. The PDC cutting elements are barely scraping the borehole bottom. In the blade leading version it is the PDC cutting elements that does most of the work, while the rolling cutters act as "depth of cut"-limiters and stabilizers.

Figure 5.4 shows the well-known fact that PDC bits are up to four times more aggressive than roller-cone bits, with the hybrid bits falling in between those two. The cone leading hybrid falls closer to the roller-cone bit and the blade leading is closer to the PDC bit. This gives the driller the alternative to choose the bit that best suits the drilling system or application.

Figure 5.5 shows the ROP as a function of torque. It is clear that all four bits require roughly the same amount of torque to drill at a given ROP. This indicates that the fundamental rock-fracture process is similar for crushing and shearing or a combination of the two [34]. In this medium-strength formation the roller-cone is slightly more efficient, but the torque generated with this bit is limited. The WOB and torque operating window is narrow. Due to this the roller-cone bit cannot take advantage of the new more powerful rigs and motors. The hybrid bits have a much broader operating window and are able to exploit the full torque and power that modern drilling systems can provide. It can be seen in Figure 5.6 that the roller-cone has a poor response to the increase in rpm, while the hybrid

and the PDC bits has a proportional response to the increase in rpm. The roller-cone bits poor response to rpm in rock under confining pressure is well known and is attributed to increased tracing at low depth of cut and less effective bottom scouring and cleaning by jets traversing at high speed [34]. The Kymera hybrid bit cleans the bottomhole mechanically as the blades on the bit act as scrapers that break up the tracking pattern. Both torque and rpm can be optimized to transfer maximum power to the bit, which is a huge benefit in performance drilling.
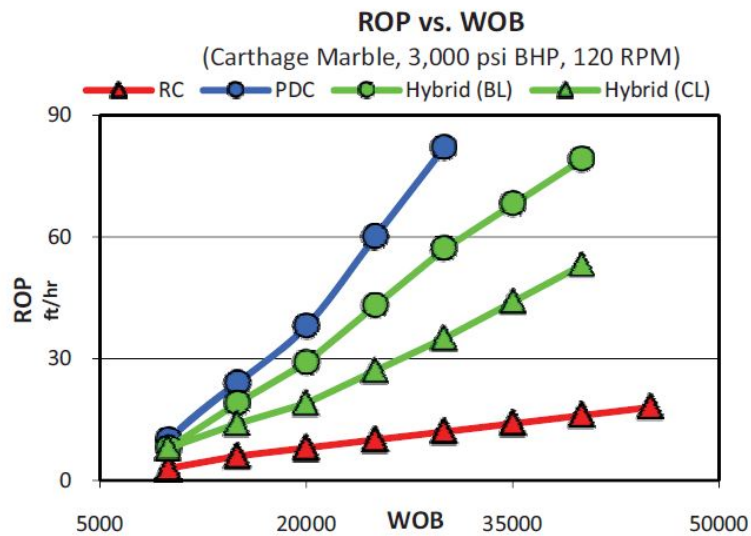
FIGURE 5.4: ROP vs. WOB, Carthage marble [34].
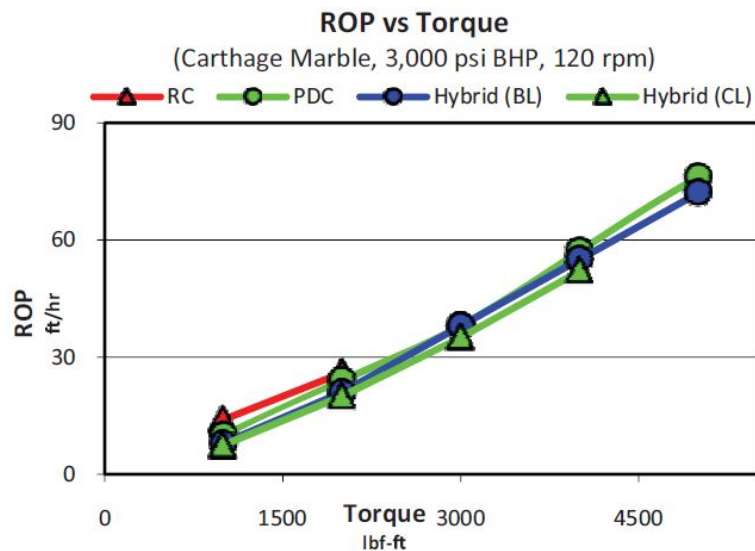
FIGURE 5.5: ROP vs. torque, Carthage marble [34].
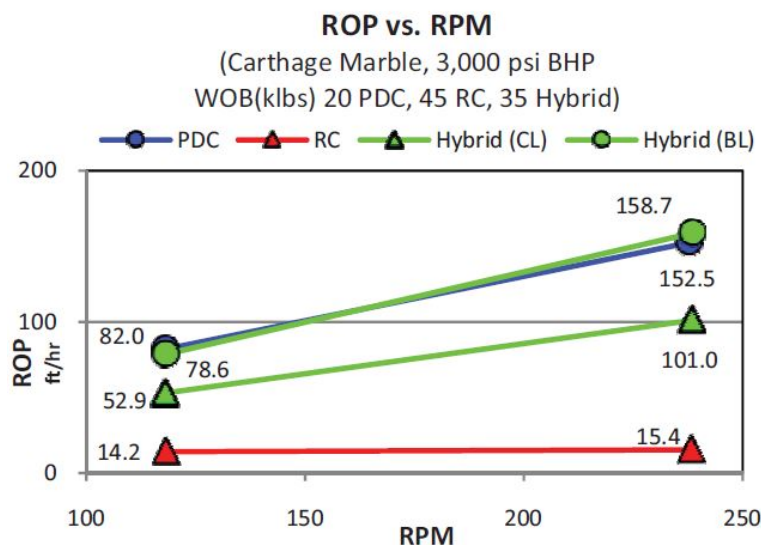
FIGURE 5.6: ROP vs. rpm, Carthage marble [34].

Soft Shale. For this test Catoosa shale with UCS of approximately 3.000 psi was chosen and it was run at 4.000 psi BHP with 9.5 lbm/gal WBM. It is shown in Figure 5.7 that the PDC is almost ten times more aggressive than the roller-cone bit at minimum WOB, and that the difference increases with higher WOB. Even though this is advantageous with regard to ROP, it can be negative when small changes in WOB can cause large variations in torque and ROP. Erratic torque and ROP response can result in bit balling and severe stick-slip. The Kymera bits response to WOB is moderately increasing, but it is still as much as four (cone leading) and eight (blade leading) times faster than the roller-cone bit. Since the WOB response of the hybrid bits is not as abrupt as for the PDC bit it ensures a smoother running and a resistance against sudden balling. The weakness of roller-cone bits is clearly evident in Figure 5.8. For a roller-cone to be able to match the ROP of the PDC bit it requires approximately three times more torque. This is because PDC bits are much more efficient in shale due to its scraping and shearing action. The Kymera hybrid bit cannot match the PDC bit at higher WOB or at greater depth of cut, but it is two (cone leading) or three (blade leading) times more efficient than the roller-cone bit at light WOB. For pure shale drilling the PDC bit is clearly the preferred choice.
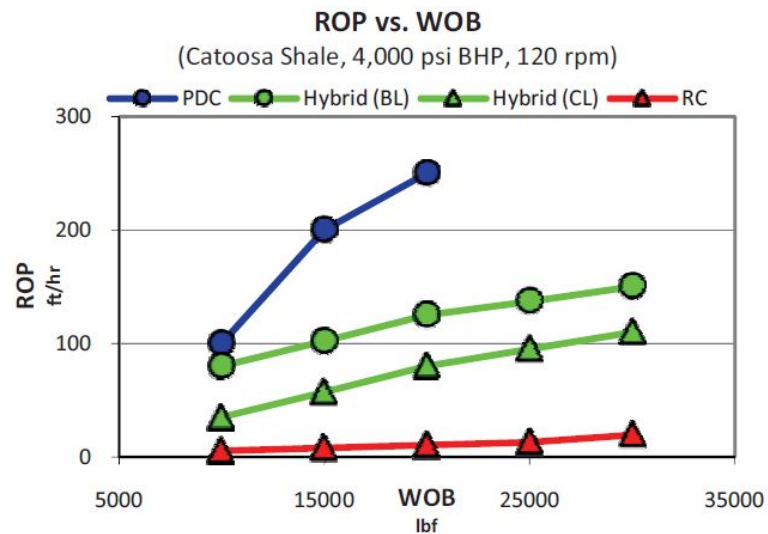
FIGURE 5.7: ROP vs. WOB, Catoosa shale [34].
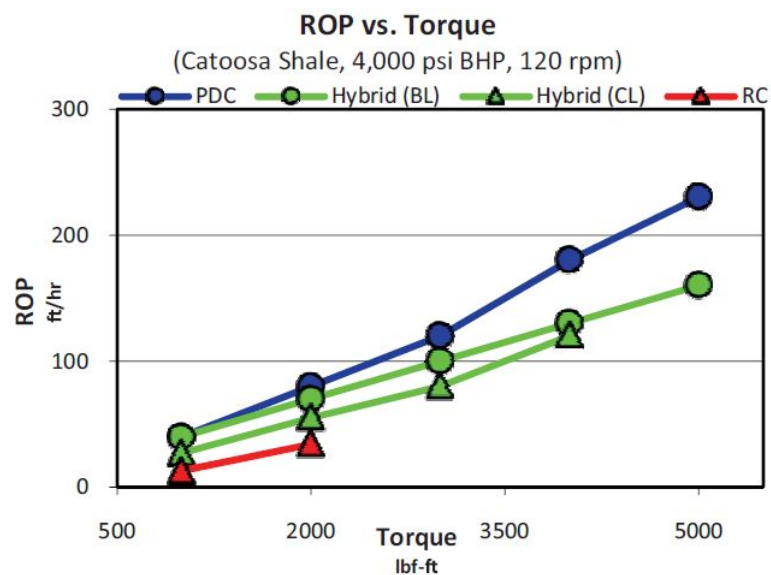
FIGURE 5.8: ROP vs. torque, Catoosa shale [34].

Hard, Abrasive Quartzite. In the third test Jasper quartzite at 36.000 psi UCS and Gabbro at 49.000 UCS was selected. A 12-1/4" three-cone, three-bladed hybrid bit was used at 4.000 psi BHP with 9,5 lbm/gal WBM, at 120 rpm and constant WOB of 30, 40 and 70 kip for the PDC, Kymera, and roller-cone bit, respectively. The reason for the different WOB for the three bits was to reach comparable torque. There is a third option in the cone/blade arrangement that is possible when using the three-cone, three-bladed bit, which is putting the matching pairs of cones and blades opposite of each other (cone opposite) and thereby sharing the drilling load equally between the two cutting structures. The resulting aggressiveness when using this setup is roughly right in the middle of the roller-cone and PDC bits.

From Figure 5.9 and 5.10 it shows that the Kymera hybrid bit achieved the highest ROP followed by the PDC and the roller-cone bit, but that it also used slightly more torque. Figure 5.11 gives the specific energy for each test, which indicates the true efficiency of the three bits. As seen in Figure 5.11, the roller-cone bit is the most efficient bit in hard rock. However, as in the medium strength rock, the roller-cone bit has already reached the maximum WOB limit, hence, no further ROP can be gained using this bit unless its aggressiveness is increased. The specific energy for the Kymera hybrid bit is lower than for the PDC bit. This might be an indication on that there is a synergy between the crushing and shearing action [34]. The cutting elements of the roller-cone bit creates a deep damage zone in the formation that might pre-fracture the hard rock and, therefore, makes it easier for the PDC cutting elements to penetrate and shear it. The wear and damage experienced with conventional fixed-cutter or PDC bits might be reduced if the hard and abrasive material has been pre-fractured. In addition, the shearing could be performed more effectively by using hybrid bits. When drilling in hard rock, the Kymera hybrid drillbit has a much wider operating window and better ROP potential than the roller-cone bit.
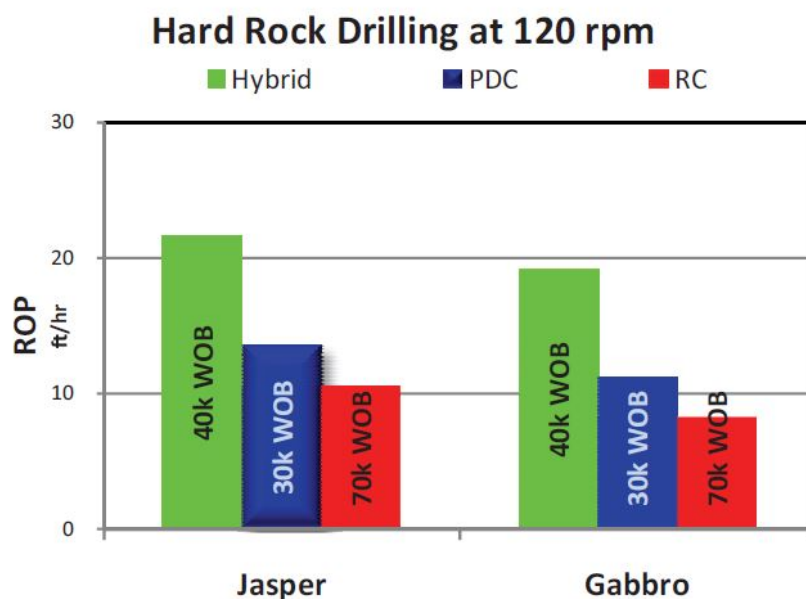
FIGURE 5.9: ROP in hard rock drilling [34].
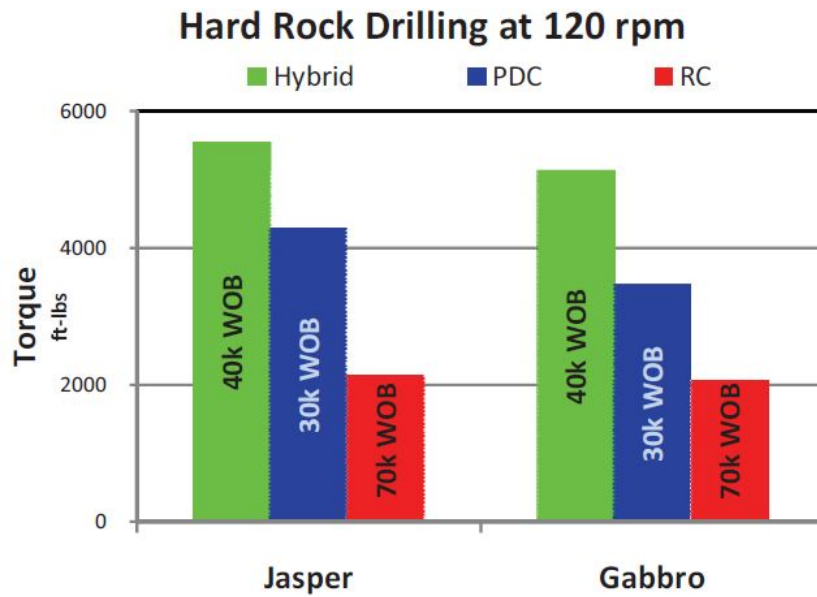
FIGURE 5.10: Torque in hard rock drilling [34].
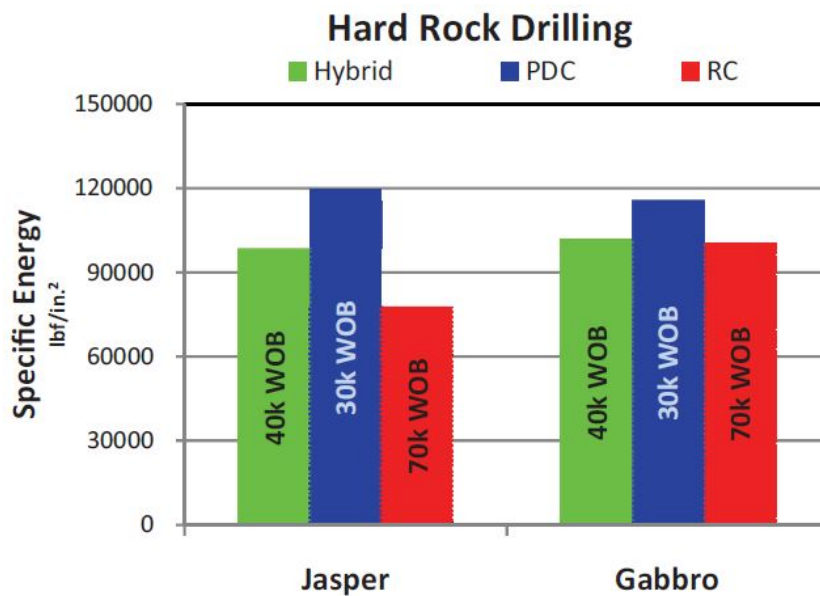
FIGURE 5.11: Specific Energy in hard rock drilling [34].

5.1.3 Drilling Dynamics

The variation and intensity of the drilling forces defines drilling dynamics. For fixed-cutter or PDC bits it is torsional forces that are dominant, while for roller-cone bits it is axial or vertical forces that characterize the dynamics. These forces

can trigger dynamic dysfunctions such as whirl[1] and stick-slip for fixed-cutter bits, and bit bounce for roller-cone bits.

Drilling Interbedded Formations. When drilling in a mix of medium-hard and hard abrasive formations, accelerated damage and wear of PDC bits are frequently observed in the field, in addition to harmful dynamics. A laboratory test was set up by Pessier and Damschen in an attempt to duplicate these conditions. This was done by creating a segmented rock core containing three different rock strengths. The three rocks that was used was Carthage marble (15.000 psi UCS), Jasper quartzite (36.000 psi UCS), and Gabbro (49.000 psi UCS). Figure 5.12 shows the thickness and sequence in which the rock layers was placed. In this test a 12-1/4" cone opposite hybrid bit and conventional roller-cone and PDC bits was used under 4.000 psi BHP and with 9,5 lbm/gal WBM. The WOB was held constant at 30.000, 40.000 and 75.000 lbf for the PDC, hybrid and roller-cone bits, respectively. The rotary speed was 120 rpm. The WOB for the roller-cone bit is at the upper end of its WOB rating. The different values for WOB was selected to achieve comparable torque levels in Carthage marble [34]. It can be seen in Figure 5.13 that the roller-cone bit is slowest overall, the PDC bit is over twice as fast as the roller-cone in Carthage, but only slightly faster in the quartzite. This is known as a negative drilling break for PDC bits in harder sandstone. The Kymera bit is slightly faster than the PDC bit in Carthage marble, but the main difference is in the harder quartzite and Gabbro. The ROP for the Kymera bit does not drop off nearly as much as for the PDC bit in these formations. In fact the ROP is almost twice as high for the Kymera bit compared to both the PDC and the roller-cone bits. Again this indicates a favorable synergy of the crushing and shearing action with the hybrid bit in harder rocks [34].

The most considerable result from this test was the variation in the average torque at constant WOB and rpm. The torque signatures for each bit type when drilling through the different layers are presented in Figure 5.14. It is evident that the torque for the PDC bit varies with more than 60 % (4.200 to 7.000 lbf-ft) when transitioning from the different rock types. The torque response of the roller-cone is not as abrupt as for the PDC bit and varies with approximately 20 % (2.500 to 3.000 lbf-ft) in the first transition. The absolute torque values for the roller-cone bit is much lower than for the PDC bit. Even with 75.000 lbf WOB it generates much

---

[1]Whirl is when the drillstring turns in the opposite direction of the drillbit. This phenomenon can be highly destructive, destroying both the tools and the borehole.

lower torque and therefore drills slower. For the Kymera bit the torque variations is about the same as for the roller-cone bit, 18 %, but at a significantly higher level (5.500 to 6.500 lbf-ft). From the obtained results it is clear that regions with highly heterogeneous formations in which torsional oscillations negatively affect the performance and durability of the drillbit as well as the reliability of the BHA and drillstring.
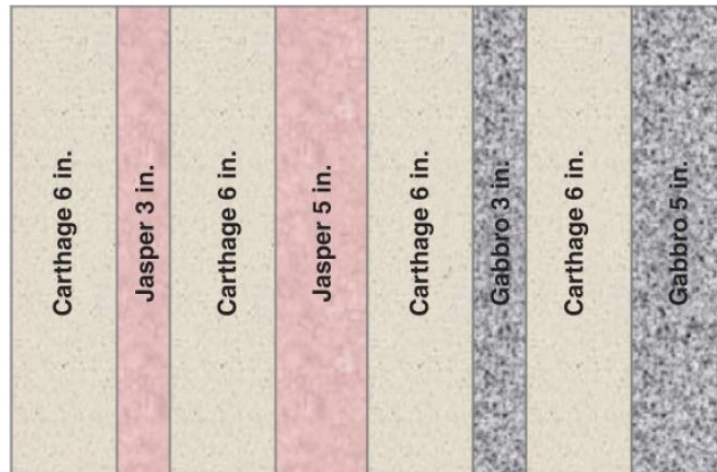
FIGURE 5.12: Segmented core section [34].
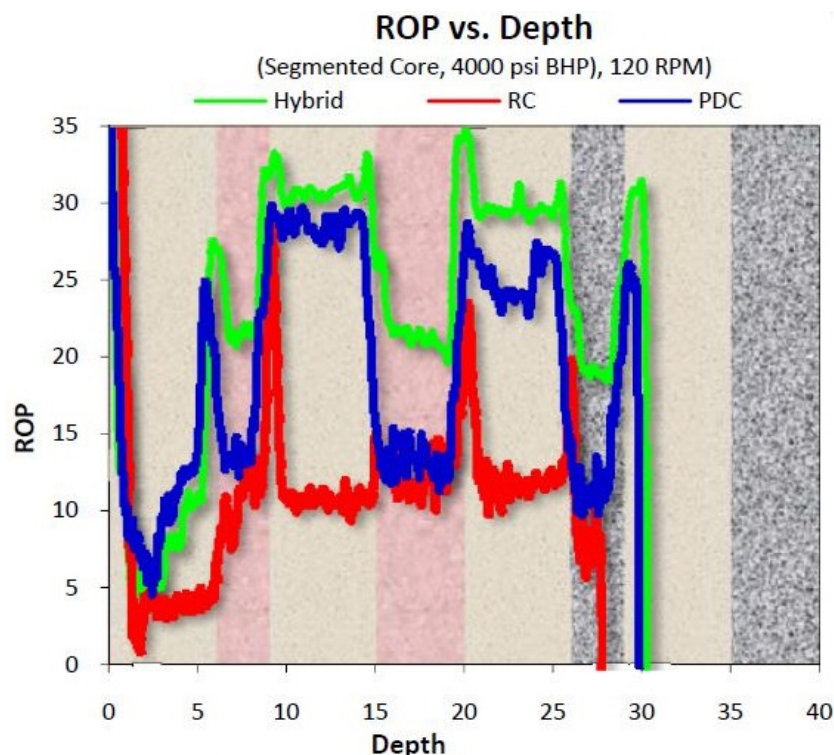
FIGURE 5.13: ROP signatures in segmented core [34].
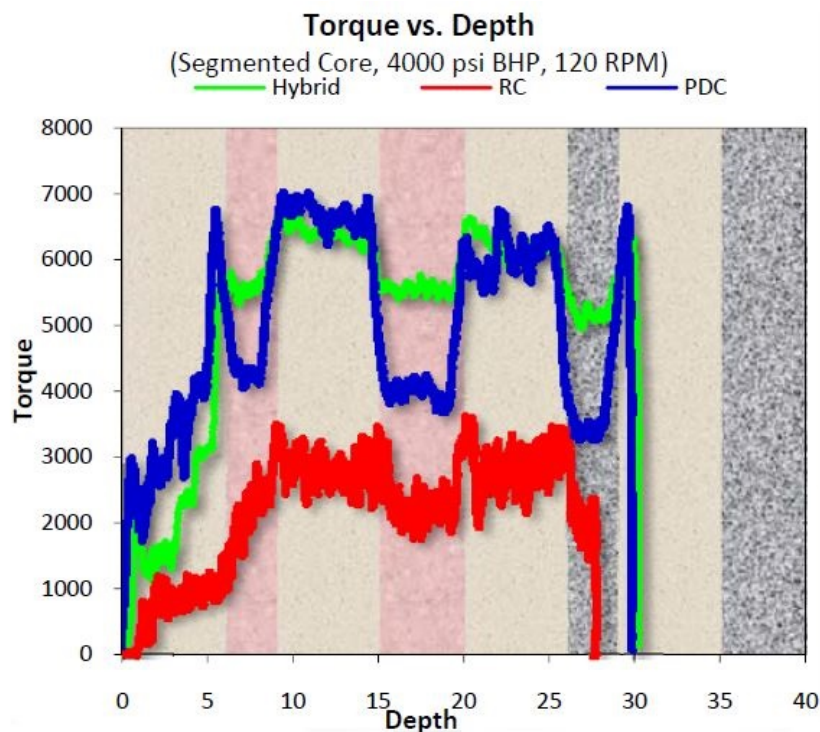
FIGURE 5.14: Torque signatures in segmented core [34].

Directional Drilling. Many drillers still use roller-cone bits for difficult and demanding jobs when drilling directionally. This is due to the issue of high torque oscillations in mixed and interbedded formations is compounded further by erratic WOB transfer, which causes additional torque spikes with aggressive PDC bits and makes tool-face control almost impossible [34]. The Kymera hybrid bit is a good alternative for these jobs as it runs smoother and more efficient than a typical PDC bit and faster and with more responsive rpm compared to a conventional roller-cone bit. The observed results from the laboratory tests support this theory.

5.1.4 Field Tests

Canada. In the field test in Canada a 12-1/4" three-cone, three-bladed hybrid bit was used in the surface hole. Here the Kymera outdrilled the PDC bit with approximately 33 % and the roller-cone bit with 134 %. It was reported that the Kymera bit could handle almost the same WOB (24 vs. 28 kip) as the roller-cone without experiencing bit bounce, as seen in Figure 5.15. Compared to the PDC bit it was able to drill with lower rpm (110 vs. 140) and much higher WOB (24 vs. 11 kip) without experiencing stick-slip. In large diameter surface hole drilling which often is torque or WOB limited, the Kymera has proven to be advantageous

due to the fact that it requires less WOB compared to roller-cone bits, and that it runs smoother than a PDC bit.
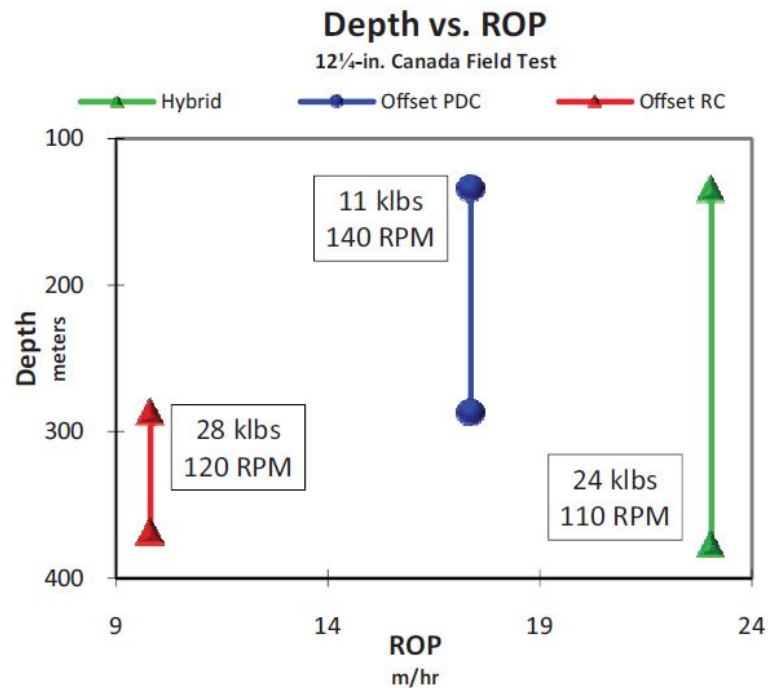
FIGURE 5.15: Depth vs. ROP, Canada field test [34].

Onshore Brazil. The Rio Grande do Norte field is known for its challenging interbedded formations, consisting of sand, shale and conglomerate sequences. Vibrations and toolface problems have caused poor performance in these formations, such as low ROP, a high number of bits and bit trips to be required, and limited tool life [34]. The Kymera bit was here tested in both the 8-1/2" and 12-1/4" sizes.

12-1/4": The Kymera bit was able to drill 362 m in one single run with an average ROP of 5,9 m/hr before it was pulled out of the hole due to a casing point [35]. In comparison, offset wellbore 1 managed to drill 417 m in four bit runs, with an average ROP of 3,4 m/hr. Offset wellbore 2 drilled 207 m in two runs with an average ROP of 1,7 m/hr. Both offset wellbores was drilled with roller-cone bits. These numbers are presented in Figure 5.16 and 5.17. During the run there was little torque fluctuation, even when transitioning from soft to hard formation and vice versa. Furthermore, there was not reported any significant fluctuation in the drilling system's steering head, indicating good toolface control and excellent stability throughout the run [35]. The Kymera bit run at 18 % lower cost per

meter (CPM) compared to offset wellbore 1 and 46 % lower than offset wellbore 2.
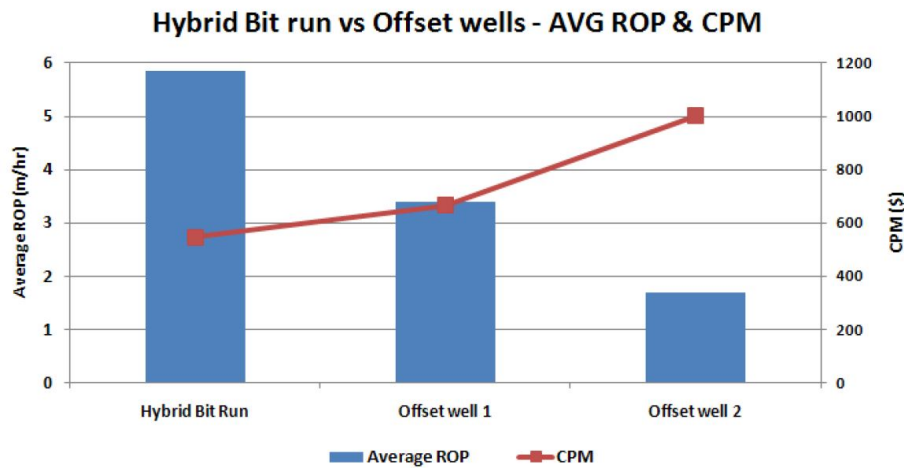
FIGURE 5.16: ROP and CPM comparison between the hybrid bit run and the offset wells 1 and 2 [35].
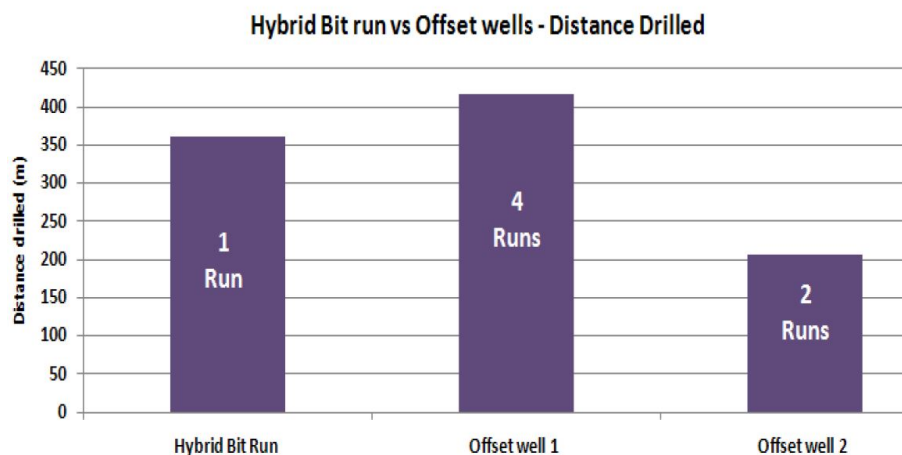
FIGURE 5.17: Distance drilled and number of runs comparison between the hybrid bit run and the offset wells 1 and 2 [35].

8-1/2": In this well two 8-1/2" Kymera bits was tested with a traditional PDC bit and a tungsten carbide insert (TCI) bit in between the two runs [34]. Figure 5.18 shows that both the Kymera bits outperformed the PDC and TCI bits in both ROP and distance drilled. The Kymera bits were able to reduce the number of days spent on the well and improve tool reliability by reducing the downhole vibrations from torque fluctuations.
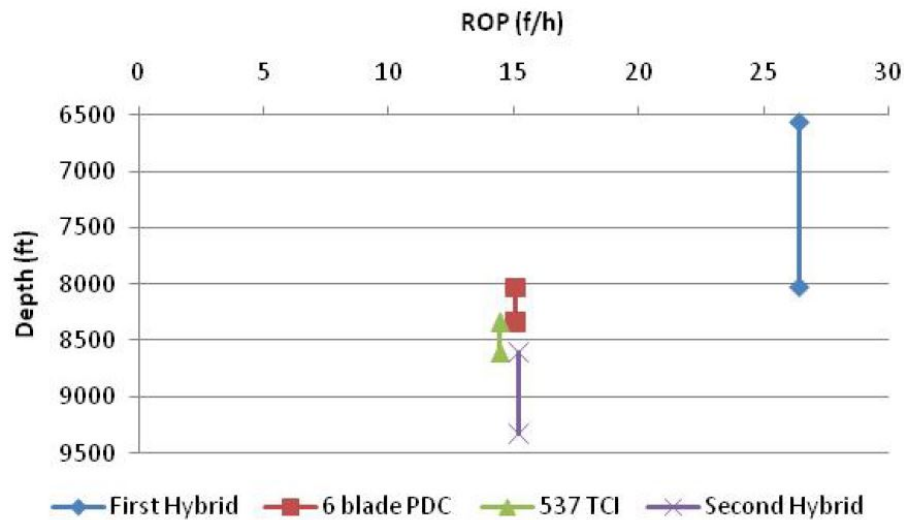
FIGURE 5.18: 8-1/2" performance of Kymera vs. TCI and PDC [34].

Several other field tests have been run which has proven the Kymera bit's ability to drill through many different formations with various BHA, delivering good results in terms of ROP, vertical control, distance drilled and stability.

5.2 PDC bit with a Stinger Element

5.2.1 Conical Diamond Element

In recent years Smith Bits, a Schlumberger company, have been developing a new concept in PDC bit in order to increase penetration rates and extend PDC bit life in non-homogeneous formations. The result is a Stinger conical shaped polycrystalline diamond element (CDE) with a thick synthetic diamond layer [36], see Figure 5.19. The geometric design of the element is supposed to deliverer a high point loading for effective formation fracture. To be able to do this the conical element is constructed with advanced synthetic diamond manufacturing systems specifically designed to generate higher pressures and temperatures during the sintering process while increasing micro-cell size for improved diamond quality [36]. Compared to the diamond layer on a conventional PDC cutter, the PCD layer on the CDE is approximately twice as thick. In addition, the conical element shows 25 % more wear resistance and the impact strength is almost doubled, see Figure 5.20.

FIGURE 5.19: Conical geometry with thick layer of synthetic diamond to enhance drilling efficiency and ROP [36].
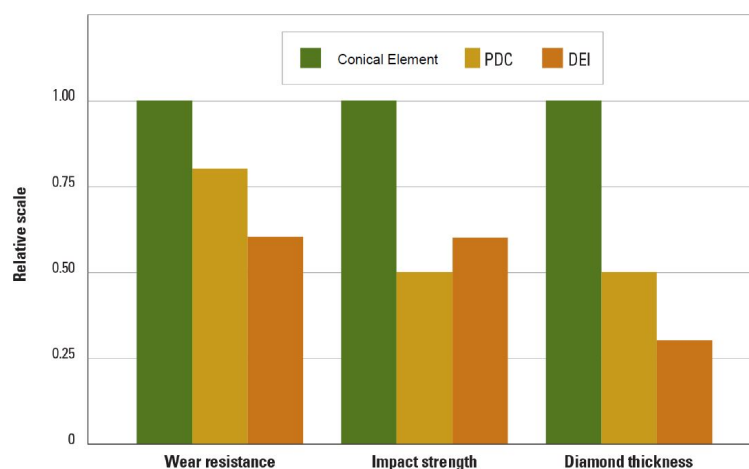
FIGURE 5.20: The conical element possesses superior wear/impact resistance compared to PDC cutters and DEI for roller-cone [36].

Single Element Testing. Extensive laboratory testing of the CDE was performed to evaluate its potential to increase total footage capabilities and to improve ROP. Compared to conventional PDC cutters, the CDE showed significant increases in resistance to impact damage and abrasive wear in a single-cutter test apparatus. The following was confirmed in a laboratory test using CDEs on a vertical turret lathe:

- At 0,02" depth of cut with 1200 lbs threshold, the CDE increased the cut efficiency with 70 % compared to the baseline PDC cutter.

- At 0,05" depth of cut with 1200 lbs threshold, the CDE increased the cut efficiency with 35 % compared to the baseline PDC cutter.

- Abrasion resistance was significantly improved over extended wet testing on a vertical turret lathe by the CDE.

PDC Performance Limiter. In order to determine how to incorporate the Stinger element into a PDC cutting structure, the focus was on the conventional PDC bit's problematic center cutting structure, or cone area which presents several distinct design challenges [36]:

1. The physical space limitation creates an inherent problem since designers cannot position multiple cutters in this location.

2. The lowest rotational velocity is experienced by the cutters at the bit center.

3. To produce an effective cutter layout to increase ROP, bit durability, stability and steerability the center most cutters, which is subjected to highest axial load, was studied in order to allow higher WOB.

4. A relatively small volume of formation is removed by the cone area cutters. This is an inefficient use of available energy to remove the rock.

There is an inherently inefficient shearing mechanism at the center of all conventional PDC bits, as can be seen in Figure 5.21. This limitation is especially evident when drilling through transitions zones with UCS variance, and when changing the WOB and rpm parameters. The depth of cut can vary considerably when the center cutters engage formation, impacting the overall behavior of the cutting structure. The resulting torque fluctuations alter the dynamic response, exposing the bit to damaging lateral/torsional shock and vibrations [36]. This will again lead to reduced ROP and the need for multiple trips to be able to complete the hole section. When drilling in hard formations the weakness of the center cutting structure design causes the cutters to break, leading to the need to change bit.
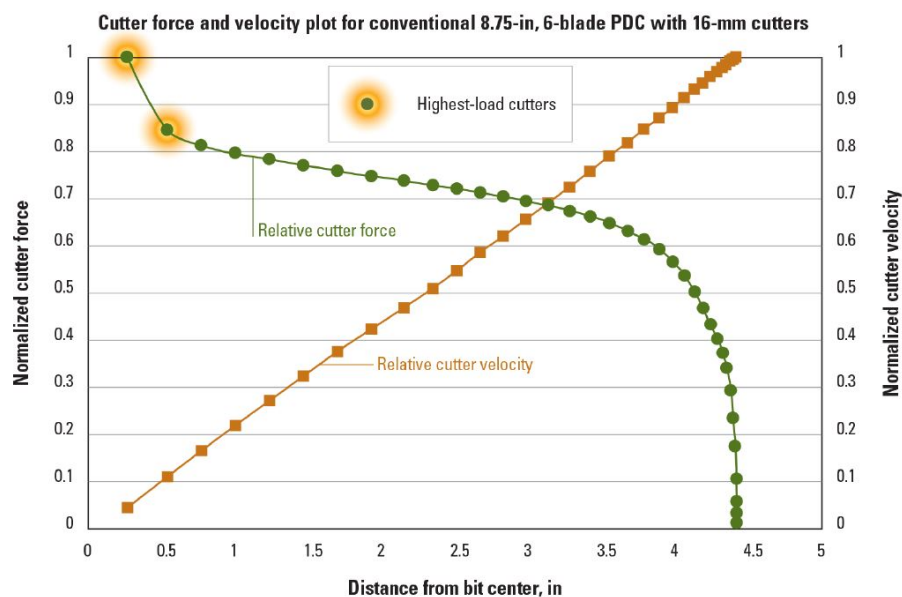
FIGURE 5.21: Conventional PDC bit design has difficulty with rock destruction at borehole center [36].

5.2.2 Design

The conical element was strategically positioned in the void space that allows a stress relieved rock column to develop in the bit's center, to allow continuously crushing of the confined rock column, see Figure 5.22. Cutter loading is improved by removing some of the standard PDC cutters which creates less division of WOB, improving overall drilling efficiency. Studies revealed that high stress conditions at the contact point can be achieved with significantly less applied force compared to conventional PDC cutters. This can increase the fracture generation within the rock. In addition, an increase in dynamic stability with less potential for vibrations have been displayed in bits equipped with a centrally located Stinger element.

Nozzle positions was adjusted to enhance cuttings removal and cleaning of the conical element and adjacent borehole [36].

Confirming Modifications. The principle of rock column formation is clearly illustrated in Figure 5.23. Significantly less energy is needed to fracture a rock column compared to a typical formation. This is because the rock column is less confined. Virtual testing confirmed that the Stinger bit would improve ROP. A full scale CDE-equipped PDC bit was tested in a pressurized drilling simulator to validate the virtual tests. The conclusions from the virtual tests were confirmed.
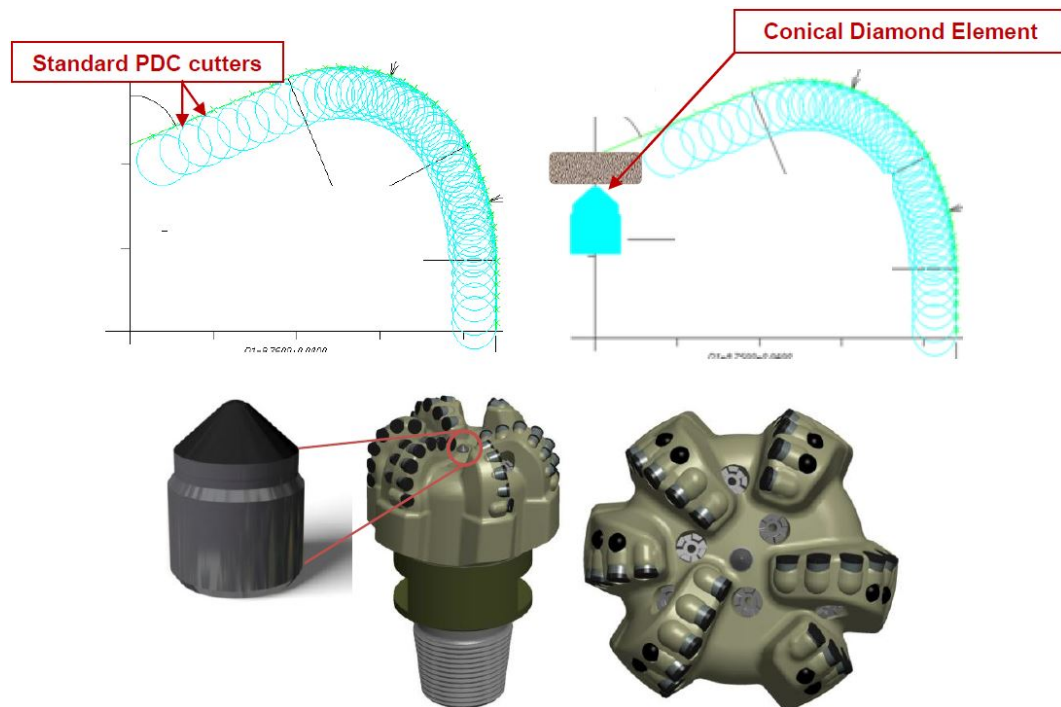
FIGURE 5.22: Conical element's center position delivers unique crushing action delivering high point loading [36].

The stress relieved rock column that is created in the center of the hole, which was crushed by the CDE, is shown in Figure 5.24.

The test also revealed that the Stinger bit creates much larger drill cuttings compared to the standard PDC bits. This is a great advantage for rock characterization at the surface by geologists or mud logging personnel. Figure 5.25 shows these enlarged cuttings. This makes the CDE PDC bit ideal for exploratory wells through a reservoir section or when determining exact wellbore position in the stratigraphic column is critical [36].
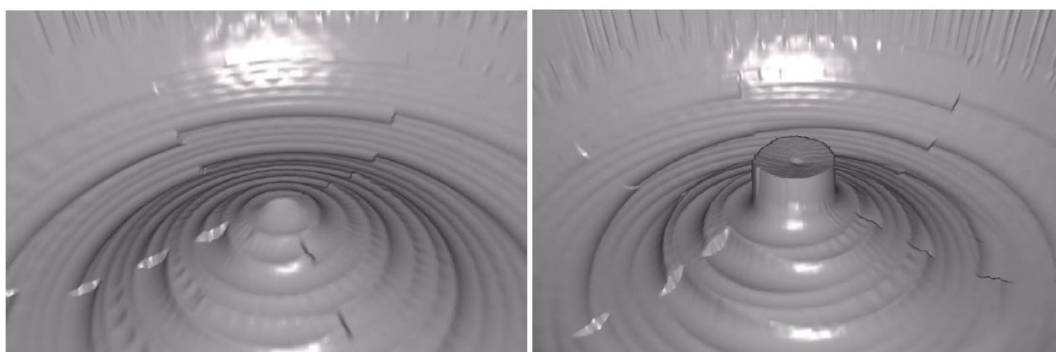
FIGURE 5.23: Modeling system used to simulate dynamic bit behavior confirmed ROP improvement in different lithologies [36].

FIGURE 5.24: Full scale drilling validated FEA-model with conventional PDC bit (left) and new CDE equipped bit (right) [36].

FIGURE 5.25: Large cuttings produced by CDE equipped PDC bit (right) greatly enhances geological/petrological evaluation [36].

Hole Quality. A laboratory test was performed in a Lazonby sandstone with UCS of 9.000 psi, constant bit revolution at 85 rpm and varying WOB, to measure variation in hole diameter. The results are presented in Figure 5.26, which shows that a conventional PDC bit have a greater tendency to produce an out-of-gauge diameter compared to the Stinger bit. Less energy was expended on unproductive movement and a more consistent hole diameter was achieved using the CDE-equipped Stinger bit.
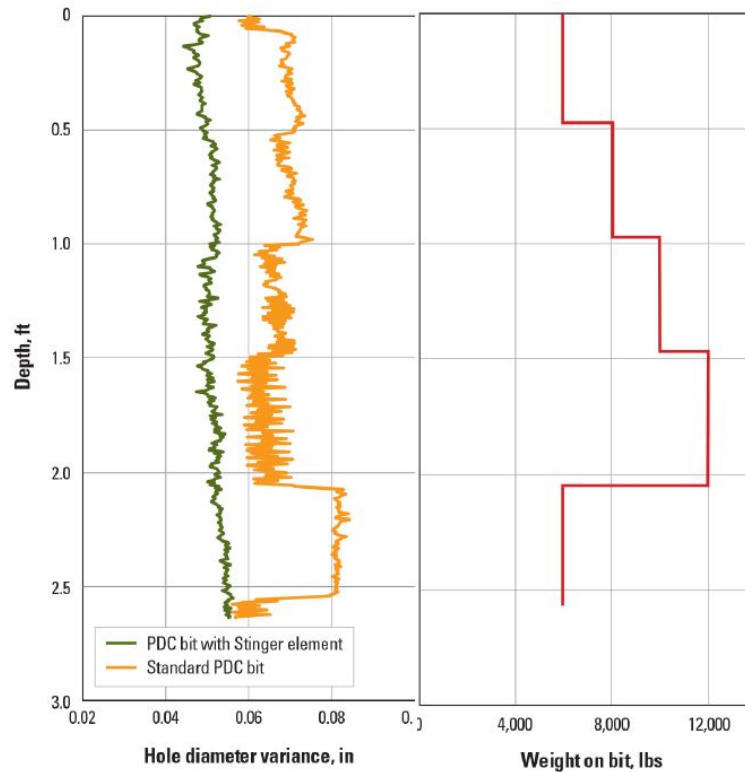
FIGURE 5.26: Laboratory testing confirmed bit with CDE demonstrates more stable drilling behavior for improved borehole quality [36].

5.2.3 Field Tests

North Dakota. An 8-3/4" Stinger bit was run on a motor BHA in three similar vertical holes through a highly mixed and interbedded sequence of formations, including limestone/dolomite/anhydrite, sand/shale and salt with UCS varying from 2.000-25.000 psi. As seen in Figure 5.27 all three CDE runs were faster compared to the best offset (131 ft/hr) and 56 % faster than the average of the 11 offset wells [36]. A new field record was set with the last run CDE bit, delivering the fastest 8-3/4" vertical drillout to kick off point in Divide County of 197,1 ft/hr. In addition, the record setting bit was in good condition with no wear on the CDE when pulled out of the hole.

East Texas. An 8-3/4" nine-bladed PDC bit with CDE and 13 mm cutters was run on a rotary steerable drive system and compared to the exact same bit, without the CDE, in the Cotton Valley field. The CDE bit drilled at 19,3 ft/hr, 5,5 % faster than the offset runs with the standard PDC, which drilled at 18,3 ft/hr. The CDE bit managed to deliver dogleg severity up to $11,2°/100\text{ft}$ and accomplished
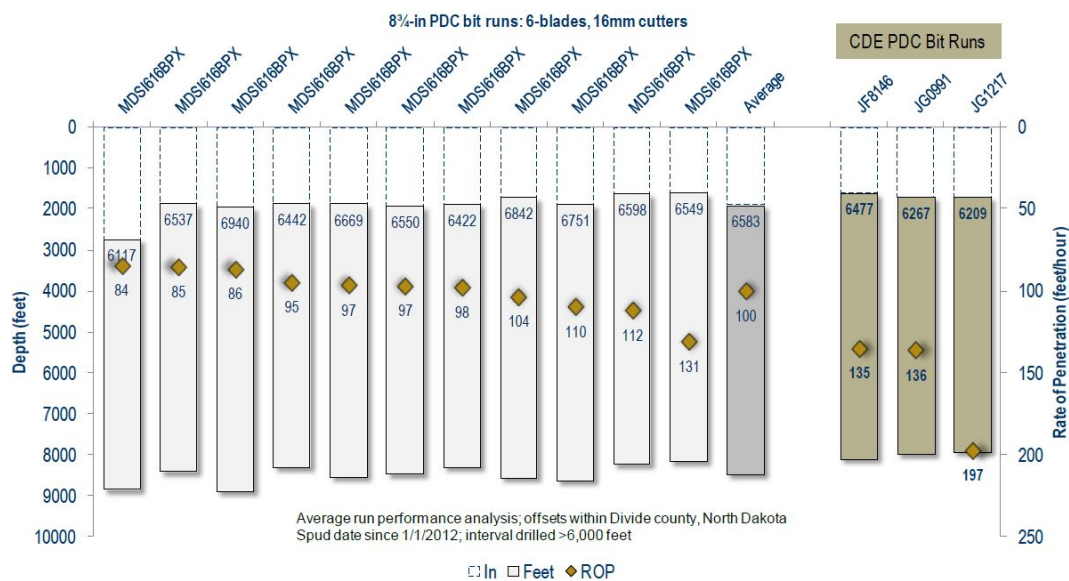
FIGURE 5.27: ROPs of three CDE runs is faster than the best offset drilled with conventional PDC bit [36].

all directional objectives. There was no significant difference in stability among the two bit types tested.

Middle East. A six-bladed 12-1/4" CDE PDC bit with 16 mm cutters was tested in the Zubair field in Iraq in an attempt to solve vibration issues causing low ROP. The formation consisted of medium-hard carbonates and interbedded intervals. A significant increase in ROP was achieved since the stick-slip and vibration levels were reduced, hence the WOB could be increased. The ROP was increased with 29 % compared to the best offset run of 18,5 m/hr, and with 56 % compared to the average of all three offset wells of 15,3 m/hr, as seen Figure 5.28. The improvement in ROP is directly attributed to the added CDE technology, as all three bits were run on the same type of rotary steerable BHA [36]. The CDE PDC bit showed no wear on the cutting structure or on the conical element after drilling 595 m. Figure 5.29 and 5.30 shows one of the conventional PDC bits compared to the CDE PDC bit after being pulled out of hole. In addition, due to the increased ROP the cost/meter was reduced by 27 % when using the Stinger bit, compared to the best offset, hence saving the operator $32.000 USD.
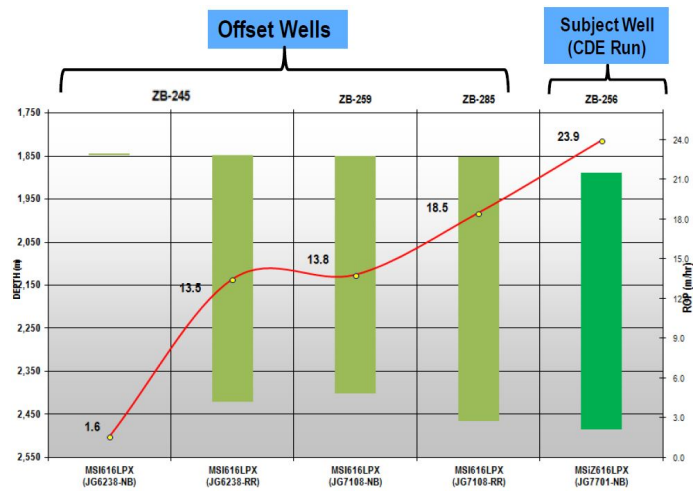
FIGURE 5.28: CDE PDC increased ROP by 29 % compared to the best offset run [36].

FIGURE 5.29: Standard PDC bit used in a offset well in Iraq [36].
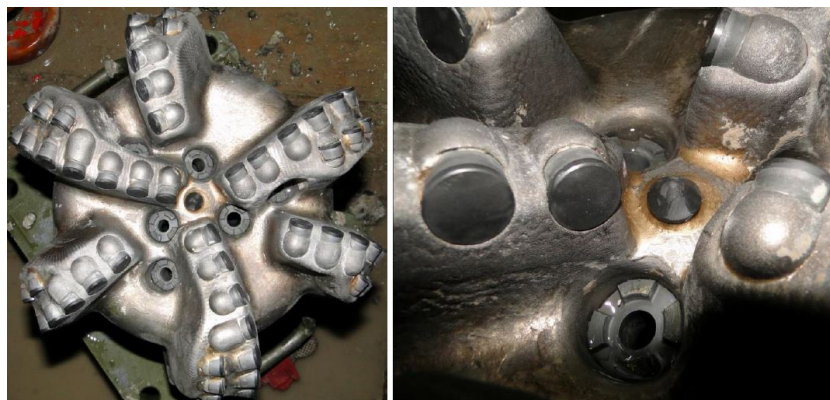
FIGURE 5.30: Removing center most cutters improved drilling efficiency and dull bit condition [36].

The results from the field tests. The field test performed indicate that the Stinger bit are improving ROP and bit stability in vertical, curved and lateral applications when drilling through difficult formations with a wide range of UCS values [36]. The improved bit stability, caused by the thick synthetic diamond on the CDE, reduces the potential for impact damage in the cone area. The conical element and void area forces the bit to rotate around its central axis, thereby increasing the dynamic stability while decreasing vibration. The result is longer runs and reduced cost of bit replacement trips.

Chapter 6

Rate of Penetration Modelling

In this chapter, the theory behind Bourgoyne and Young's ROP model is presented. Further, the procedure for how the modelling attempt was performed will be described.

6.1 Factors Affecting Penetration Rate

There are numerous factors and a large number of uncertainties that affect ROP, and their relationship is nonlinear and complex. Due to this complexity, previous studies have been focusing on the most important variables that affect ROP when trying to create ROP models. The factors that have been identified and studied are (1) bit type, (2) formation characteristics, (3) drilling fluid properties, (4) bit operating conditions (bit weight and rotary speed), (5) bit tooth wear, and (6) bit hydraulics [37].

6.1.1 Bit Type

The bit type that is used has a great effect on ROP [37]. Initially when the formation is soft the ROP is highest when rolling cutter bits are used, due to its long teeth and large cone offset angle. In hard formation, these bits are unpractical because of the quick destruction of the teeth, so drag bits are the preferred option here. Drag bits are designed to give a wedging-type rock failure. Because of this, the bit penetration per revolution depends on the number of blades and the bottom

cutting angle. The penetration per revolution for PCD and diamond depends on size, and the number of diamonds or PCD blanks on the bit.

6.1.2 Formation Characteristics

The most important formation properties affecting ROP are the elastic limit and the ultimate strength of the formation. Maurer [38] found in his studies that the crater volume produced beneath a single tooth is inversely proportional to the rock compressive strength and the rock shear strength. Bingham [39] reported in his studies that the threshold force required to initiate drilling in a given rock at atmospheric pressure could be correlated to the shear strength of the rock as determined in a compression test at atmospheric pressure.

The permeability of the formation is another parameter that has a profound effect on the ROP. This is because in permeable formations, the drilling fluid filtrates can penetrate into the formation ahead of the bit. This will equalize the differential pressure acting on the rock cutting that is formed beneath each bit tooth. This reduction in differential pressure will have a tendency to promote the more explosive elastic mode of crater formation, as described in Figure 6.1. This mechanism can also be affected by the nature of the fluid contained in the pore spaces of the formation. The reason for this is since more filtrate volume would be required to equalize the pressure in a formation containing gas than in a formation containing liquid. The last parameter of the formation characteristics that affects the ROP is the mineral composition of the formation. If the formation contains hard, rough minerals this can cause a quick dulling of the bit teeth. Bit balling can also occur in formations containing gummy clay minerals.
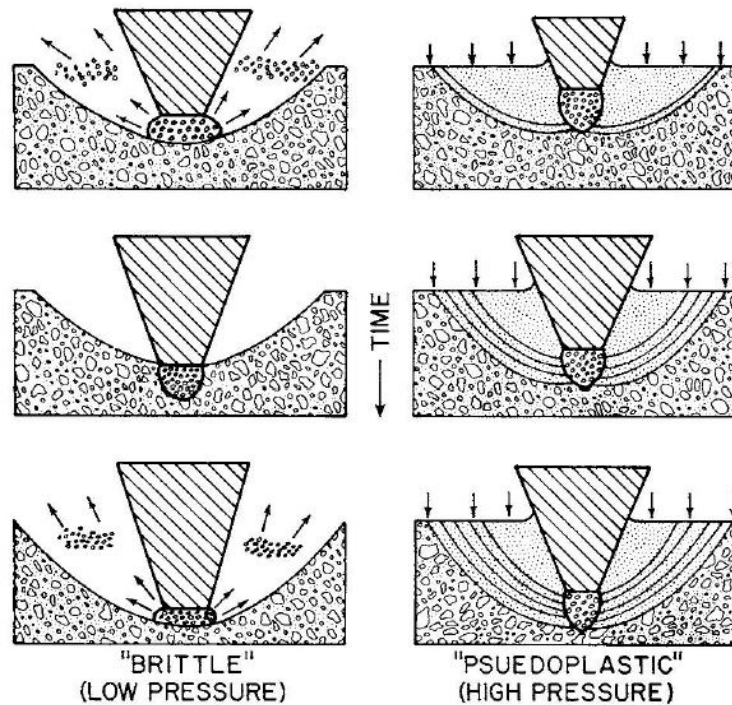
FIGURE 6.1: Fluid Pressure Affects Crater Mechanism [38].

6.1.3 Drilling Fluid Properties

The main properties reported to affect the ROP [37] include (1) density, (2) rheological flow properties, (3) filtration characteristics, (4) solids content and size distribution, and (5) chemical composition.

Penetration rate tends to decrease with increasing fluid density, viscosity, and solids content, and tends to increase with increasing filtration rate. The differential pressure across the zone of crushed rock beneath the bit is controlled by the density, solids content, and filtration characteristics of the mud. The fluid viscosity controls the parasitic frictional losses in the drillstring and the hydraulic energy available at the bit jets for cleaning. Estes [40] reported in his studies that the ROP was reduced when the viscosity is increased, even when the bit is perfectly clean. Penetration rate is affected by the chemical composition of the fluid. This is because the hydration rate and the bit balling tendency of some clays are affected by the chemical composition of the fluid.

Estes also reported that the presence of particles, which are less than 1 μm (colloid particles), is an order of magnitude more damaging to ROP than particles coarser

than approximately 30 μm. This is explained by the colloidal particles being much more efficient at plugging off the filtration beneath the bit.

Maurer [38] could obtain some insight into how an increase in drilling fluid density causes a decrease in ROP for rolling cutter bits. If the drilling fluid density is increased this causes an increase in the bottomhole pressure underneath the bit, which leads to an increase in the differential pressure between the borehole pressure and the formation fluid pressure. This is called *overbalance*, when the pressure in the borehole is larger than the pressure in the formation. Figure 6.1 shows that with increasing overbalance, the crater formation mechanism changes. This effect of overbalance can also be predicted on drag bit performance [37] by the Mohr failure criteria given by Equation (6.1). This shows that for a wedging-type failure mechanism, the normal stress at the failure plane σ_n is directly connected to overbalance.

$$\sigma_n = 0,5(\sigma_1 + \sigma_3) - 0,5(\sigma_1 - \sigma_3)\cos(2\phi) \tag{6.1}$$

The effects of overbalance on ROP were studied by Cunningham and Eenink [41] on numerous rock permeabilities. The results acquired in Berea sandstone with permeability between 150 to 450 mD are shown in Figure 6.2. The results acquired in Indiana limestone with permeability between 8 to 10 mD are shown in Figure 6.3. The effect of overbalance is similar in both cases. Apparently, the formation damage underneath the bit caused by the filter cake, and the formation solids prevented a flow of mud filtrate ahead of the bit sufficient to equalize the pressure differential [37]. Note that the effect of overbalance on ROP is more significant at low values compared to high values. It has basically no effect on ROP if a high overbalance is increased.

In the report made by Garnier and van Lingen [42] they concluded that the effective overbalance during rock chip removal by a drag bit often can be larger than the difference between the static borehole and rock pore pressures. There can be created a vacuum under the chip when it is lifted, unless adequate amounts of liquid are able to fill the opening void space. This empty space can only be filled by (1) formation fluid entering the void space from the rock beneath the chip, (2) drilling fluid flowing into the void through the fracture created, and (3) drilling fluid flowing through the pores of the chip and into the void space. Garnier and van Lingen found that when using clay/water as drilling fluid in a low permeability
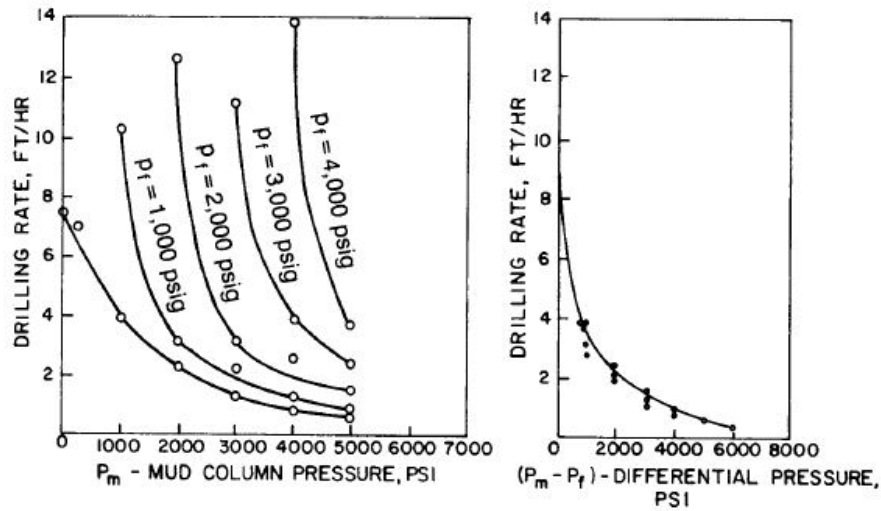
FIGURE 6.2: The effect of overbalance on ROP in Berea sandstone with clay/water mud and 1,25" rolling cutter bit [37].
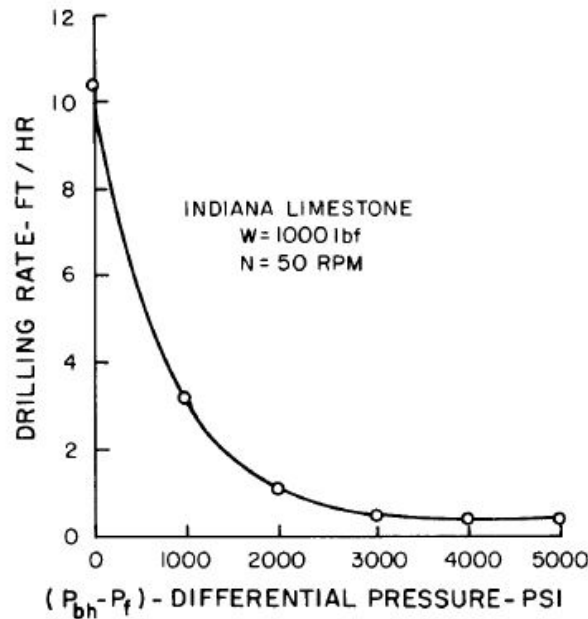
FIGURE 6.3: The effect of overbalance on ROP in Indiana limestone with clay/water mud and 1,25" rolling cutter bit [37].

formation, the filter cake created will slow down the flow of liquid. The flow into the void beneath the chip will be to slow to prevent a pressure reduction beneath the chip. This is shown in Figure 6.4, which was acquired keeping the static pore pressure and the wellbore pressure at the same value. Note from the figure that ROP decreases with increasing mud pressure when mud is used as drilling fluid, although the static overbalance is being held constant. This shows that the static overbalance was surpassed by the effective dynamic overbalance during

chip formation. When water was used as drilling fluid, the pressure equalized at a quicker rate for formations of moderate permeability, and the ROP remained constant when the mud pressure was increased.
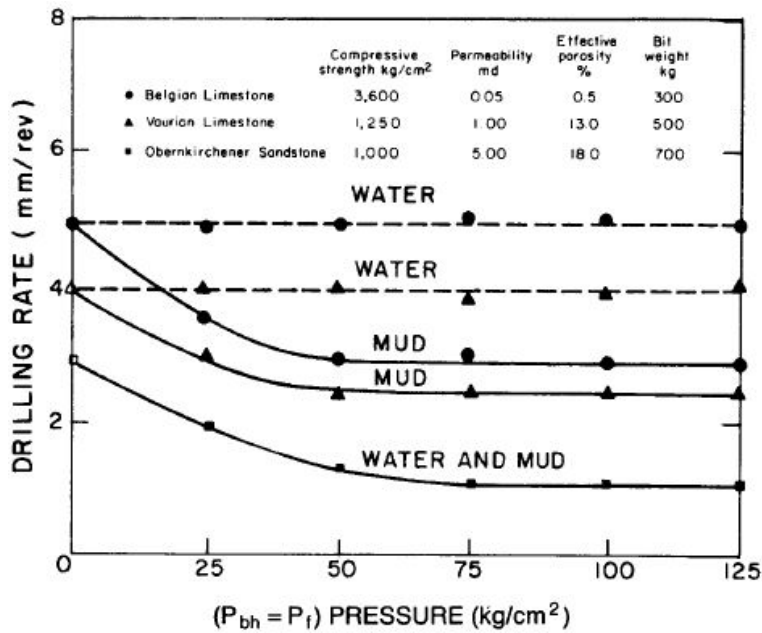
FIGURE 6.4: Effect of drilling fluid and rock permeability on effective overbalance at 32 rpm [37].

To achieve their results, Garnier and van Lingen used several levels of borehole pressure while keeping the pore pressure constant at an atmospheric pressure. Since the pore pressure was low, both the static and dynamic overbalance was basically equal. Figure 6.5 shows the results obtained using a (1) 1,25" double-blade drag bit, (2) diamond core bit, and (3) 3 7/8" tricone rolling cutter bit.
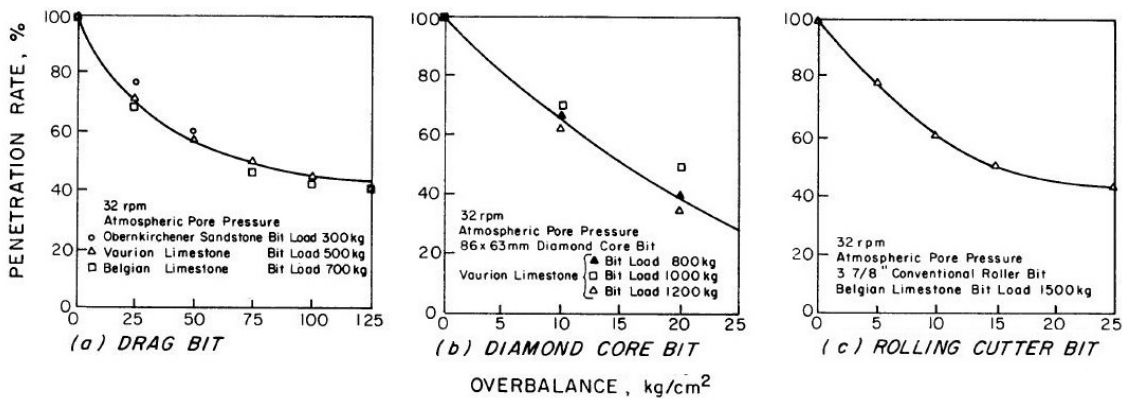
FIGURE 6.5: Comparison on effect of overbalance on penetration rate [37].

Black and Green [43] could confirm the results regarding the effect of overbalance on ROP made in small-scale laboratory tests by using full-scale bits in a high-pressure wellbore simulator. Figure 6.6 shows the results obtained in a Colton Sandstone with permeability of 40 μD and unconfined compressive strength of 7600 psi.
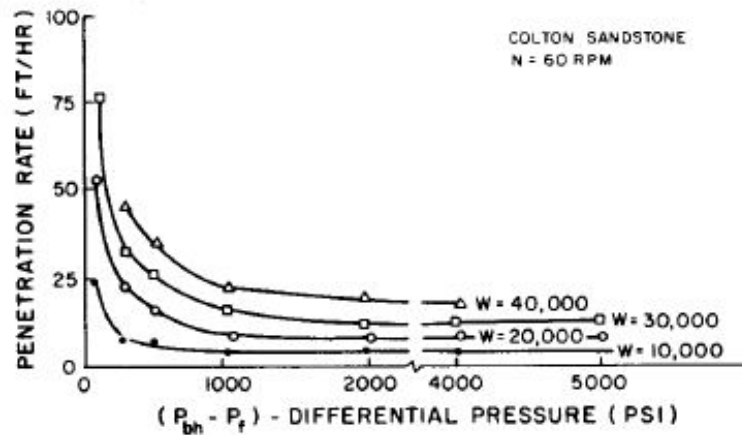
FIGURE 6.6: Penetration rate as a function of overbalance for Colton Sandstone [37].

Vidrine and Benit [44] studied the effect of overbalance on ROP when gathering field data in seven wells drilled in south Louisiana. The results made by Vidrine and Benit are similar to the results made by Cunningham and Eenik. Figure 6.7 shows data obtained in well D with an 8,5" rolling cutter bit at approximately 12000 ft.

In their study, Bourgoyne and Young [45] found that the relationship between ROP and overbalance could be represented by a straight line on a semi-log plot for the most common ranges of overbalance used in the field. They also proposed normalizing the ROP data by dividing by the ROP equal to zero overbalance. Figure 6.8 shows the suggested model by Bourgoyne and Young. It appears that a relatively straight line can be drawn to represent the data for moderate values of overbalance. The equation for this straight line can be expressed by

$$log \frac{R}{R_0} = -m(p_{bh} - p_f) \tag{6.2}$$

where

$R = $ ROP,

$R_0 = $ ROP at zero overbalance,

$p_{bh} = $ bottomhole pressure in the borehole,

$p_f = $ formation fluid pressure, and

$m = $ the slope of the line.

If the expression for overbalance is expressed in terms of equivalent circulating mud density $(ECD)_{\rho_c}$ and pore pressure gradient g_p, it gets

$$(p_{bh} - p_f) = 0,052D(\rho_c - g_p).$$

Putting this expression into Equation 6.2 yields

$$log\frac{R}{R_0} = -0,052mD(\rho_c - g_p) = 0,052mD(g_p - \rho_c)$$

Bourgoyne and Young chose to replace the constants $(0,052m)$ with the coefficient a_4, so the final expression relating changes in mud density or pore pressure to ROP is

$$log\frac{R}{R_0} = a_4D(g_p - \rho_c) \tag{6.3}$$
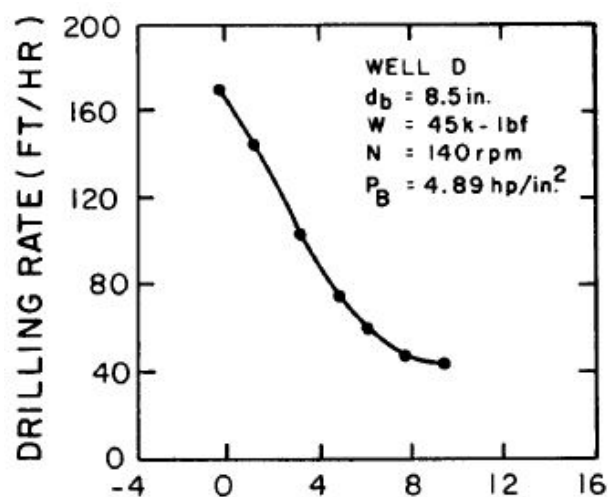
FIGURE 6.7: Field measurement of the effect of overbalance on penetration rate in shale [37].
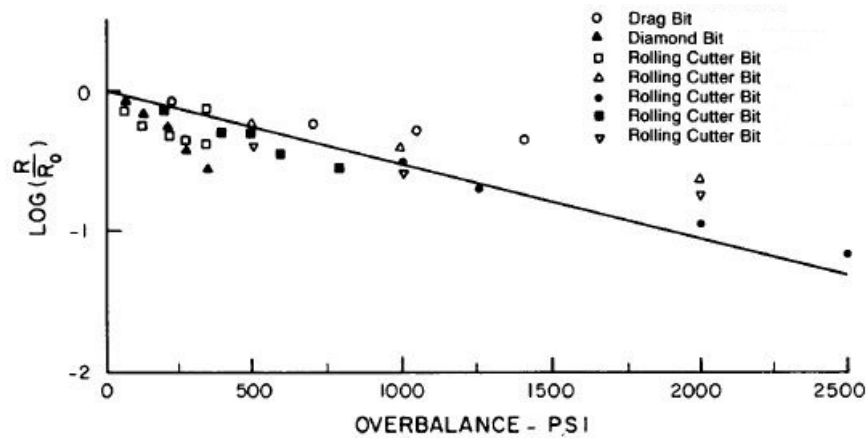
FIGURE 6.8: Exponential relation between ROP and overbalance for rolling cutter bits [37].

6.1.4 Operating Conditions

Two of the most important parameters on ROP are the bit weight and rotary speed. The characteristic plot of ROP against bit weight obtained when holding all other variables constant is shown in Figure 6.9. As the figure shows, penetration is not initiated until the threshold bit weight has been reached (point a). When penetration starts it increases quickly with increasing values of bit weight (segment ab). At moderate rates of bit weight, a linear curve can be observed (segment bc). When the bit weight gets to a certain level, any increase in bit weight will only increase the ROP slightly (segment cd). In extreme levels of bit weight, the ROP can actually decrease. This is called *bit floundering*. This halt or decrease in ROP is usually due to poor bottomhole cleaning at high rates of cutting generation or to a complete penetration of the cutting element into the hole bottom.
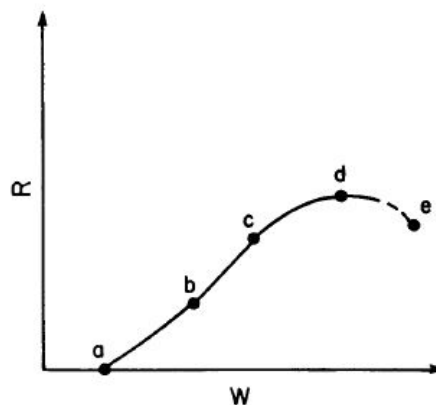
FIGURE 6.9: The response of ROP to increasing bit weight [37].
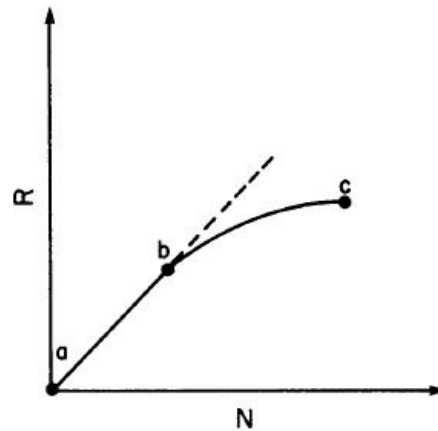
FIGURE 6.10: The response of ROP to increasing rotary speed [37].

The characteristic plot of ROP against rotary speed obtained when holding all other variables constant is shown in Figure 6.10. At low values of rotary speed, the ROP normally increases linearly (segment ab). At high values of rotary speed the ROP decreases (segment bc). This decrease is also explained by poor bottomhole cleaning.

Maurer [46] could derive a theoretical equation for rolling cutter bits connecting ROP to bit weight, rotary speed, bit size, and rock strength. The experiments were done with single tooth impact, and the following observations were found; (1) The crater volume is equivalent to the square of the depth of cutter penetration, and (2) the depth of cutter penetration is inversely proportional to the rock strength. Note that this equation assumes perfect bottomhole cleaning and incomplete bit tooth penetration.

The ROP, R, is given by

$$R = \frac{K}{S^2} \left(\frac{W}{d_b} - (\frac{W_0}{d_b})_t \right)^2 N \tag{6.4}$$

Where

K = constant of proportionality,

S = compressive strength of the rock,

W = bit weight,

W_0 = threshold bit weight

d_b = bit diameter, and

N = rotary speed.

By using experimental data acquired at low values of bit weight and rotary speed, the theoretical equation of Maurer can be confirmed. This is equivalent to segment ab in Figure 6.9 and 6.10. When the bit weight is increased to a moderate value, the weight exponent is actually closer to a value of one than the predicted value of two given by Equation 6.4. When the bit weight reaches high values, the weight exponent usually is less than one. Based on the substantial laboratory and field data, Bingham [39] proposed the following equation

$$R = K \left(\frac{W}{d_b} \right)^{a_5} N \tag{6.5}$$

K is still the constant of proportionality that takes into account rock strength, and a_5 represent the bit weight exponent.

Bingham chose to assume the threshold bit weight to be negligible in this equation. He also used a constant rotary speed exponent of one, despite some of his data showed behavior comparable to that described in segment bc in Fig 6.10. The bit weight exponent must be found experimentally for the existing conditions.

Young [47] developed a computerized system in which both bit weight and rotary speed could be varied. These two parameters were systematically changed when a new lithology was encountered. The bit weight and rotary speed exponent were automatically computed from the ROP response. The results obtained for the bit weight exponent value is between 0,6 and 2,0 and 0,4 to 0,9 for the rotary speed exponent.

Measuring ROP from bit weight and rotary speed can be difficult as lithology changes frequently. Often the lithology change before the test is complete, and this will give inaccurate results. To overcome this problem a *drilloff* test can be executed. Drilloff tests are performed by applying a large WOB, lock the brakes while keeping the rotary speed constant and monitoring the reduction in bit weight. The next step is to calculate the amount the drillstring has stretched as the as the bit weight decreased and the hook load increased. This is done by using Hooke's law of elasticity. By following this procedure the response in ROP to change in bit weight can be determined over a short depth interval.

Hooke's law says that the change in stress is directly proportional to the change in strain.

$$\Delta\sigma = E\Delta\epsilon \tag{6.6}$$

In a drillstring, the stress change is equal to the change in axial tension (bit weight) divided by the cross-sectional area of the drillpipe. The change in strain equals the change in drillpipe length per unit length. This gives

$$\frac{\Delta W}{A_S} = E\frac{\Delta L}{L}$$

Solving for ΔL gives

$$\Delta L = \frac{L}{EA_S}\Delta W$$

By dividing this equation by the time elapsed to drill off the bit weight ΔW we get the average ROP given for the change in bit weight.

$$R = \frac{\Delta W}{\Delta t} = \frac{L}{EA_S}\frac{\Delta W}{\Delta t}$$

Approximately 5 % of the total length of range two drillpipes consist of tool joints, which in essence does not contribute to the length change in the pipe, due to a larger cross-sectional area. Therefor the L in the equation is replaced by 0,95L. This gives the final equation

$$R = 0,95\frac{L}{EA_S}\frac{\Delta W}{\Delta t} \tag{6.7}$$

Note that the length change in drill collars is small enough to be neglected.

6.1.5 Bit Tooth Wear

Gradually as bits are used, they tend to drill slower due to tooth wear. The tooth length of milled tooth rolling cutter bits is continually shrunk by abrasion and

chipping. Even though the bit teeth are designed to have a self-sharpening type of tooth wear, this does not compensate for the reduction in tooth length. A method to reduce the tooth wear is to use tungsten carbide insert-type rolling cutter bits. The teeth of these bits fail by breaking instead of wear and tear, and often the entire tooth breaks of. This also applies for diamond bits, which fail from tooth breakage or loss of diamonds from the matrix. Since the milled tooth bits wear quicker than insert bits, unless a large number of teeth break of, the reduction in ROP is larger for these bits.

Several mathematical models have been proposed by different authors for calculating the effect tooth wear has on ROP for rolling-cutter bits. Galle and Woods [48] suggested this model

$$R \propto \left(\frac{1}{0,928125h^2 + 6h + 1} \right)_7^a \tag{6.8}$$

where h represents the tooth height that has been worn down, and a_7 is an exponent with the recommended value of 0,5.

Bourgoyne and Young [45] proposed another model that is similar but simpler

$$R \propto e^{-a_7 h} \tag{6.9}$$

The a_7 exponent in this equation is supposed to be determined based on ROP declination and bit wear observations previously made when drilling in similar conditions.

6.1.6 Bit Hydraulics

In 1953, the jet-type rolling cutter bits was introduced. By improving the jetting action at the bit, and thereby improving the bottomhole cleaning and the bit teeth cleaning, the jet-bit made a significant increase in ROP. Eckel could prove that when the discharge ends of the jets are close to the formation this will provide the most effective jetting action [49]. This occurs when using extended-nozzle bits that bring the jet closer to the bottom of the hole. Pratt [50] found in his studies that the ROP would be increased by 15 - 40 % by using extended-nozzle bits. To

prevent bit balling, a center jet is necessary when using the extended-nozzle bits. Figure 6.11 shows a drawing of an extended-nozzle bit.

The flounder point of the bit is thought to be affected by the level of hydraulics achieved at the bit. When the ROP and bit weight is small, there is not much need for hydraulics for hole cleaning. However, as the ROP and the generated level of cutting's increases, eventually a flounder point is reached where the generation of cuttings is larger than the rate of removal. The higher the level of hydraulics, the more WOB can be used before this floundering point occurs. Figure 6.12 shows hypothetical relationship between ROP and bit hydraulics.

As mentioned earlier, Eckel has studied the effect of hydraulics on ROP, working with microbits in a laboratory drilling machine. When applying constant WOB and rotary speed, he could show that ROP could be related to a Reynold's number group given by

$$N_{Re} = K \frac{\rho \ vd}{\mu_a} \tag{6.10}$$

K = a scaling constant,

ρ = drilling density,

v = flow rate,

d = nozzle diameter, and

μ_a = apparent viscosity of drilling fluid at 10000 seconds^{-1}.

As there are shear rates present in the bit nozzle, the shear rate of 10000 seconds^{-1} was chosen to represent these. Eckel chose to use a constant value of 1/1976 for the scaling constant K to get a suitable range of the Reynold's number, but this value seems somewhat arbitrary.

When Eckel experimented with increasing the Reynold's number, the ROP increased as shown in Figure 6.13. When the bit weight was increased, Eckel found that the correlation curve was moved upwards as shown in Figure 6.14

Even though the correlation shown in Figure 6.13 and 6.14 is quite convincing, Eckel's results have not been widely used in practice. When developing correlations
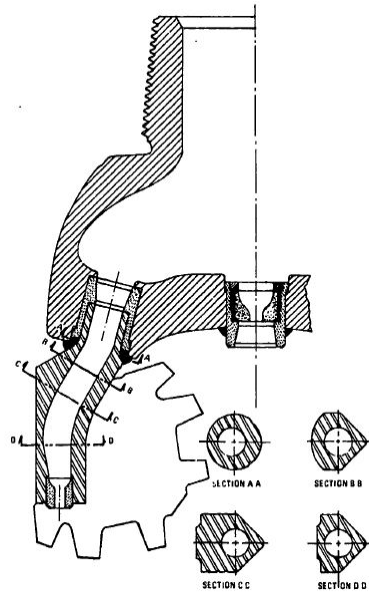
FIGURE 6.11: Conceptual drawing of a extended-nozzle bit [50].
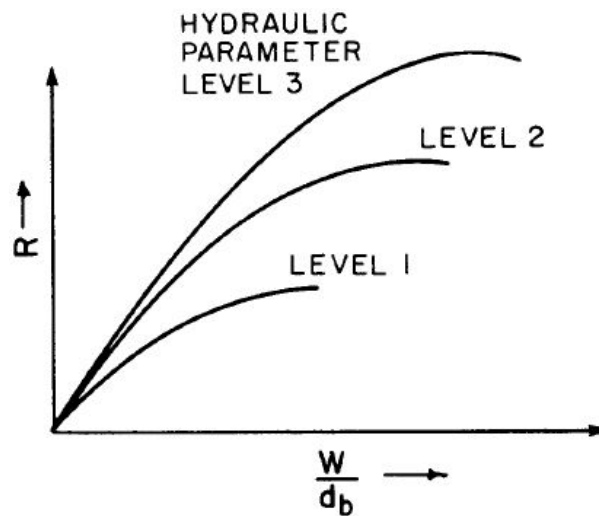
FIGURE 6.12: Expected relationship between bit hydraulics and penetration rate [37].

between ROP and bit hydraulics, jet impact force and hydraulic horsepower are more often used compared to Eckel's jet Reynold's number group. During Tibbitts' [51] full-scale laboratory drilling experiment under simulated borehole conditions, he found that the jet impact force, hydraulic horsepower and jet Reynold's number group all gave equal results when used to correlate the ROP to the effect of jet bit hydraulics. These results, obtained in Mancos shale with a 7 7/8" Smith F3 bit are shown in Figure 6.15, 6.16 and 6.17.
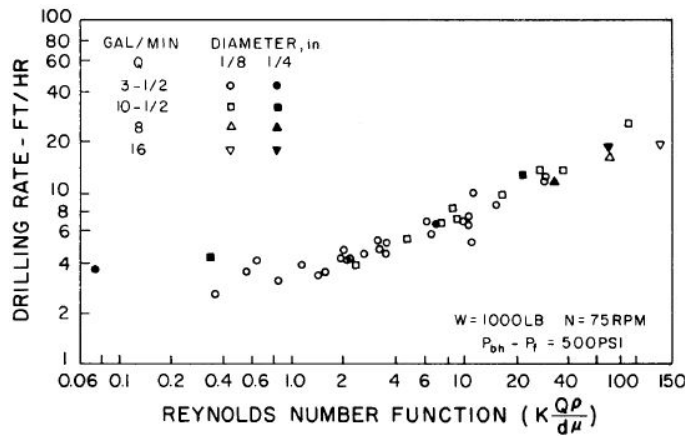
FIGURE 6.13: Penetration rates as a function of bit Reynold's number [37].
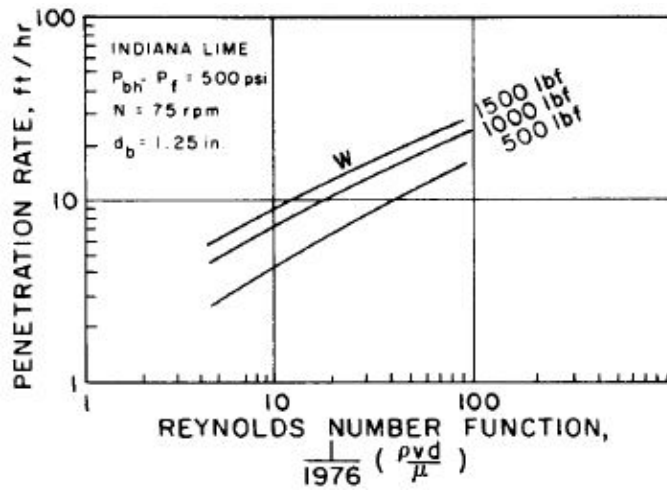
FIGURE 6.14: Observed effect of bit weight and bit Reynold's number on penetration rate [37].
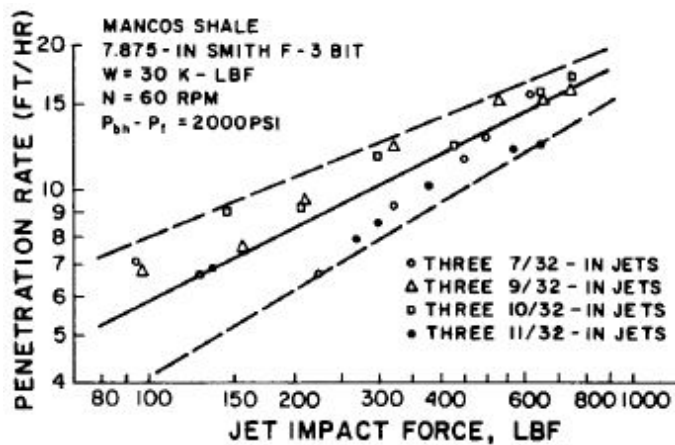
FIGURE 6.15: Observed correlation using jet impact force as hydraulics parameter on penetration rate in Mancos shale under simulated borehole conditions [37].
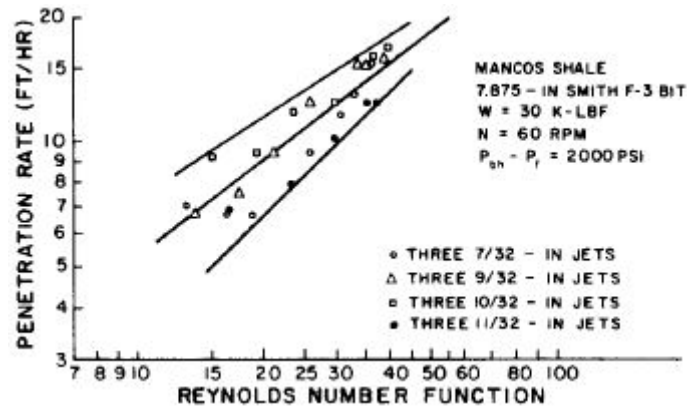
FIGURE 6.16: Observed correlation using Reynold's number function as hydraulics parameter on penetration rate in Mancos shale under simulated borehole conditions [37].
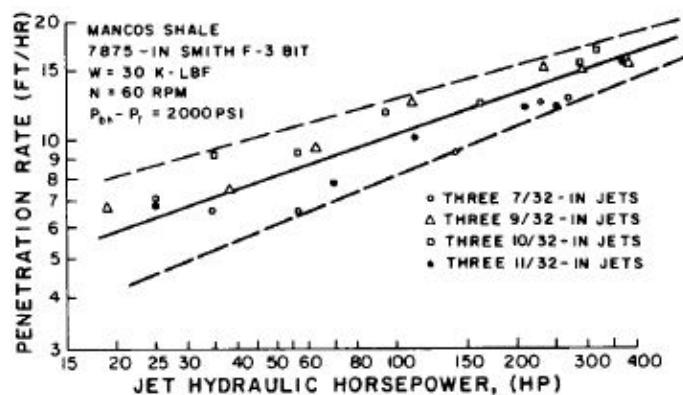
FIGURE 6.17: Observed correlation using jet hydraulic horsepower as hydraulics parameter on penetration rate in Mancos shale under simulated borehole conditions [37].

6.1.7 Penetration Rate Equation

How the parameters, discussed in this chapter, affect ROP is complex, and therefore, are they only partially understood. As a result, there has still not been developed a completely accurate mathematical model of the rotary drilling process. However, there have been many attempts to create a arithmetical model that can take into account the known relationship between the different parameters. These models have been applied by using formal optimization methods to solve the problem of selecting the best rotary speed and bit weight to achieve as low as possible cost per foot drilled. There has been reported [45], [47], [48] several successful applications of these approximate mathematical models, which have resulted in significant reductions in drilling cost.

Some bits are designed to give a maximum penetration per revolution, in particular, diamond bits and other types of drag bits. If the conditions are perfect, the bit weight and torque are such that the bit keeps feeding into the formation at the design cutting rate. For a given penetration of the cutting element into the formation, the ROP of a drag bit is given by

$$R = L_{pe}n_{be}N \tag{6.11}$$

L_{pe} = effective penetration of each cutting element,

n_{be} = effective number of blades, and

N = rotary speed.

There has been developed theoretical equations for the effective number of blades n_{be} and for the efficient penetration L_{pe} by Peterson [52]. To be able to derive the equations, Peterson used a simplified model which assumes the following:

- The face of the bit is flat and perpendicular to the axis of the hole.

- The diamond in each bit is aligned as a helix as shown in Figure 6.18a.

- The stones have a spherical shape as shown in Figure 6.18b.

- The diamonds are spaced so that the cross-sectional area removed per stone is a maximum for the design depth of penetration.

- The bit is operated at the design depth of penetration.

- There is perfect bottom hole cleaning provided by the bit hydraulics.

Under these conditions, the equations for effective penetration L_{pe} and the effective number of blade's n_{be} yields

$$L_{pe} = 0,67L_p \tag{6.12}$$

and

$$n_{be} = 1,92 \left(\frac{C_c}{s_d}\right) d_b \sqrt{d_b L_p - L_p^2} \tag{6.13}$$

where

C_c = concentration of diamond cutters, carats/in^2,

L_p = actual depth of penetration of each stone, in.,

d_b = bit diameter, in.,

d_c = average diameter of the face stone cutters, in., and

s_d = diamond size, carats/stone.

To find the bit weight required to acquire the design penetration L_p, a formation property named the *formation resistance, r_f*, is used to compute the bit weight. To be able to penetrate the rock with the stone, the formation strength needs to be overcome. The pressure needed to do so is the formation resistance, given by

$$r_f = \frac{W_e}{A_{dt}} \tag{6.14}$$

where A_{dt} is the total diamond area in contact with the formation, and W_e is the effective weight applied to the bit when including the hydraulic pumpoff forces. In order to calculate the formation resistance, the observed ROP for a bit operated in the formation of interest needs to be used.

The contact area for a spherical stone as shown in Figure 6.18b is given by

$$A_{dt} = \frac{\pi^2 d_b^2}{4} \left(\frac{C_c}{s_d}\right) (d_c L_p - L_p^2) \tag{6.15}$$
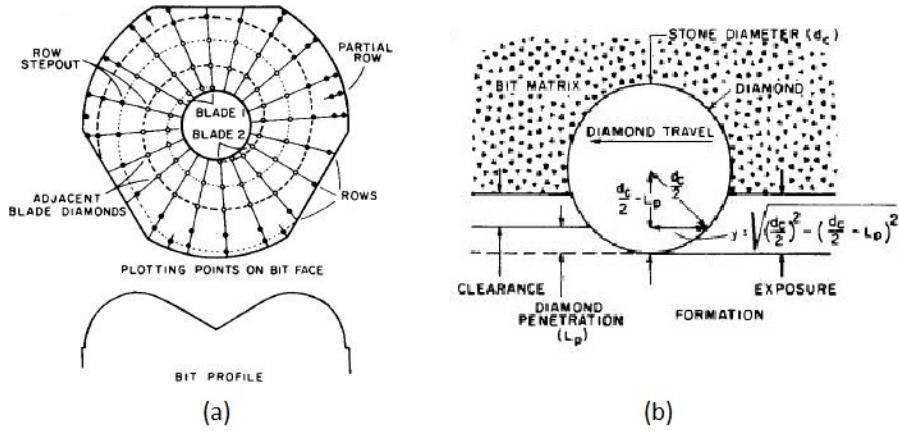
FIGURE 6.18: Diamond bit stone layout assumed in penetration rate equation [37].

When ROP models have been suggested, the approach has been to assume that the effects of the different parameters effecting ROP are all independent of each other and that the combined effect can be computed with an equation like this

$$R = (f_1)(f_2)(f_3)(f_4)...(f_n) \tag{6.16}$$

where f_1, f_2, f_3, f_4, etc., is the functional relationship between the different drilling parameters and ROP. The operational relations are normally based on trends observed in laboratory or field studies. To find empirical mathematical equations, some authors have chosen to define the functional relation graphically and others have used curve fitting techniques.

Bourgoyne and Young [45] have presented what is probably the most complete mathematical drilling model used for rolling cutter bits. Their model involves using eight different functions to model the effect of most of the drilling parameters discussed. The Bourgoyne-Young is defined by Equation 6.16 combined with these functional relations

$$f_1 = \exp^{2,303a_1} = K \tag{6.17}$$

$$f_2 = \exp^{2,303a_2(10000-D)} \tag{6.18}$$

$$f_3 = \exp^{2,303a_3 D^{0,69}(g_p - 9,0)} \tag{6.19}$$

$$f_4 = \exp^{2,303a_4 D(g_p - p_c)} \tag{6.20}$$

$$f_5 = \left[\frac{\left(\frac{W}{d_b}\right) - \left(\frac{W}{d_b}\right)_t}{4 - \left(\frac{W}{d_b}\right)_t} \right]^{a_5} \tag{6.21}$$

$$f_6 = \left(\frac{N}{60}\right)^{a_6} \tag{6.22}$$

$$f_7 = \exp^{-a_7 h} \tag{6.23}$$

$$f_8 = \left(\frac{F_j}{1000}\right)^{a_8} \tag{6.24}$$

where

D = true vertical well depth, ft,

g_p = pore pressure gradient, lbm/gal,

ρ_c = equivalent circulating density,

$(W/d_b)_t$ = threshold bit weight per inch of bit diameter, 1000 lbf/in.,

h = fractional tooth dullness,

F_j = hydraulic impact force beneath the bit, lbf, and

a_1 *to* a_8 = constants that must be chosen based on local drilling conditions.

To acquire the constants a_1 through a_8 detailed drilling data obtained in the area must be used for computation. In addition to drilling optimization calculations, this drilling model can be used to detect changes in formation pore pressure, but how to do this will not be presented in this report.

The effects of formation strength and bit type on ROP are represented by the function f_1. This function includes the effect of drilling variables such as type of mud, solids content, etc., which are not included in the drilling model. For computing the values of a_1 through a_8 Bourgoyne and Young [45] suggested using a multiple regression technique. The exponential expression for f_1 is useful when applying this multiple regression technique. The reason for the coefficient "2,303" is to allow the constant a_1 to be defined easily in terms of the common logarithm of an observed ROP.

The compaction effect on ROP is modeled by the functions f_2 and f_3. Here f_2 takes into account the rock strength increase due to normal compaction of the formation with depth. The f_3 function represents the effect of under-compaction that can occur in abnormally pressured formations. The product of $f_2 f_3$ is equal to 1,0 when the pore pressure gradient equivalent to 9,0 lbm/gal and a depth of 10000 ft.

The effect of overbalance in the borehole on ROP is modeled by the function f_4. If the formation pressure is identical to the borehole pressure in the well – i.e., there is no overbalance, then the value of f_4 is equal to zero.

The functions f_5 and f_6 represent the effect of bit weight and rotary speed on ROP. If the bit weight (W/d_b) is 4000 lbf/in. of bit diameter subsequently f_5 has a value of 1,0 and if the rotary speed is 60 rpm, then f_6 is equal to 1,0. The reason for this is so that the product of $f_2 f_6$ would have a value close to 1,0 for the most common drilling conditions. Where the formation is soft, the threshold bit weight is small and can be ignored. In harder formations, the threshold bit weight can be estimated from drilloff tests performed at low bit weight. The upper limit of the function f_5 corresponds to the bit flounder point, which must be established from drilloff tests. The constants a_5 and a_6 can in addition be established from a drilloff test. The reported values of a_5 range between 0,4 to 2,0 and the values of a_6 is between 0,4 to 1,0.

The effect of tooth wear on ROP is modeled by the function f_7. To estimate the value of a_7, the ROP measurements taken in a related formation at similar bit operating conditions, at the start and at the end of a bit run is used. If the tooth wear is nonexistent, then the value of f_7 is equal to 1,0. This is often the case when operating with tungsten carbide insert bits at moderate bit weight and rotary speed. The bit wear is then insignificant, and the f_7 term can be neglected.

For a_7 the typical values' ranges from 0,3 to 1,5. Note that this is for milled tooth bits.

The effect of bit hydraulics on ROP is modeled by the function f_8. The hydraulic parameter used is jet impact force, with a normalized value for f_8 of 1,0 at 1000 lbf. As seen in Figure 6.15, 6.16 and 6.17 the choice of hydraulic impact force is random. By using the bit hydraulic horsepower or nozzle Reynold's number, the results would be similar as to jet impact force. The normal values for a_8 range between 0,3 to 0,6.

When applying this method and these equations it is wise to select the best average value for the values of a_2 through a_8 for the formation types in the depth interval of interest. The value of f_1 varies with the strength of the formation that is being drilled. The term f_1 is usually called the drillability of the formation because it is expressed in the same units as ROP. If the drilling is performed in a normally compacted formation, with a new bit, there is zero overbalance, the bit weight is 4000 lbf/in., the rotary speed is 60 rpm, and at a depth of 10000 ft, then the drillability would be numerically equal to the ROP that would be observed in the given formation type. By using drilling data collected in previous wells in an area, it is possible to compute the drillability of various formations.

6.2 Procedure

Bourgoyne and Young's drilling model uses eight different parameters for modelling the ROP. These are (1) depth [ft], (2) actual ROP [ft/hr], (3) WOB [lbf], (4) rotary speed of the bit [rpm], (5) tooth wear, (6) jet impact force [lbf], (7) ECD [lbm/gal], and (8) the pore pressure gradient [lbm/gal]. All of these parameters must be acquired from drilling data. When these parameters have been obtained, there are four steps to follow before the modelling is complete.

Step 1 - Choose Data Points. Since the ROP model by Bourgoyne and Young takes into account eight variables, this gives eight equations with eight unknowns, $a_1 - a_8$. This requires at least eight independent equations to be able to find these unknowns, which again requires eight distinctive data points from the drilling data. However, in order to increase the accuracy of the model, Bourgoyne and Young suggested a minimum number of data points to be used, depending on how many variables that are used [45], see Table 6.1. Bourgoyne and Young also suggested a

minimum range for the variables used, as seen in Table 6.2. It is not stated what these ranges are based upon.

TABLE 6.1: Recommended minimum number of data points relative to the number of parameter [45].

Number of independent variables	Minimum number of data points
8	30
7	25
6	20
5	15
4	10
3	7
2	4

TABLE 6.2: Recommended minimum data range for the independent variables [45].

Variable	Recommended minimum data range
x_2	2000
x_3	15000
x_4	15000
x_5	0,40
x_6	0,50
x_7	0,20
x_8	0,50

Step 2 - Calculate the x-variables. The x-variables $x_2, x_3, ..., x_8$ and $\ln(ROP)$ can be calculated when the data points from the drilling data have been selected. The x-variables are given by:

$$x_2 = 10.000 - D \tag{6.25}$$

$$x_3 = D^{0,69}(g_p - 9,0) \tag{6.26}$$

$$x_4 = D(g_p - \rho_c) \tag{6.27}$$

$$x_5 = \ln\left(\frac{\left(\frac{W}{d_b}\right) - \left(\frac{W}{d_b}\right)_t}{4 - \left(\frac{W}{d_b}\right)_t}\right) \tag{6.28}$$

$$x_6 = \ln\left(\frac{N}{60}\right) \tag{6.29}$$

$$x_7 = -h \tag{6.30}$$

$$x_8 = \ln\left(\frac{F_j}{1000}\right) \tag{6.31}$$

$$\ln(ROP) = \ln(ActualROP) \tag{6.32}$$

These x-variables model the following:

- x_2 and x_3 - the effect of compaction.

- x_4 - the effect of differential pressure.

- x_5 - the effect of bit weight and bit diameter.

- x_6 - the effect of rotary speed of the drillstring.

- x_7 - the effect of bit tooth wear.

- x_8 - the effect of bit hydraulics

These variables must be calculated for all the chosen data points. If any of the x_n-variables are basically constant, Bourgoyne and Young recommended that the corresponding regression constants, a_n, should be estimated from previous studies. The regression analysis is performed for the remaining constants [45].

Step 3 - Perform Multiple Regression. When all the x_n-variables have been calculated, the next step is to find the coefficients a_1 - a_8 using multiple linear regressions on the x-variables. There are several methods for doing this, but in this thesis, the LINEST function in Excel is used. This function calculates the statistics for a line by using the "least squares" method to calculate a straight

line, that best fits the data, and returns an array which describes the line [54]. Bourgoyne and Young suggested that the a-coefficients obtained should be within a given boundary. These boundaries are presented in Table 6.3. These boundaries are based on reported ranges for the coefficients from various formations in different areas, and average values of them. The reliability of the predictor system will be increased if these boundaries are used.

The linear regression method will sometimes deliver values for the a-coefficients that are outside these suggested boundaries. This is because this regression method does not handle bound constraints [55]. If the obtained a-coefficients are negative or zero, these results are mathematically correct, but physically meaningless. If a a-coefficient is negative, this means that if the variable that the coefficient represents is increased, then the ROP will decrease. In most cases, this will be illogical. This will be discussed in further detail later in Chapter 8.

The multiple linear regression equations for obtaining the a-coefficients is given by:

$$x_{2,n} + x_{3,n} + x_{4,n} + x_{5,n} + x_{6,n} + x_{7,n} + x_{8,n} = \ln(ROP_n) \tag{6.33}$$

TABLE 6.3: Recommended bounds for the a_n-coefficients [45].

Coefficient	Lower bound	Upper bound
a_1	0,5	1,9
a_2	0,000001	0,0005
a_3	0,000001	0,0009
a_4	0,000001	0,0001
a_5	0,5	2
a_6	0,4	1
a_7	0,3	1,5
a_8	0,3	0,6

Step 4 - Estimate the ROP. When the a-coefficients have been obtained, the last step is to calculate the estimated ROP. This is done by:

$$\ln(Est.ROP) = a_1 + a_2 x_2 + a_3 x_3 + a_4 x_4 + a_5 x_5 + a_6 x_6 + a_7 x_7 + a_8 x_8 \tag{6.34}$$

$$Est.ROP = \exp(\ln(Est.ROP)) \tag{6.35}$$

This method for calculating the estimated ROP differs slightly from the method presented earlier in this chapter by avoiding the calculations of the functions f_1 - f_8. This method calculates the estimated ROP directly from the obtained a- and x-values. The result is exactly the same, it just makes the calculation simpler.

Chapter 7

Results

7.1 ROP Modelling Using Drilling Data from Salt

The Bourgoyne and Young drilling model was chosen for modelling the ROP. This is one of the most important optimization methods because it is based on statistical analysis of past drilling parameters [53] from previously drilled wells. It then uses multiple regressions to analyze the effect that several independent variables ($x_1, x_2, etc.$) has on a dependent variable (y). The objective of the ROP modelling attempt was to determine which parameters have the greatest impact on ROP when drilling in salt formations.

7.1.1 Incomplete Drilling Data

The drilling data provided to the author was from a salt section in one single deepwater well. Some of the variables that are used in Bourgoyne and Young's drilling model were missing in these drilling data. These absent variables were:

Tooth wear. Since the tooth wear variables were missing, this value was assumed to be zero for all depths. The x_7-variable is therefore excluded from all calculations.

Jet impact force. Although the jet impact force was missing in the drilling data, it was possible to calculate an estimated value for this variable using other variables that were included in the drilling data. The jet impact force is given by:

$$F_j = 0,01823 C_d q \sqrt{\rho \Delta p_b} \tag{7.1}$$

where

F_j = jet impact force, lbf,

C_d = discharge coefficient,

q = flow rate, gpm,

ρ = mud density, lbm/gal,

Δp_b = pressure drop across the bit, lb/in^2.

Eckel and Bielstein [56] found, through experiments with bit nozzles, that the discharge coefficient, C_d, can be as high as 0,98, but they recommended a value of 0,95 as a more practical limit. In this report 0,95 will be used.

The bit pressure drop, Δp_b, can be estimated from the standpipe pressure. It is fair to assume that Δp_b is half of the standpipe pressure given in the drilling data. Typically, 50 % of the pump pressure is lost in the drillbit, and the remaining 50 % is lost to friction in the drillstring and annulus [57]. This justifies this assumption.

Pore pressure gradient. The change in pore pressure is minimal in short intervals, so the pore pressure was assumed to be constant throughout the interval.

Threshold bit weight. This parameter is included in the x_5-variable, but was assumed to be zero for all data points. This is justified by the UCS of salt being relatively low, and therefore, are high values of WOB not needed in order to be able to penetrate salt formations.

7.1.2 First ROP Modelling Attempt

The drilling data provided contained 10.703 data points. These were obtained when drilling in deepwater salt formations using a 12-1/4" PDC bit with 14-3/4" reamer. Several of the data were incomplete or contained errors, so in order to increase the accuracy of the regression, a filter was set up to remove the fault values. Extreme values were also unwanted, as they may represent a short interval which does not reflect the section as a whole. The filter criterion was:

- ROP between 10 and 100 ft/hr.

- Rotary speed between 100 and 200 rpm.

- WOB above 1000 klb.

After putting on this filter, 4442 data points remained. The obtained range for the remaining data points are presented in Table 7.1. It can be seen that the range for x_3, x_5, and x_6 is below the recommended minimum value. The values acquired for the coefficients a_1 to a_8 after performing the regression are presented in Table 7.2. Here only one (a_5) of the coefficients was within the recommended boundaries. The resulting r^2-value was 0,101.

TABLE 7.1: Recommended minimum range vs. obtained range.

Variable	Minimum range recommended	Obtained range
x_2	2000	2298,25
x_3	15000	31,54
x_4	15000	17354,44
x_5	0,40	0,13
x_6	0,50	0,21
x_8	0,50	1,62

TABLE 7.2: Recommended bounds for the a-coefficients vs. obtained value.

Coefficient	Lower bound	Upper bound	Obtained value
a_1	0,50	1,90	286,48
a_2	0,000001	0,0005	-0,0166
a_3	0,000001	0,0009	1,22
a_4	0,000001	0,0001	-0,000042
a_5	0,50	2,0	1,49
a_6	0,40	1,0	-0,22
a_8	0,30	0,60	-0,009

7.1.3 Troubleshooting

The dataset was divided into five subsets in an attempt to find out why several of the a-coefficients were of unphysical value. The parameter that varied the most in the drilling data was the actual ROP. In addition, this is the dependent variable. Therefore, this parameter was chosen as the basis when dividing the dataset into

subsets. The average value for ROP in the drilling data was 45 ft/hr, hence the filtration criterion was:

- 10<ROP<30

- 40<ROP<50

- 30<ROP<60

- 20<ROP<80

- 80<ROP<100

The resulting ranges, a-coefficients and r^2 values, after calculating the x-variables and the a-coefficients for the different subsets, are presented in Table 7.3 and 7.4.

TABLE 7.3: Range obtained for the different subsets.

Dataset	x_2	x_3	x_4	x_5	x_6	x_8
10<ROP<30	2271,17	31,17	16691,11	0,12	0,21	1,14
40<ROP<50	2294,47	31,49	17281,51	0,12	0,21	1,25
30<ROP<60	2297,15	31,53	17289,10	0,13	0,21	1,30
20<ROP<80	2298,25	31,54	17297,13	0,13	0,21	1,62
80<ROP<100	2283,00	31,34	17244,58	0,10	0,21	1,03

TABLE 7.4: The a-coefficients and r^2-values obtained for the different subsets.

Dataset	a_1	a_2	a_3	a_4	a_5	a_6	a_8	r^2
10<ROP<30	184,65	-0,011	0,802	-0,0000050	4,94	-0,23	0,0084	0,032
40<ROP<50	28,43	-0,0014	0,105	-0,000002	0,116	-0,057	0,012	0,013
30<ROP<60	86,04	-0,0049	0,350	0,0000008	-0,142	-0,049	0,013	0,090
20<ROP<80	139,84	-0,0080	0,580	-0,000023	-1,153	-0,066	0,039	0,095
80<ROP<100	1,148	0,00038	-0,017	-0,000017	0,125	-0,298	-0,072	0,123

7.1.4 Second Attempt - Locking Variables

Another effort was made in order to increase the accuracy of the model. The next act was to lock some parameters to one, so they would not affect the outcome of the regression. This was performed on the subsets 10<ROP<100, 20<ROP<80, and 30<ROP<60 to cover both large and small specters of ROP. It was decided

that the most logical variables to lock were the ones with the least variation in the parameters. The variables and their parameters are shown in Equation 6.25 to 6.31. The parameter variations in the different variables are shown in Table 7.5. Clearly, the pore pressure and ECD have the least variation. Therefore, all variables containing these parameters will be locked to one. In addition, since depth is a parameter that cannot be adjusted in order to increase ROP, it was also locked to one. The remaining parameters that will be used in the regression are WOB, rotary speed, and jet impact force, in the variables x_5, x_6, and x_8, respectively. The resulting a-coefficients and r^2-values are presented in Table 7.6, and the resulting S and p-values for the different a-coefficients are presented in Table 7.7.

TABLE 7.5: The difference between the maximum and minimum value in each parameter.

| Dataset | Depth | WOB | rpm | Jet force | ECD | Pore pres. |
(-)	(%)	(%)	(%)	(%)	(%)	(%)
10<ROP<100	13,4	12,3	18,9	80,2	1,8	0,0
20<ROP<80	13,3	9,7	18,6	64,4	1,6	0,0
30<ROP<60	13,4	12,0	18,9	72,8	1,7	0,0

TABLE 7.6: The a-coefficients and r^2-values obtained for the different subsets with locked variables.

Dataset	a_1	a_5	a_6	a_8	r^2
10<ROP<100	-6,01	4,26	0,31	0,014	0,072
20<ROP<80	-2,10	2,83	0,22	0,04	0,064
30<ROP<60	0,46	1,65	0,10	0,014	0,064

TABLE 7.7: S and p-values obtained for the a-coefficients in the different subsets using locked variables.

30<ROP<60			20<ROP<80			10<ROP<100		
Coeff.	*S*	*P-value*	*Coeff.*	*S*	*P-value*	*Coeff.*	*S*	*P-value*
a_1	0,31	0,14	a_1	0,45	0,00	a_1	0,82	0,00
a_5	0,14	0,00	a_5	0,20	0,00	a_5	0,26	0,00
a_6	0,09	0,24	a_6	0,12	0,07	a_6	0,15	0,05
a_8	0,02	0,57	a_8	0,04	0,26	a_8	0,05	0,77

7.1.5   Other Parameters Affecting ROP

The probability that there are parameters affecting ROP, which are not taken into account in Bourgoyne and Young's drilling model, is high. An attempt was made in order to see if this was the case for this modelling attempt. The ROP ranged from 10 to 100 ft/hr in the drilling data, so it was checked if this large difference in ROP could be explained by one of the drilling parameters being highly different for the high ROPs, compared to the low ROPs. The average parameter values in the interval 10<ROP<30 and 80<ROP<100 was compared against each other. The result is presented in Table 7.8.

TABLE 7.8: Difference in the parameters average value, for high and low ROP.

Dataset	*ROP*	*Depth*	*WOB*	*rpm*	*Jet force*	*ECD*	*Pore pres.*
(-)	(ft/hr)	(ft)	(1000 lbf/in)	(-)	(lbf)	(ppg)	(ppg)
80<ROP<100	86,9	15830,9	26,2	158,6	3192,8	15,88	8,60
10<ROP<30	20,9	16042,0	26,4	159,4	3087,9	15,90	8,60
Difference (%)	75,95	1,32	0,69	0,49	3,29	0,14	0,0

7.2   Modelling Attempt to Verify Results

To check if the results acquired from modelling with drilling data from salt formations were meaningful, another modelling attempt was carried out. This time using data obtained from the tests performed by Pessier and Damschen [34] in Carthage marble. The data were extracted from the graphs in Figure 5.4, and 5.6. This modelling attempt will be performed using only data for WOB and rpm, and for four different bit types. These bit types are (1) roller-cone, (2) PDC, (3) blade leading hybrid bit, and (4) cone leading hybrid bit. The aim of this experiment was to see if the same results were obtained, in terms of which parameter that affects ROP most, compared to the results obtained in Chapter 7.1.4. The attempt will be conducted in the following manner:

1. Extract the data for WOB and rpm from the graphs, for all four bits.

2. Calculate the variables x_5 and x_6 using Equation 6.28 and 6.29.

3. Perform regression to find a_1 and a_5 for WOB, and a_1 and a_6 for rpm.

4. Use the obtained a_5 and a_6-coefficients together with the average value for a_1 from the two regressions.

5. Perform a new combined regression using the a_5-coefficient obtained from the WOB regression, and the a_6-coefficient obtained from the rpm regression, together with the average value for a_1 from the two regressions.

7.2.1 Verifying Results

The obtained results for the a-coefficients, standard error, and p-values are presented in Table 7.9, 7.10, 7.11, and 7.12. The r^2 value was one in all four regressions.

TABLE 7.9: The a-coefficients, S, and p-values obtained for the roller-cone bit.

Roller-cone bit

Coefficient	Coefficient value	Standard error	P-value
a_1	2,54	0,00	0,00
a_5	1,22	0,00	0,00
a_6	0,12	0,00	0,00

TABLE 7.10: The a-coefficients, S, and p-values obtained for the PDC bit.

PDC bit

Coefficient	Coefficient value	Standard error	P-value
a_1	4,13	0,00	0,00
a_5	1,89	0,00	0,00
a_6	0,95	0,00	0,00

TABLE 7.11: The a-coefficients, S, and p-values obtained for the blade leading hybrid bit.

Blade leading hybrid bit

Coefficient	Coefficient value	Standard error	P-value
a_1	3,89	0,00	0,00
a_5	1,65	0,00	0,00
a_6	0,96	0,00	0,00

TABLE 7.12: The a-coefficients, S, and p-values obtained for the cone leading hybrid bit.

Cone leading hybrid bit

Coefficient	Coefficient value	Standard error	P-value
a_1	3,45	0,00	0,00
a_5	1,41	0,00	0,00
a_6	0,93	0,00	0,00

7.3 ROP Increase Due to Parameter Increase

Using the a-coefficients obtained in the second modelling attempt in Chapter 7.1.4, an effort was made in order to find the parameter/ROP correlation. This was done simply by finding the average value of the a-coefficients in Table 7.6. These mean values are presented in Table 7.13.

TABLE 7.13: Average values for the a-coefficients obtained using locked variables.

Coefficient	Avg. value
a_5	2,91
a_6	0,21
a_8	0,023

Chapter 8

Discussion

In this chapter, challenges regarding drilling in salt formations and how to overcome these challenges will be discussed, in addition to the benefits of two new drillbit technologies. Further, the results from the modelling attempts are reviewed.

8.1 Drilling in Salt

Salt possesses characteristics that distinguish it from ordinary rocks, and that makes drilling in these formations a challenge. Several potential risks lie within and/or around salt sections. In order to perform safe and successful drilling operations in these sections, knowledge of these risk is essential and must be implemented when planning each well.

8.1.1 Challenges of Drilling in Salt

When drilling in salt sections, it is salt's unique characteristics, which create the difficulties encountered. After burial, salt sheets maintain a relatively low density compared to the surrounding formations. This is because these formations around the salt will increase in density over time as overburden is added. As a result of salt's density being lower than of the surrounding formations, the salt will rise if the overlying sediments offer little resistance [2]. The rise of salt creates a difficult rubble zone at the salt's base and sides. When exiting the salt, well

control becomes a challenge. This is because the existence and extent of natural fractures are difficult to predict, in addition to the pore pressure and fracture gradients. When salt bodies undergo large lateral movement, complex near salt sediment deformation can be created, making nearby formations highly fractured, faulted and overturned. In these areas wellbore instability, losses and rubble zones are a challenge.

Drilling through the salt presents a unique challenge in itself. When subjected to constant stress, salt will deform/creep significantly as a function of time, physical properties and loading conditions. This feature makes salt able to flow into the wellbore and replace the volume removed by the bit. This is especially a problem at elevated temperatures as this increases salt creep rate [2]. If the invasion occurs fast enough it can cause a stuck-pipe situation, and the well might have to be abandoned or sidetracked. To overcome this problem, it is essential to find the appropriate mud weight that will stop salt from creeping into the wellbore.

When subjected to water, salt can dissolute. If this occurs while drilling, hole enlargement can be a problem. To overcome this problem, several inhibitors have been developed to supersaturate salt muds. Another solution to this problem is to use oil based muds, although this has its negative effects, such as increased reaming time. Cementing casing strings across large salt formations has proven to be a challenge, due to salt dissolution. It is therefore, important to use cement slurries that are salt saturated to prevent this problem [2]. However, when the salt concentration is high in cement slurries, it makes mixing difficult and the cement can become over-retarded. With time, cement failure may eventually occur due to ion exchange between calcium and magnesium. Several chemical solutions have been proposed to rectify this problem, but the authors' favorite is to let salt creep around the casing. The need for cement jobs can thereby be avoided. However, this requires a highly uniform hole to avoid non-uniform casing loads, which may be difficult to achieve.

Shock and vibration are another problem that must be faced when drilling in salt. This can become acute if shock and vibration levels get too high. This can be attributable to inappropriate drilling-fluid design, poor tool selection and BHA design, ratty or laminated salt intervals, salt creep, and suboptimal drilling parameters (especially WOB and rotary speed) [2]. Vibration can cause tool twist-off or failure, leading to expensive fishing or additional trips. Vibration can also be caused by overly aggressive bits and a poor matched bit-reamer combination.

Often the bit and reamer are up to 90 ft apart, so it is possible that the bits are drilling salt while the reamer is drilling an inclusion. This will lead to one component drilling faster than the other, which can lead to poor weight transfer who manifests into shock and vibration.

Attaining drilling targets have proven to be a challenge when drilling in salt. This is because modelling the base of salt is very difficult. Seismic waves travels through salt at a higher velocity than the surrounding layer, causing poor survey images below or near salt. In addition, the salt may be structurally complex. Considerable error margin is caused by this when estimating pore pressure and other properties of the sub-salt formations.

Pressure traps inside the salt can cause a kick while drilling. These high pressures are associated with seams or inclusions. Even though these flow volumes are usually small, the pressure may be sufficiently elevated to cause well control problems. If these high pressure zones can be detected by seismic, the recommended measure is to set casing so that mud weight can be used to counteract these influxes.

8.1.2 New Drillbit Technology

In Chapter 5, two brand new and modern drillbit technologies were presented. These bits are Baker Hughes Kymera Hybrid drillbit, and Schlumberger's CDE PDC Stinger bit. The author believes these bits can help overcome many of today's salt drilling challenges. This is based on the properties of these two drillbits.

Currently, the preferred drillbit when drilling in salt is a common PDC bit. As mentioned before, ROP is an important factor in order to drill successfully in salt formations. Compared to the roller-cone bit, the PDC is superior in terms of achievable ROP. However, the aggressiveness of the PDC has proven to be a problem in these formations, and large shock and vibrations may occur due to this. Both the Kymera and Stinger bit has proven to reduce the downhole vibrations and drill smoother than a common PDC bit [34], [35], [36]. This is a great advantage when it comes to improving wellbore measurements, and reducing the stress on the BHA. Increasing the reliability of the downhole equipment may make it easier for drillers to improve the accuracy of models through inclusions, reducing the pore pressure uncertainty when exiting the salt, and locate targets while drilling.

One important parameter in order to increase ROP when drilling is WOB. When drilling with PDC bits, stick-slip can occur when the WOB becomes excessively large. As the Kymera and the Stinger bit are able to drill smoother than conventional PDC bits [34], [35], [36], the chance of stick-slip is reduced. This may again allow an increase in WOB without experiencing stick-slip, and thereby increase ROP.

Reamers are often used when drilling salt formations in order to increase the wellbore diameter. This will give the drillers more time to drill to target, pull out of hole, and run casing. A problem that may occur when using reamers in non-homogeneous formations is that the bit and reamer may drill in different formations. As the ROP may vary between formations, this can result in the bit out-drilling the reamer, or vice versa, and thereby result in a poor weight transfer. This can, in turn, result in large shock and vibration levels, which may damage the BHA components. If the ROP can be increased sufficiently when drilling with the Kymera or the Stinger bit, the need for reamers may be reduced or eliminated.

Tests performed with the Kymera, and the Stinger bit has shown that these bits have an improved bit life [34], [35], [36]. By increasing the bit life, longer sections can be drilled; NPT is reduced and the operations can be performed in a shorter amount of time. This may reduce the chance of borehole closure as sections can be drilled quicker, in addition to reducing the operation's cost.

As mentioned in the previous subsection, cementing can be an issue in salt formations. The author believes that one of the best solutions to this problem is to eliminate the need for cementing completely. Since salt can creep, it will close around the casing by itself after some time. This requires a uniform borehole so the loads will be equally distributed across the casing, preventing deformation and/or collapse of the casing. Both the Kymera and the Stinger bit has proven in tests, to deliver more consistent hole diameters and improved borehole quality compared to both PDC and roller-cone bits. The author believes that these bits would greatly increase the possibility of eliminating the cement job, and allow the casing to be held in place by the salt itself. If successful, this would not only increase the safety by eliminating poor cement jobs, it would also save the operator the cost of the whole cementing process.

The Stinger bit has one unique ability that the Kymera bit does not possess. Due to the conical diamond element's characteristics, the resulting cuttings from the

Stinger bit are larger than standard cuttings [36]. This may provide better rock characterization, which can be an advantage for determining wellbore position in the stratigraphic column.

8.2 Rate of Penetration Modelling in Salt

8.2.1 Regression Output Statistics Explained

a-coefficients. The coefficients obtained after performing a regression, represents the mean change in the response for one unit of change in the predictor. This is while holding the other predictors in the model constant [58]. E.g. if the a_5-coefficient is 2,5 after performing a linear regression, it means that if a_5 is increased with one unit, then the response variable (in this case ROP) will increase with an average of 2,5 units. This statistical control that the regression provides is important. This is because the role of one variable is isolated from all the others in the model [59].

r^2 **(R-squared).** Whether the r^2-value can be used to interpret the results of the regression or not, depends on the objective for the linear regression [58]. Is the goal to describe the relationship between the predictors and response variable, or is it to predict the response variable?

- r^2 **used to interpret the relationship between the predictors and response variable.** If the goal of the regression is to determine how changes in the predictors relate to changes in the response variable, then r^2 are irrelevant. The r^2-value does not affect how to interpret the relationship between the response variable and predictors, if the regression model is correctly specified [58]. A low r^2 do not change the meaning of the coefficients or negate a significant predictor. Therefore, this meaning of the r^2-value will not be discussed in further detail later in this report.

- r^2 **used to predict the response variable.** When the goal of the regression is to produce precise predictions for the response variable, r^2 become valuable. This is because predictions are not as simple as a single predicted value, and because a margin of error is included [58]. Low values for r^2 indicate that the model has more error and can warn of imprecise predictions.

The Standard Error of the Regression (S). The standard error of the regression, also known as the standard error of the estimate, represents the average distance that the observed values fall from the regression line [60]. Using the units of the response variable, it tells how wrong the regression model is on average. The smaller the values the better, because this means that the observations are close to the fitted line. S can be used to asses the precision of the predictions.

P-value. The p-value tests, for each term, the null hypothesis that the coefficient is equal to zero (that it has no effect). If the p-value is below 0,05, it indicates that the null hypothesis can be rejected. Changes in the predictor's value are related to changes in the response variable. Therefore, if the predictor has a low p-value, it is likely to be a meaningful addition to the model [59]. Conversely, if the p-value is large (insignificant) for a predictor, it suggests that changes in the response are not associated with changes in the predictor. The coefficient p-values are often used to determine which terms to keep in the regression model and which to remove.

8.2.2 First Modelling Attempt

The aim of this study was to determine which parameters have the greatest impact on the ROP in salt. Therefore, a modeling experiment was conducted, as described in Chapter 7, using data from a previously drilled well in salt formation. In this first attempt only the drilling data with ROP between 10 and 100 ft/hr were used.

a-coefficients. As seen in Table 7.2 the only a-coefficient within the recommended boundaries was a_5. In addition, four out of seven a-coefficients were negative. As explained above, when a coefficient is negative, it means that if the variable in which the coefficient represents is increased, the dependent variable (y) will decrease. This applies if all the other variables are held constant. This can of course be correct in some situations, as long as these negative a-coefficients give meaningful results. However, in this modelling attempt, the negative coefficients are not meaningful; they are of unphysical values. E.g. the a_6-coefficient which represents the x_6-variable, which takes into account the rotary speed of the drillstring. In the result of the regression, the a_6-coefficient was negative (-0,22), so if the rotary speed of the drillstring was increased with one unit, the resulting ROP would decrease with -0,22 ft/hr, if all other parameters were held constant. From the theory presented in Chapter 6, clearly the rotary speed of the drillstring is one of

the parameters that increases ROP the most, and therefore, it is illogical that this parameter should affect the ROP in a negative manner. The result is accordingly, not meaningful.

r^2**-values.** The coefficient of determination indicates that this dataset cannot predict the response variable. The r^2-value was only 0,101, which indicates that the prediction of ROP is imprecise.

The standard error of the regression and the p-values will not be discussed in this first modelling attempt as the unphysical a-coefficients were enough to conclude that this modelling attempt was unsuccessful.

There are strong indications that the parameters used in this first modelling attempt, were not varied enough to give a good result. The initial indications are shown in Table 7.1. Here, 50 % of the variables are below the minimum range recommended by Bourgoyne and Young. Another indication that the variation in the drilling data was too small, is presented in Table 7.5. It can be seen in the first row that the variation in ECD is quite low. In the pore pressure, the variation is non-existing, because this value was assumed to be constant throughout the dataset.

8.2.3   Troubleshooting

The dataset used in the initial modelling attempt was divided into five subsets in order to find out why the attempt was unsuccessful. The reason for breaking the dataset into five subsets is because when the range is large, unwanted data, which is impossible to model using this method, may be included. Changes in the formation, or the use of a different bit are examples of data that are not included in Bourgoyne and Young's model. It is, however, important not to use too small ranges, as this may result in loss of data that may be of interest.

x-variable range. It can be seen in Table 7.3, that the differences in range between the five intervals of ROP are of insignificant value. This is a clear indication that the variation throughout the dataset is too small, regardless of interval.

a-coefficients. As seen in Table 7.4, several of the a-coefficients are of unphysical value (negative value). The only coefficient that was consistent for all spectra of ROP was a_6, which was negative. Again this indicates that there is too little

variation in the input variables. It also indicates that there are other parameters, which are not taken into account in Bourgoyne and Young's drilling model, but which affects the ROP in the provided drilling data.

r^2**-value.** To be able to predict the response variable, it is important that the coefficient of determination is good. Table 7.4 shows that this is not achieved in any of the subsets. The highest r^2-value obtained was for the subset using ROP between 80 and 100, where the acquired value was 0,123. As mention above, one is the best achievable result, while zero is the worst. A low r^2 indicate that the model has imprecise predictions. This confirms that these datasets cannot be used to predict ROP.

8.2.4 Second Attempt with Locked Variables

Since the first modelling attempt was unsuccessful, and the test with five subsets showed that the parameter variation is too small, the next attempt was to lock some of the variables to one. By doing so, these variables could not affect the result of the regression. The specters of ROP used in this test was 30<ROP<60, 20<ROP<80, and 10<ROP<100.

a-coefficients. As seen in Table 7.6 the resulting values for the coefficients a_5, a_6, and a_8 are positive, and therefore, physical. This applies to all three specters of ROP. In addition, the rankings of the values for these coefficients are consistent for all three datasets. a_5 is greatest, a_6 is second largest, and a_8 is smallest. This means that in these datasets, using only three variables, WOB affects ROP the most, before rpm, and jet impact force the least. This result coincides with the theory regarding in which degree parameters affect ROP. The result is, therefore, meaningful and intuitive.

Table 7.6 shows that the a_1-coefficient is negative for the specters 10<ROP<100 and 20<ROP<80. The a_1-coefficient is also known as the y intercept, which basically means this is the value at which the fitted line will cross the y-axis. This coefficient is often described as the mean response value, when all predictor variables are set to zero. This is mathematically correct, but a zero setting for all predictors in a model is often a meaningless combination. If all predictors cannot be zero, a meaningful interpretation of the a_1-coefficient is impossible. In addition, even if it is possible for all the predictor variables to be zero, the data

point might be outside the range of the observed data [61]. From Figure 8.1, 8.2, and 8.3 clearly setting the predictor variables to be zero, are outside the range of the observed data in this modelling attempt.

Using a regression model to make a prediction for a data point that is outside the data range should not be done. This is because the relationship between the variables might change. The value for a_1 is a prediction for the response value if all predictor variables are zero. If the data are not collected for this all-zero ranges, then the value of a_1 cannot be trusted. The relationship for the observed data can be locally linear, but beyond that it might change. This explains why the regression constant might have a meaningless value [61]. It should be said that even though a zero setting for all predictors is plausible, and if the data are collected within the all-zero ranges, the a_1 might still be meaningless. This is because it serves as a garbage bin for any bias that is not accounted for by the terms of the model. It is important to use this coefficient in the regression model since it guarantees that the residuals have a mean of zero. In addition, if it is not added, the regression line is forced to go through the origin. If the fitted line does not naturally go through the origin, the regression coefficients and predictions will be biased, if a_1 is not included. Based on the foregoing, it must not be placed too much emphasis on the meaning of a_1.

r^2**-value.** The coefficient of determination is poor for all three specters of ROP, as seen in Table 7.6. This is not unexpected, as 50 % of the parameters (depth, ECD, pore pressure, and bit tooth wear) used in Bourgoyne and Young's model are missing in this altered model. This means that these regression results cannot be used to predict ROP. However, since the main goal is to interpret the relationship between the predictors and the response variable, these poor r^2-values do not have to be taken into consideration.

The Standard Error of the Regression (S). As seen in Table 7.7, the standard error of the regression is best for a_8 in all three spectra of ROP. This means that the a_8-coefficient is closest to the fitted line. This could be explained by the range for jet impact force, which a_8 represents, being larger than for the other two parameters, as seen in Table 7.5. The a_8-coefficient for 30<ROP<60 is the only parameter in which the value for S falls within a sufficiently narrow 95 % prediction interval ($<(0,05/2)$). This is an indication that the variation in the data is too small and that the model needs to be more precise.

P-value. The p-value has to be smaller than 0,05 to indicate that changes in the predictor's value are related to changes in the response variable. As seen in Table 7.7 the a_5-coefficient is consistently 0,00 for all three spectra of ROP, which argue that this parameter has the largest impact on ROP. The a_5-coefficient represent WOB, so this observation agrees well with the theory. a_6 are consistently the second-lowest p-value, and for 10<ROP<100 it equals 0,05. This indicates that of the three parameters taken into the model, this is the one who affects ROP the second most. In addition, it indicates that changes in ROP are related to changes in rotary speed, which a_6 represents. Again, this agrees well with the theory. The p-values for jet impact force, a_8 are large, saying that this parameter does not affect changes in ROP in this model.

Based on the above-mentioned results from the regression, clearly locking the parameters with the least variation had a positive effect on the outcome of the a-coefficients. Although the datasets cannot be used to model ROP, they say something about how the parameters affect ROP individually. From the obtained results, the author interprets that the parameters affecting ROP the most when drilling in salt, from greatest to smallest, is in the following order:

1. Weight on bit

2. Rotary speed of the drillstring

3. Jet impact force

Note that the jet impact force is included, although the p-value suggested that this parameter had no effect on changes in ROP. Based on the theory presented in Chapter 6.1.6, clearly bit hydraulics will have an impact on ROP. The author, therefore, chose to include the jet impact force in his findings.
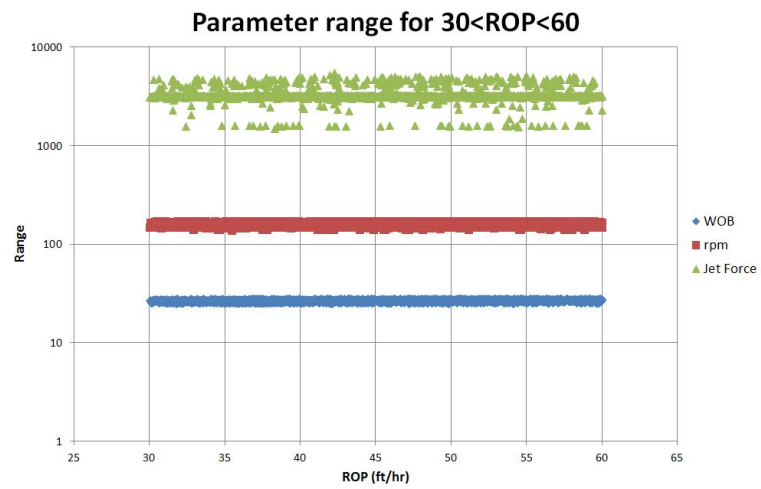
FIGURE 8.1: Parameter range for the specter 30<ROP<60.
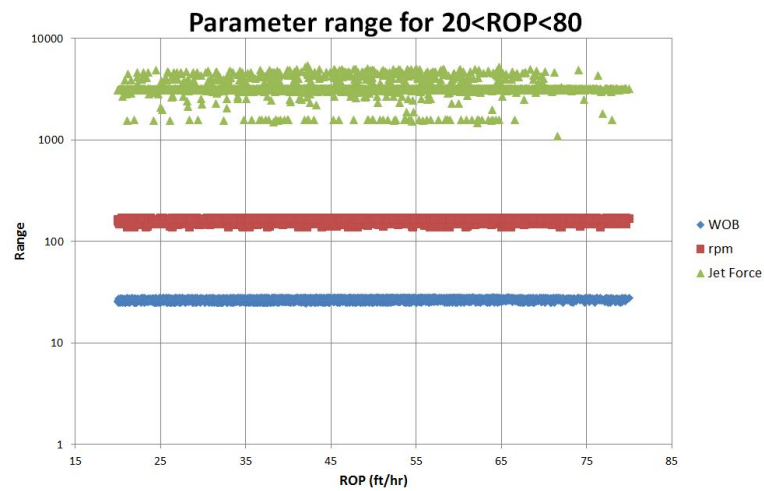
FIGURE 8.2: Parameter range for the specter 20<ROP<80.
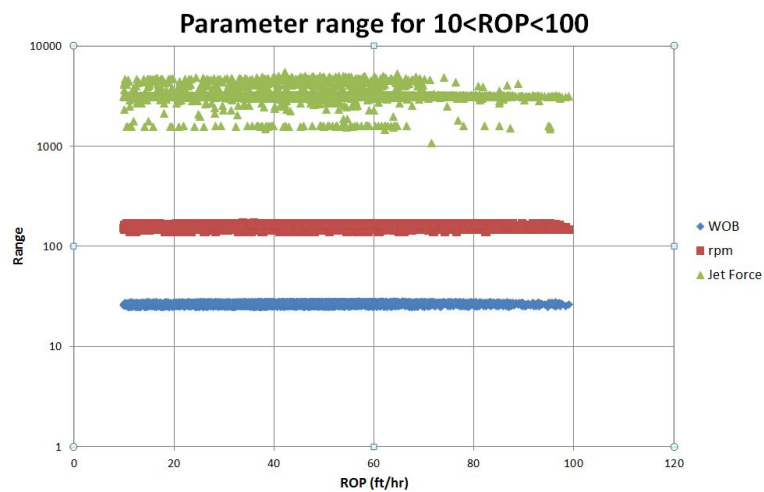
FIGURE 8.3: Parameter range for the specter 10<ROP<100.

8.2.5   Other Parameters Affecting ROP

Because of the low r_2-values obtained in both modelling attempts, and the poor S and p-values obtained in the second attempt, it was suspected that there were other parameters affecting ROP that was not taken into the model. The bad results of these regression output statistics indicate that the correlation between the actual ROP, and the modeled ROP is insufficient. This was tested by checking if the difference in high and low values of ROP could be explained by one of the parameters (used in the model) was highly different between the ROP-spectra. Two intervals of ROP on the opposite side of the scale were chosen for this test, 10<ROP<30, and 80<ROP<100. The differences found between the parameter's mean values in these two ranges are presented in Table 7.8. As seen, there is an insignificant difference between the average values in the parameters, compared to the large difference in ROP. This implies that there are other parameters affecting ROP, which are not taken into account in the model used and, therefore, explains the poor results obtained when predicting the response variable.

8.3   Modelling Attempt to Verify Results

In this modelling attempt, using the drilling data obtained by Pessier and Damschen [34], it emerges that the same results are obtained as in the second attempt with locked variables. Table 7.9, 7.10, 7.11, and 7.12 reveals that for all four bit types, WOB (a_5) affects ROP more than rotary speed (a_6). Note that all values for the standard error, S, and for the p-values equals 0,00. This suggests that the observed values coincide perfectly with the regression line. This is supported by r^2 being one in all four regressions. This result is, therefore, to be trusted, and gives reason to rely on the parameter relationship obtained using the drilling data from salt.

The results obtained in this modelling attempt agrees well with the theory regarding the relationship between ROP, and the combination of bit aggressiveness and WOB. The magnitude of a_5 is in the identical order as the aggressiveness of the bits. It is greatest for the PDC bit, followed by the blade leading hybrid bit, the cone leading hybrid bit, and then the roller-cone bit.

8.3.1 How to Increase the ROP in Salt

In the modelling attempt using data from a salt formation, it was found that the parameter that affects ROP the most was WOB, before rotary speed, and jet impact force, in that order. This result was supported by the modelling attempt using drilling data from Carthage marble. The results showed in both cases that WOB had a greater impact on ROP than the rotary speed. Based on the results from these two modelling attempts, to increase ROP when drilling in salt, the best parameter to increase is WOB, before rpm and jet impact force.

8.3.2 Limitations to Parameter Increase

WOB, the rotary speed and jet impact force cannot be increased indefinitely. Certain limitations exist, which needs to be taken into consideration.

Limitation to WOB:

- **Rig hook load capacity.** The derrick and hoisting systems on drillrigs/drillships presents a limitation to the WOB available, by having a maximum hook load capacity. The WOB can never exceed the hook load capacity, as this is the highest weight of the drillstring that the rig/ship can handle. However, the hook load capacity of modern drillrigs/drillships surpasses 1.000 tonnes, which should be sufficient in almost any scenario.

- **Buckling.** When subjected to a vertical compression load, drillpipes tend to fail by buckling, as they have a low resistance to any applied bending moments [37]. Buckling can occur in the lower portion of the pipe if the drillpipe is confined by a wellbore or casing, and is subjected to a compression load on the bottom that is less than the hook load. These buckling forces are resisted by the moment of inertia of the pipe, but for long and slender drillpipes this moment of inertia is small and often negligible. Drilling when the drillstring is in a buckled condition will fatigue the tool joints quickly and lead to failure. Buckling tendency can be avoided, to some extent, by using enough heavy walled drill collars in the lower section of the drillstring.

- **Stick-slip.** By applying too much WOB, the friction between the drillbit and the formation can get excessively high, causing the bit to "stick." This

will lead to a reduced, or complete stop in rotation. When this occurs, the energy stored in the drillstring will accumulate and be stored as several turns of twist in the string. When the energy level gets to a certain point, it will overcome the friction force and be released. The string will then spin out of control and create destructive vibrations.

- **Bit tooth strength.** If the drillbit is subjected to high WOB, excessive torque will increase tooth wear and may lead to broken or chipped cutters/inserts, and bit failure. Recommendations for maximum allowable WOB will be delivered by the bit supplier.

- **Shocks and vibrations.** Shock and vibration can occur when too much WOB is applied. It can be in the form of axial vibration (bounce), and torsional vibration (stick-slip). This can be destructive and lead to BHA failure, twistoffs, bit failure, and tool failure.

- **Bit floundering.** When extreme levels of WOB are applied, a decrease in penetration rate can be observed. This is usually due to poor bottomhole cleaning at high rates of cutting generation [37].

Limitation to rpm.

- **Bit damage.** Too high rotary speed can lead to broken teeth and, in worst case, bit failure. Recommendations for maximum allowable rpm will be delivered by the bit supplier.

- **Shocks and vibrations.** Bit and/or BHA whirl can be caused by excessive rpm. This can cause BHA failure, overgauged hole, broken PDC blades, wear on stabilizers, and damaged cutters/inserts.

- **Rig capacity.** On drilling rigs/ships, the top drive is the limiting factor. The best top drives are capable of rotary speeds up to 280 rpm. However, the most common maximum rotary speeds for top drives are plus/minus 200 rpm.

Limitations to jet impact force.

- **Surface operating pressure.** The surface operating pressure is the maximum pump pressure capacity of the mud pump. The newest and largest mud pumps can handle pressures up to 7500 psi.

- **Pump hydraulic horsepower.** The pump hydraulic horsepower is the power available in a positive displacement mud pump. The largest mud pumps are equipped with approximately 1600 horsepowers.

8.3.3 ROP/Parameter Increase Correlation

A simple attempt was made in order to answer how much ROP can be increased by adjusting the parameters affecting it. The a-coefficients describe the change of the dependent variable with one-unit change in the independent variables. This was used to find the increase in ROP due to altering the parameters. This was done by calculating the average values for the a_5, a_6, and a_8 coefficients obtained in the second modelling attempt. These values are presented in Table 7.13.

Increase in ROP due to WOB. The unit used for WOB in this modelling attempt was 1000 lbf/inch. From the resulting average value for a_5, increasing WOB with one unit, or 1000 lbf/inch, should result in an increase in ROP by 2,91 ft/hr. This result does seem realistic, considering that salt formations are relatively soft. The mean value for WOB in the used dataset was 26,5 (1000 lbf/in). If the circumstances allowed a 10 % increase in WOB, this would have resulted in 7,7 ft/hr increase in ROP. The difference between the smallest and largest value for WOB in the dataset was 12,3 %.

Increase in ROP due to rotary speed. The results in Table 7.13 shows that increasing the rotary speed by one rpm should increase the ROP by 0,21 ft/hr. The author believes that this result also seems realistic. The average value for rotary speed in the drilling data was 160,1 rpm. If this value was increased to the most common rotary speed limitation for top drives of 200 rpm, the resulting increase in ROP would be 8,4 ft/hr.

Increase in ROP due to jet impact force. The unit used for jet impact force was lbf. Increasing the jet impact force with one lbf should, according to the acquired result, increase ROP by 0,023 ft/hr. The author believes this result is too large to be realistic. This is based on the fact that the difference between the smallest and largest value of jet impact force in the drilling data was 4386,9 lbf. Increasing the jet impact force with 4386,9 lbf should then result in 100,9 ft/hr increase in ROP, which is unrealistic. In addition, the high p-values obtained for jet impact force (see Table 7.7) indicates that this parameter is insignificant for the

predictor. The author, therefore, believes that the result for jet impact force/ROP increase correlation are invalid.

8.3.4   Comparison of ROP in Salt vs. Marble

Two modelling attempts have been carried out in which meaningful results for the a-coefficients have been obtained. One attempt was using data from salt drilling, and the second using data from drilling in marble. To get a better understanding of the ROP/parameter interaction when drilling in salt, these two results were compared to see if any significant difference was found. It should be mentioned that these data were obtained under completely different conditions, one being a deepwater well and the other a simulated laboratory experiment.

The results of four different bit types were obtained from the modelling attempt in Carthage marble. However, since a PDC bit was used to drill the salt formation, only the results from the PDC bit (Table 7.10) were used. These results were compared to the average values for the a-coefficients presented in Table 7.13. As seen in Table 8.1 the effect of increasing WOB is 35,1 % greater in salt than in Carthage marble. Increasing the rotary speed will have 77,9 % more effect in Carthage marble compared to salt.

This observed difference in the effect of WOB might be due to the UCS of Carthage marble being five times larger than in salt (15.000 psi in Carthage marble vs. 3.000 psi in salt). The higher UCS, the more WOB is required to overcome the threshold bit weight. In addition, Maurer [46] found in his experiments that the depth of cutter penetration is inversely proportional to the rock strength. This may also describe the better ROP response in low UCS rocks.

An explanation for the rotary speed response being lower in salt than in Carthage marble could be due to salt creep. Excessive rotary speed in salt is known to cause downhole vibrations, which will decrease ROP.

As mentioned above, the drilling data used in these modelling attempts were obtained under various conditions, therefore, the differences in these results should not be emphasized too greatly. The most important result from these two tests is that the order of which the parameters affect ROP is similar. This is an indication that the results obtained in the salt modelling attempt, may be used to predict which parameters affect ROP the most.

TABLE 8.1: a-coefficients obtained in salt vs. Carthage marble.

Coefficient	Avg. value Salt	Salt	Difference (%)
a_5	2,91	1,89	35,1
a_6	0,21	0,95	77,9

Chapter 9

Conclusion

The following conclusions were drawn based on the presented theory and the modelling results:

- Geomechanical risks related to drilling in salt formations:

  - Tectonically instable areas around the salt. Thrust faulting stress regimes may occur where the minimum horizontal stress is close to the overburden stress, and the maximum horizontal stress surpasses the overburden stress. This occurs due to active lateral salt deformation.

  - Rubble zones or depressions near the salt. This may occur if the neighboring rock is not able to withstand the imposed stresses developed from salt emplacement of fluid migration.

  - Recumbent beds. Salt movement can make nearby formations overturned and highly fractured and faulted.

  - Squeezing sediments entrapped in salt seams or occurring as inclusions within the salt. The pore pressure in these sediments may be high, and the sediment itself may be highly plasticized.

  - Casing loading from deformable salt. Creep rate is governed by the temperature of the salt, and the stress difference between the overburden stress and the borehole pressure. Changes in one of these may cause a non-uniform casing load, leading to casing collapse.

  - Drilling in tight-hole conditions, due to salt flow.

- Pore pressure risks related to drilling in salt:

  - High pressure zones, found in seams or inclusions within salt, or above the salt in carapace sediments. These zones occur if higher pressured sediments were forced upwards by the underlying salt, and have not been "bled-off".

  - Pore pressure uncertainty when exiting the salt, due to poor seismic imaging.

- Recommendations when drilling in salt:

  - RSS are the best option for drilling salt. This is based on the improvements seen in ROP, directional control and hole quality.

  - To increase ROP over extended salt intervals, use RSS in combination with motors, as these deliver higher torque and rpm at the bit.

  - Define salt exits as targets, plan salt exits across a tangent section, and at a flat or low dipping area of the salt base. This is to ensure that the well exits the salt in an area least susceptible to problems.

  - Plan a low DLS ($< 2{,}0°/100$ ft). This is to make sure that the assembly still has enough capability to drill the desired trajectory, even when steering is required to counteract salt tendency.

  - Avoid the use of drilling jars in hole sections larger than 18". This is because jars represents a weak point in the drillstring. In addition, stuck-pipe problems are rare in these large hole sizes.

  - If under-reamers are used, make sure these are matched with the bit, to avoid shocks from a poor bit-reamer combination.

  - When entering and exiting salt, monitor and control the drilling parameters until both the under-reamer and the bit are in the same formation. This is to avoid shock and vibration related problems.

  - Use real-time monitoring of the drilling parameters in salt. This is to increase BHA life and optimizing drilling performance. This can be done either at the rig-site or from remote centers.

- New drillbit technology:

  - By reducing the shock and vibration levels while drilling, the Kymera and the Stinger bit can improve borehole quality, improve BHA tool

reliability, increase ROP by being able to increase WOB and rpm, and improve bit and BHA life.

– The Stinger bit provides better rock characterization as the cutting size is increased.

- Parameter effect on ROP:

  – It was found that of the three parameters used in this modeling attempt, they affect ROP in the following order:

    1. WOB
    2. Rotary speed of the drillstring
    3. Jet impact force

Chapter 10

Future Work

Based on the uncertainty of the findings in this thesis, the author recommends that further research is performed to validate the results. Both Bourgoyne and Young's model and the multiple linear regression method should suffice for obtaining valid results. However, they both depend on a good variation in the drilling data. It is not necessary to use data from just one single well. Data from several wells in the same formation can be used, if available. This may increase variation and improve the accuracy of the model. A suggestion for increasing the data quality is to make sure that all the parameters needed are included in the drilling data. This can be achieved by planning the modelling attempt ahead of drilling a well. It is then known which parameters which must be measured and recorded.

It would be interesting to perform tests in salt formations, using the new drillbit technology presented in this paper. The author strongly believes that this technology will be of great benefit when drilling in salt. A suggestion for further work is to test and see if these new drillbits are able to improve ROP when drilling in salt formations. This can be performed either as a laboratory or a field study. To achieve the most realistic results, the author recommends a field study. This is because the performance of the Kymera and the Stinger bit can be directly compared to conventional bits. The author also recommends performing studies on borehole quality when using these bits in salt formations. The author believes that the need for cement jobs may be reduced, by utilizing the salt creep tendency to hold the casing in place. This can only be achieved in high-quality boreholes.

Bibliography

[1] BP. Bp energy outlook 2035, January 2014. URL `http://www.bp.com/content/dam/bp/pdf/Energy-economics/Energy-Outlook/Energy_Outlook_2035_booklet.pdf`.

[2] M.A. Perez, D'Amrosio P. Clyde, R. and, R. Israel, T. Leavitt, and L. Nutt. Meeting the subsalt challenge. *Oilfiel*, –:33, 2008.

[3] Stephen M. Willson and Joanne T. Fredrich. Geomechanics considerations for through- and near-salt well design. In *SPE Annual Technical Conference and Exhibition, 9-12 October, Dallas, Texas*. Society of Petroleum Engineers, 2005.

[4] Maurice B. Dusseault, Vincent Maury, Francesco Sanfilippo, and Frederic J. Santarelli. Drilling through salt: Constitutive behavior and drilling strategies. In *Gulf Rocks 2004, the 6th North America Rock Mechanics Symposium (NARMS), 5-9 June, Houston, Texas*. American Rock Mechanics Association, 2004.

[5] David Biello. *Has Petroleum Production Peaked, Ending the Era of Easy Oil?* Scientific American, January 2012. URL `http://www.scientificamerican.com/article/has-peak-oil-already-happened/`.

[6] Riaz R. Israel, Pedro D'Ambrosio, Anthony D. Leavitt, John Martin Shaughnessy, and John F. Sanclemente. Challenges of directional drilling through salt in deepwater gulf of mexico. In *IADC/SPE Drilling Conference, 4-6 March, Orlando, Florida, USA*. Society of Petroleum Engineers, 2008.

[7] ARLO F Fossum and JOANNE T Fredrich. Salt mechanics primer for near-salt and sub-salt deepwater gulf of mexico field developments. Technical report, Sandia, July 2002.

[8] J.W. Barker, K.W. Feland, and Y.H. Tsao. Drilling long salt sections along the u.s. gulf coast. *Society of Petroleum Engineers Journal*, 9:185 – 188, 1994.

[9] Maurice B. Dusseault, Vincent Maury, Francesco Sanfilippo, and Frederic J. Santarelli. Drilling around salt: Risks, stresses, and uncertainties. In *Gulf Rocks 2004, the 6th North America Rock Mechanics Symposium (NARMS), 5-9 June, Houston, Texas*. American Rock Mechanics Association, 2004.

[10] Encyclopaedia Britannica Online. *Salt Dome*, 2014. URL `http://www.britannica.com/EBchecked/topic/519806/salt-dome/6385/Origin-of-salt-domes`.

[11] E.A. Leyendecker and S.C. Murray. Properly prepared oil muds aid massive salt drilling. *World Oil*, –:93–95, 1975.

[12] N.B. Muecke. Heated mud systems: A solution to squeezing-salt problems. *Society of Petroleum Engineers Journal*, 9:276 – 280, 1994.

[13] J. Yearwood, P. Drecq, and P. Rae. Cementing across massive salt formations. In *Annual Technical Meeting, June 12 - 16, Calgary, Alberta*. Petroleum Society of Canada, 1988.

[14] W.H. Grant, E.L. Dodd, and C.A. Gardner. Simplified slurry design increases wellsite success. *SPE Drilling Engineering*, 4:255 – 260, 1989.

[15] Jr. Cheatham, J.B. and J.W. McEver. Behavior of casing subjected to salt loading. *Journal of Petroleum Technology*, 16:1069 – 1075, 1964.

[16] R.M. Hackney. A new approach to casing design for salt formations. In *SPE/IADC Drilling Conference, 5-8 March, New Orleans, Louisiana*. Society of Petroleum Engineers, 1985.

[17] A.A.H. El-Sayed and Fouad Khalaf. Resistance of cemented concentric casing strings under nonuniform loading. *SPE Drilling Engineering*, 7:59 – 64, 1992.

[18] J.T. Fredrich, D. Coblentz, A.F. Fossum, and B.J. Thorne. Stress perturbations adjacent to salt bodies in the deepwater gulf of mexico. In *SPE Annual Technical Conference and Exhibition, 5-8 October, Denver, Colorado*. Society of Petroleum Engineers, 2003.

[19] I. R. MacDonald, Gerhard Bohrmann, E. Escobar, Friedrich Abegg, P. Blanchon, V. Blinova, Warner Bruckmann, Manuela Drews, Anton Eisenhauer,

X. Han, K. Heeschen, F. Meier, C. Mortera, T. Naehr, B. Orcutt, B. Bernard, J. Brooks, and M. D. Farago. Asphalt volcanism and chemosynthetic life, campeche knoll, gulf of mexico. *Science*, 304:999 – 1002, 2004. URL `http://oceanrep.geomar.de/7342/`.

[20] Ian Davison, Dan Bosence, G. Ian Alsop, and Mohammed H. Al-Aawah. Deformation and sedimentation around active miocene salt diapirs on the tihama plain, northwest yemen. *Geological Society, London, Special Publications*, 100(1):23–39, 1996. doi: 10.1144/GSL.SP.1996.100.01.03. URL `http://sp.lyellcollection.org/content/100/1/23.abstract`.

[21] I. Davison, G.I. Alsop, N.G. Evans, and M. Safaricz. Overburden deformation patterns and mechanisms of salt diapir penetration in the central graben, north sea. *Marine and Petroleum Geology*, 17(5):601–618, 2000-05-01T00:00:00. doi: doi:10.1016/S0264-8172(00) 00011-8. URL `http://www.ingentaconnect.com/content/els/02648172/2000/00000017/00000005/art00011`.

[22] G. I. Alsop, J. P. Brown, I. Davison, and M. R. Gibling. The geometry of drag zones adjacent to salt diapirs. *Journal of the Geological Society*, 157(5):1019–1029, 2000. doi: 10.1144/jgs.157.5.1019. URL `http://jgs.lyellcollection.org/content/157/5/1019.abstract`.

[23] D. D. Schultz-Ela. Origin of drag folds bordering salt diapirs. *AAPG Bulletin*, 87(5):757–780, 2003. doi: 10.1306/12200201093. URL `http://aapgbull.geoscienceworld.org/content/87/5/757.abstract`.

[24] Daniel L. Orange, Michael M. Angell, John R. Brand, Jim Thomson, Tim Buddin, Mark Williams, William Hart, and III Berger, William J. Geological and shallow salt tectonic setting of the mad dog and atlantis fields: Relationship between salt, faults, and seafloor geomorphology. In *Offshore Technology Conference, 5/5/2003, Houston, Texas*, pages –. Offshore Technology Conference, 2003.

[25] H.L. Harrison. Base of salt structure and stratigraphy - data and mmodel from pompano field, vk 989/990, gulf of mexico. In *GCSSEPM 24th Annual Research Conference Technical Papers and abstracts*, pages 243 – 269, 2004.

[26] Douglas E. Caughron, Douglas K. Renfrow, James R. Bruton, Catalin D. Ivan, Paul N. Broussard, Tom R. Bratton, and William B. Standifird. Unique

crosslinking pill in tandem with fracture prediction model cures circulation losses in deepwater gulf of mexico. In *IADC/SPE Drilling Conference, 26-28 February, Dallas, Texas*. Society of Petroleum Engineers, 2002.

[27] William B. Bradley. Bore hole failure near salt domes. In *SPE Annual Fall Technical Conference and Exhibition, 1-3 October, Houston, Texas*, pages –. Society of Petroleum Engineers, 1978.

[28] K.P. Seymour, Graeme Rae, J.M. Peden, and Keith Ormston. Drilling close to salt diapirs in the north sea. In *Offshore Europe, 7-10 September, Aberdeen, United Kingdom*. Society of Petroleum Engineers, 1993.

[29] S.M. Willson, A.F. Fossum, and J.T. Fredrich. Assessment of salt loading on well casings. *SPE Drilling & Completion*, 18:13 – 21, 2003.

[30] P. Copercini, F. Solomon, M. El Gamal, and I. McCourt. Powering up to drill down. *Oilfield Review*, 8:4 – 9, 2004.

[31] Louis A. Romo, John Martin Shaughnessy, and Ed T. Lisle. Challenges associated with subsalt tar in the mad dog field. In *SPE Annual Technical Conference and Exhibition, 11-14 November, Anaheim, California, U.S.A.*, pages –. Society of Petroleum Engineers, 2007.

[32] U. Albertin, J. Kapoor, R. Randall, M. Smith, G. Brown, C. Soufleris, P. Whitfield, F. Dewey, J. Farnsworth, G. Grubitz, and M Kemme. The time for depth imaging. *Oilfield Review*, 14:–, 2002.

[33] F.L. Scott and I.H. Bettis. Combination rolling and scraping cutter drill., August 1932.

[34] Rudolf Pessier and Michael Damschen. Hybrid bits offer distinct advantages in selected roller-cone and pdc-bit applications. *SPE Drilling & Completion*, 26:96 – 103, 2011.

[35] Ian James Thomson, Raul M. Krasuk, Nalon Silva, and Kertis Romero. Hybrid drill bit improves drilling performance in heterogeneous formations in brazil. In *Brasil Offshore, 14 - 17 June, Macae, Brazil*. Society of Petroleum Engineers, 2011.

[36] Suman Velvaluri, Karim Beheiry, Michael Azar, Allen White, and Mohamad Mustafa Johny. Middle east hard/abrasive formation challenge: Reducing pdc cutter volume at bit center increases rop/drilling efficiency. In

SPE/IADC Middle East Drilling Technology Conference & Exhibition, 7 - 9 October, Dubai, UAE. Society of Petroleum Engineers, 2013.

[37] A.T. Bourgoyne. *Applied Drilling Engineering.* SPE textbook series. Society of Petroleum Engineers, 1986.

[38] William C. Maurer. Bit - tooth penetration under simulated borehole conditions. *Journal of Petroleum Technology*, 17:1433 – 1442, 1965.

[39] G. Bingham. *A New Approach to Interpreting Rock Drillability.* Petroleum Publishing Company, 1965.

[40] Jack C. Estes. Selecting the proper rotary rock bit. *Journal of Petroleum Technology*, 23:1359 – 1367, 1971.

[41] R.A. Cunningham and J.G. Eenink. Laboratory study of effect of overburden, formation and mud column pressures on drilling rate of permeable formations. *Petroleum Transactions*, 217:9 – 17, 1959.

[42] A.J. Garnier and N.H. van Lingen. Phenomena affecting drilling rates at depth. *Petroleum Transactions*, 216:232 – 239, 1959.

[43] S.J. Black, A.D. & Green. Laboratory simulation of deep well drilling. *Petroleum Engineer*, –:40 – 43, 1978.

[44] D.J. Vidrine and E.J. Benit. Field verification of the effect of differential pressure on drilling rate. *Journal of Petroleum Technology*, 20:676 – 682, 1968.

[45] Jr. Bourgoyne, A.T. and Jr. Young, F.S. A multiple regression approach to optimal drilling and abnormal pressure detection. *Society of Petroleum Engineers Journal*, 14:371 – 384, 1974.

[46] W.C. Maurer. The "perfect - cleaning" theory of rotary drilling. *Journal of Petroleum Technology*, 14:1270 – 1274, 1962.

[47] Jr. Young, F.S. Computerized drilling control. *Journal of Petroleum Technology*, 21:483 – 496, 1969.

[48] E.M. Galle and H.B. Woods. Best constant weight and rotary speed for rotary rock bits. In *Drilling and Production Practice, 1 January, New York, New York.* American Petroleum Institute, 1963.

[49] John R. Eckel. Microbit studies of the effect of fluid properties and hydraulics on drilling rate, ii. In *Fall Meeting of the Society of Petroleum Engineers of AIME, 29 September-2 October, Houston, Texas*, 1968.

[50] C.A. Pratt. Increased penetration rates achieved with new extended nozzle bits. *Journal of Petroleum Technology*, 30:1191 − 1198, 1978.

[51] Gordon A. Tibbitts, John L. Sandstrom, Alan D. Black, and Sidney J. Green. Effects of bit hydraulics on full-scale laboratory drilled shale. *Journal of Petroleum Technology*, 33:1180 − 1188, 1981.

[52] J.L. Peterson. Diamond drilling model verified in field and laboratory tests. *Journal of Petroleum Technology*, 28:213 − 222, 1976.

[53] S. Irawan, A. Mahfuz, A. Rahman, and S.Q. Tunio. Optimization of weight on bit during drilling operation based on rate of penetration model. *Journal of Applied Science*, 4:1690 − 1695, 2012.

[54] Microsoft. *Microsoft Office Support, Linest.*, May 2014. URL `http://office.microsoft.com/en-001/excel-help/linest-HP005209155.aspx`.

[55] Bahari A. Nejati Moharrami F. Bahari, M.H. and M.B. Naghibi Sistani. Determining bourgoyne and young model coefficients using genetic algorithm to predict drilling rate. *Journal of Applied Science*, 8:3050 − 3054, 2008.

[56] John R. Eckel and W.J. Bielstein. Nozzle design and its effect on drilling rate and pump operation. In *Drilling and Production Practice, 1 January, New York, New York*. American Petroleum Institute, 1951.

[57] Pal Skalle. *Drilling Fluid Engineering*. Bookboon.com, 3 edition, 2012.

[58] Jim Frost. How high should r-squared be in regression analysis?, January 2014. URL `http://blog.minitab.com/blog/adventures-in-statistics/how-high-should-r-squared-be-in-regression-analysis`.

[59] Jim Frost. How to interpret regression analysis results: P-values and coefficients, July 2013. URL `http://blog.minitab.com/blog/adventures-in-statistics/how-to-interpret-regression-analysis-results-p-values-and-coefficients`.

[60] Jim Frost. Regression analysis: How to interpret s, the standard error of the regression, January 2014. URL

`http://blog.minitab.com/blog/adventures-in-statistics/`
`regression-analysis-how-to-interpret-s-the-standard-error-of-the-regression`

[61] Jim Frost. Regression analysis: How to interpret the constant (y intercept), July 2013. URL `http://blog.minitab.com/blog/adventures-in-statistics/` `regression-analysis-how-to-interpret-the-constant-y-intercept`.